TOWARD THE DEVELOPMENT OF AN IMPROVED RICIN VACCINE

By

JUSTIN CODY THOMAS

Submitted to the graduate degree program in Pharmaceutical Chemistry and the Graduate Faculty of the University of Kansas in partial fulfillment of the requirements for the degree of Doctor of Philosophy.

Date Defended: September 5, 2013

The Dissertation Committee for JUSTIN CODY THOMAS

certifies that this is the approved version of the following dissertation:

TOWARDS THE DEVELOPMENT OF AN IMPROVED RICIN VACCINE

_____

Chairperson Dr. C. Russell Middaugh

Date approved: September 5, 2013

Abstract

To date, there is no approved antidote to treat or prevent the toxic effects of ricin exposure. RiVax, a recombinant ricin A chain subunit vaccine antigen, is one such antidote being developed as a prophylaxis. While it has been shown to be protective in numerous animal studies, RiVax is currently limited by its ability to elicit a robust toxin-neutralizing antibody (TNA) response. The underlying hypothesis of this dissertation is that a RiVax-based antigen with improved structural stability would result in an enhanced TNA response due to the preservation of conformationally-sensitive epitopes. To that end, two complimentary and orthogonal computational approaches were employed to design twelve point mutations predicted to stabilize the structure of RiVax. Differential scanning calorimetry across a range of pH values revealed seven of the twelve mutations were more stable than RiVax, two had essentially no effect, and three were destabilizing. Serological analysis of mice immunized with RiVax, one of two stabilized mutants, or one of two destabilized mutants suggested that the stabilized antigens induced a qualitatively better immune response. Eight double point mutants and a triple point mutant were then produced by combining the seven stabilizing mutations in various ways. Circular dichroism and fluorescence thermal unfolding curves showed that all nine derivatives were, to varying degrees, more stable than RiVax. Differential scanning calorimetry (DSC) detected two distinct transitions – one which was rather dramatically affected by the mutations and a second which showed more meager gains in stability more in line with the spectroscopic techniques. The first transition was speculated to arise from changes to the rather unstable C-terminal region of RiVax. Serological analysis of mice immunized with RiVax or one of four multi-site derivatives (selected on the basis of highest $T_{m,1}$ from DSC analysis) showed that three of the derivatives elicited a more rapid and statistically superior TNA response relative to RiVax. When the mouse study was repeated with a lower antigen dose, a RiVax derivative containing mutations V81I, C171L, and V204I was clearly superior to RiVax and the other three derivatives at eliciting TNA. Furthermore, pepscan analysis suggested that the improvement in

TNA was due to preservation of conformationally-sensitive, neutralizing epitopes because reactivity differences with the overlapping peptides did not adequately explain the dramatic improvement in TNA elicited by the abovementioned triple mutant. Due to the results presented in this dissertation, the RiVax triple mutant warrants further development as a ricin vaccine candidate.

Dedicated to my parents, Bill and Carol, and my wife Angela

Acknowledgements

First and foremost I would like to thank my advisor, Dr. Russ Middaugh. It has been an absolute pleasure being a member of your lab. I will remain forever grateful for all that you've taught me these past five years. I would also like to thank all of the Middaugh and Volkin lab members, both past and present, for their friendship and scientific conversation. A special thank you goes to Dr. Sangeeta Joshi for all her help and guidance throughout my graduate work.

I would like to thank my committee members: Drs. Jennifer Laurence, Teruna Siahaan, David Volkin and John Karanicolas. In particular, I would like to John Karanicolas for his help in the early stages of my work involving the design of some of the RiVax mutants.

I would also like those people who contributed to my work through their collaborative efforts including F. Philip Gao, Ph.D.; Jianwen Fang, Ph.D.; Lei Hu, Ph.D; and Robert N. Brey, Ph.D. In particular, this work would not have been possible had it not been for Dr. Nicholas Mantis and his group at the Wadsworth Center, in particular Joanne O'Hara, Ph.D. and Erin Sully, Ph.D.

Finally, I would like to thank my family. To my mother, father, and sister: you have always been there for me whenever I have needed you. I will never be able to thank you enough for that. Most importantly, I would like to thank my incredible wife Angela. I don't know how I would have finished had I not had you to come home to. I love you!

Table of Contents

Chapter 1 Introduction

A brief history of vaccines

In 1805, Thomas Jefferson wrote to Edward Jenner:

> *"…You have erased from the calendar of human afflictions one of its greatest…"*

What President Jefferson was referring to was Dr. Jenner's "discovery" in 1796 that inoculating humans with cowpox virus prevented subsequent infection from smallpox. The practice of inoculating individuals as a means of protection against disease was certainly not novel at the time; it had been practiced by at least the Africans, Indians, and Chinese well before Jenner ever vaccinated little James Phipps. But, as Sir Francis Darwin so shrewdly stated, *"…in science the credit goes to the man who convinces the world, not to whom the idea first occurs.*" Nonetheless, Jenner's experiment was the first scientifically rigorous study in a series of landmark events that have advanced the field of vaccine research to where it stands today. Perhaps not surprisingly, his findings were relatively overlooked until the procedure had been replicated by himself and others over the course of the next couple of years. Once Jenner's results had been sufficiently repeated, word spread quickly about the success of this inoculation and much of the developed world began to implement the practice. In Europe alone, it has been estimated that before the practice of vaccination took hold 8–20% of all deaths were caused by the smallpox virus [1]. While lack of a concerted, worldwide effort prevented the complete eradication of smallpox until 1979, Dr. Jenner's breakthrough proved to be the first of what would go on to become one of the world's most effective human health interventions — the

vaccine. Today, there are over 70 FDA approved vaccines that provide some level of protection against roughly 25 agents. Two diseases that once took the lives of millions are now either considered eradicated (smallpox) or on the verge of eradication (poliomyelitis) by the World Health Organization due, in large part, to the development of vaccines against those pathogens.

One might presume that, given Dr. Jenner's discovery of a vaccine to protect against smallpox, the scientific community would have immediately put forth a tremendous amount of effort to discover similar medicines to protect against other diseases of that time. This, however, was not the case, as the field of vaccinology lay more or less dormant for 80 years until the work of Louis Pasteur. Pasteur's seminal contribution to the development of vaccines was his inquiries into pathogen attenuation. Instead of immunizing with a live pathogen related to the one that is of real concern (i.e., Jenner using cowpox for smallpox), Pasteur showed that he could vaccinate chickens with a weakened (but replication-competent) form of chicken cholera to protect the animals from subsequent infection [2]. As the story goes, Pasteur told one of his assistants to vaccinate the chickens with non-attenuated chicken cholera before leaving for vacation. The assistant forgot, leaving the cultures exposed to air for many weeks. Upon his return, the assistant injected the chickens with the air-exposed cholera cultures. The cultures ultimately protected the chickens from succumbing to a challenge with fresh, non-attenuated bacteria. This serendipitous demonstration marked a major turning point in vaccine development since vaccines could now be made in the laboratory under somewhat controlled conditions. In addition to the chicken cholera vaccine, Pasteur developed attenuated vaccines against anthrax (for livestock) and rabies (for humans). Interestingly enough, the case has been made that Pasteur really did not understand the theoretical basis underlying why attenuation was an effective way of making a vaccine [3]. Nonetheless, attenuated viruses remain one of the most effective classes of vaccines reinforcing the importance of Pasteur's observations. In fact, the

soon-to-be complete eradication of poliomyelitis is due largely to the oral, attenuated vaccine developed by Albert Sabin and co-workers in the late 1950s and early 1960s.

The next major advances in vaccine development were the introduction of the various inactivated vaccine classes. Daniel Salmon and his research assistant Theobald Smith are credited with discovering that vaccination with whole organisms completely inactivated by heat would provide protection against the live pathogen [4]. This influential breakthrough paved the way for the many derivatives of the inactivated vaccine class.

The toxoid class started with the work of Emil von Behring and Shibasaburo Kitsato, among others. Von Behring and Kitsato showed that sublethal doses of a diphtheria exotoxin could induce the production of protective antibodies [5]. Working from that basis, Gaston Ramon became the first to produce a stable, non-toxic diphtheria vaccine by using formalin to disable the toxin's ability to cause disease [6]. The 1950s saw the development of the world's first polio vaccine when Jonas Salk introduced his killed whole organism vaccine, although the aforementioned Sabin attenuated vaccine largely replaced Salk's killed vaccine everywhere in the world after its introduction. Salk, however, may have gotten the last laugh in their home country (Sabin was a naturalized U.S. citizen) since the attenuated vaccine was discontinued in the U.S. in 2000, although it remains in use elsewhere. The first polysaccharide vaccines for meningococcal and pneumococcal disease were then introduced in the 1970s. These vaccines were eventually superseded by the corresponding conjugated polysaccharide vaccines that arrived in the late 1980s. The first demonstration of a successful conjugate vaccine was accomplished by Frederick Robbins and co-workers when they conjugated diphtheria toxoid to the H. influenzae type b capsule [7]. The subunit viral vaccine (Heptavax-B; hepatitis B) class was successfully conceived by Maurice Hilleman and did not arrive on the market until 1981. Heptavax-B was made using purified human blood products and was quickly succeeded in 1986

by a fully recombinant version (Recombivax HB) made in yeast that did not require the use of human plasma. Although his name is not as instantly recognizable as Jenner or Pasteur, Dr. Hilleman is arguably the most practically important scientist in the history of vaccinology. He and his teams at Merck developed more than half of the vaccines on the Centers for Disease Control's child immunization schedule resulting in millions of saved lives [8].

The final transformative event in the history of vaccines that will be discussed here (although more could be discussed) came with the advent of recombinant DNA technology. Genetic engineering has revolutionized vaccine research. This breakthrough is crucial for the work presented in this dissertation, since without it the mutant versions of the RiVax antigen could not have been produced. Nobel Prize winner Paul Berg was the first to introduce the DNA of one organism into that of a different, living organism; by splicing together a fragment of the lambda genome into the DNA of simian virus SV40, he and his colleagues created the first man-made recombinant DNA [9]. Herb Boyer and Stanley Cohen followed that landmark discovery with experiments that showed that recombinant DNA could be inserted into bacteria in such a way that the foreign DNA would replicate as if it was part of the host genome [10]. Another watershed moment came when Boyer harnessed this technology to produce the first functional polypeptide from a synthesized gene [11]. Although still in its relative infancy, genetic engineering has already been instrumental in the development of four licensed vaccines. Hepatitis B and human papillomavirus (HPV) vaccines are made by inserting the appropriate viral surface protein gene into a yeast or Baculovirus expression system. The proteins produced by these hosts are then purified and assembled into the non-infections virus-like particles (VLPs) that are used for vaccination. The live typhoid vaccine has been genetically modified to not cause illness. Lastly, the attenuated influenza vaccine has been engineered to replicate effectively in the mucosa of the nasopharynx but not in the lungs [12]. It is really quite difficult

to understate the impact genetic engineering has had (and will continue to have) not only on vaccine research but on every biologically-oriented branch of science.

Vaccine classes

As alluded to in the previous paragraphs, there are two basic classes of vaccines: live, attenuated vaccines and inactivated vaccines. In the vast majority of cases, the antigen is of viral or bacterial origin. Inactivated vaccines can be further classified into whole organisms or fractional extracts. Fractional vaccines can be either protein- or polysaccharide-based. Toxoid and subunit vaccines constitute the protein-based vaccines, whereas polysaccharide-based vaccines can be pure sugars or sugars conjugated to a carrier protein. The focal point of this dissertation is an improvement of a subunit vaccine (outlined in green in Figure 1) that protects against ricin toxin. Unlike the majority of vaccines, it is not comprised of or derived from a virus or bacteria. Instead, it is a plant toxin and the antigen used in the vaccine is based on one of the toxin's two chains. In the following sections, a brief discussion of some of the advantages and disadvantages of the various classes will be presented. Each section also contains a list of currently licensed vaccines in the respective class.

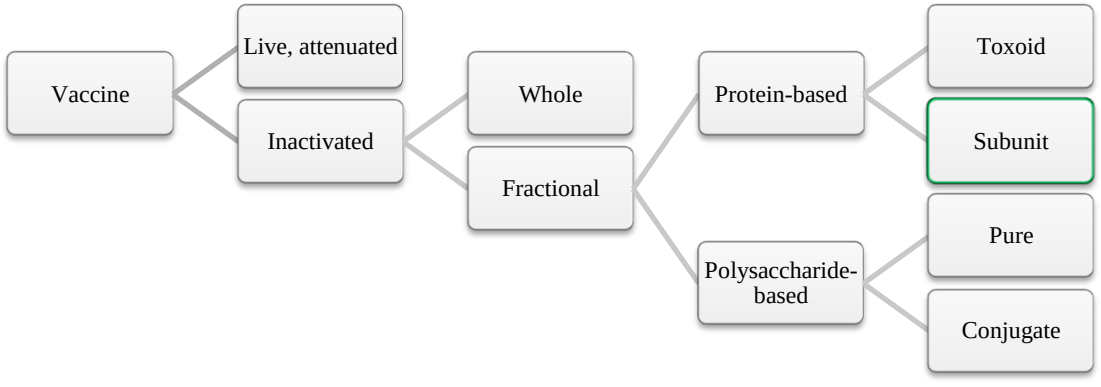

Figure 1. Classification of vaccines. The design of a ricin subunit vaccine will be the focus of this dissertation.

Live, attenuated vaccines. Since Pasteur's discovery of pathogen attenuation, this class of vaccines has been incredibly successful in preventing disease. Attenuation is typically achieved by passaging the virus (or bacteria) in tissue cultures or animal embryos in which the virus does not reproduce well [13]. This is done many times over after which the virus's ability to cause disease in a human host is severely limited. The pathogen does, though, replicate after injection and essentially causes "disease", but the disease state is extremely mild and temporary; it also pales in comparison to the disease state that would be caused by encounter with the wild pathogen. As one can imagine, people with immunodeficiencies should be very mindful when receiving live, attenuated vaccines because the replication of the pathogen once injected is not controlled and could potentially cause fatal adverse events. Another drawback of such a vaccine is that they require very precisely controlled conditions due to the fact the pathogen is alive. Any excursion from the specified storage conditions (exposure to light or temperature) can be particularly harmful to this class of vaccines because it may prevent the weakened pathogen from

replicating after injection [12]. This is certainly not an ideal situation for vaccines that have a significant patient population in places with poor chances of maintaining a cold chain.

On the positive side, the immune response against the attenuated pathogen remains very strong. Because a live pathogen is injected into the body, it is the most inherently immunogenic vaccine class and generally requires only one or two injections for lifetime immunity [2]. This is due to the vigorous cellular and humoral (antibody-mediated) immune response that is induced by vaccination, which mimics the response to natural infection. FDA approved vaccines of this class include those that protect against measles; mumps; rubella; vaccinia; varicella/zoster; yellow fever; rotavirus; influenza (intranasal version); and the only attenuated bacterial vaccine, typhoid.

Whole, inactivated vaccines. Whole, inactivated vaccines are comprised of an entire disease-causing organism, but the pathogen has been inactivated by heat and/or chemicals, such as formaldehyde or formalin. Unlike the case of attenuated vaccines, inactivated vaccines and their derivatives induce a considerably weaker immune response, with many of them relying solely on the vaccine's ability to invoke an antibody response [2]. As will be discussed in a subsequent section, many adjuvants are being developed that seek to stimulate a cellular response so that the response to vaccinations more closely resembles that of natural infection. Because the antigen is not alive, this class of vaccines requires multiple (i.e., booster) immunizations so that the body can maintain the memory immune cells required to fight infection upon contact with the natural pathogen [12]. As it pertains to storage conditions, inactivated vaccines have generally less restrictive conditions than their attenuated counterparts because the antigen is no longer living. These types of vaccines are often lyophilized such that they can even be stored at room temperature, avoiding the need for a strict cold chain. Vaccines in this class are limited to polio,

hepatitis A, and rabies; several inactivated bacterial vaccines are no longer available in the United States.

Protein-based vaccines. In the decades since the advent of recombinant DNA technology, there has been an increasing trend towards developing vaccines based on purified components of the infectious agent. For pathogenic species, this typically involves delivering a recombinantly-expressed surface protein(s). How one selects which surface protein to deliver is not necessarily an easy task – a pathogen can have hundreds of proteins on its surface. As will be discussed in a later section, thanks to modern computational techniques this selection process has become much easier and more rational. From a safety perspective, the isolated protein is almost always safer than the parent agent. Unfortunately, protein-based vaccines suffer from poor immunogenicity, even more so than whole, inactivated vaccines [2]. To combat this weaker response, subunit vaccines are typically administered in conjunction with adjuvants (as is also the case with the inactivated hepatitis A virus and some polysaccharide-based vaccines). The types of compounds used as adjuvants will be discussed in a later section. Subunit vaccines are available for four diseases: hepatitis B, influenza, acellular pertussis, human papillomavirus, and anthrax. Another type of protein-based vaccine is the toxoid vaccine. These are made by inactivating (typically by using formaldehyde) the toxic exoproteins of pathogenic organisms so they can no longer cause disease. Toxoid vaccines are available against diphtheria and tetanus; some also consider the aceullular pertussis and anthrax vaccines as part of this class.

Polysaccharide-based vaccines. Polysaccharide vaccines come in two types: pure and conjugated. Pure polysaccharide vaccines are just as the name implies: vaccines composed solely of long chains of sugar molecules. Conceptually, there is no limit to the number of

distinct sugar chains that can be incorporated into a polysaccharide vaccine. As the extreme example, Merck's pure polysaccharide vaccine against pneumococcal disease is comprised of 23 different polysaccharide antigens. Vaccines of this type typically generate a T cell-independent immune response [12]. In stark contrast to other inactivated vaccines, the booster response to pure polysaccharide vaccines is nonexistent. Pure polysaccharide vaccines are available for three diseases: pneumococcal disease, meningococcal disease, and *Salmonella typhi* (typhoid fever).

Due to the underwhelming immune response produced by pure polysaccharide vaccines (especially in young children), the 1980s saw the introduction of the conjugated polysaccharide vaccine class. In this type of vaccine, the poorly immunogenic polysaccharide antigen(s) is chemically conjugated to a protein carrier to help boost the immune response against the sugars. The conjugation to a protein carrier changes the type of immune response elicited from T cell-independent to T-cell dependent [12]. The vaccines that provide protection against infection from *Neisseria meningitides*, *Streptococcus pneumoniae*, and *Haemophilus influenzae* type b (Hib) all show an improved immune response when conjugated to a carrier protein [14]. There are five main carrier proteins used in vaccines today: tetanus toxoid (TT), diphtheria toxoid (DT), cross- reactive material 197 (CRM197), N. meningitides outer membrane protein (OMP), and non-typeable H. influenza derived protein D (PD) [15]. Conjugated polysaccharide vaccines are available for three diseases: Haemophilus influenzae type b (Hib), pneumococcal disease, and meningococcal disease.

DNA-based vaccines. This concise introduction to vaccine classes would be remiss not to include a few sentences about nucleic acid vaccines. Firstly, there are no nucleic acid vaccines approved for human use since these remain purely experimental at this point; however, four veterinary vaccines using DNA plasmids are approved suggesting that human use will eventually

become a reality [16]. The idea behind a nucleic acid vaccine is a cell will express a DNA-encoded protein (usually in the form of a plasmid) after which the protein would be subject to surveillance by the immune system. A huge advantage of this type of vaccine is that they should inherently produce a cellular immune response in addition to a humoral response – the goal towards which all vaccines aspire [17]. From a manufacturing perspective, this class of vaccine would be relatively simple and cost effective to produce. Perhaps the most significant hurdle for nucleic acid vaccines to overcome is that of efficient delivery [18]. Some of the delivery technologies being considered include viral particles; formulations involving lipids, emulsions, or DNA complexes formed with cationic carriers; and physical methods, such as electroporation.

Vaccine adjuvants

Due to the lack of a strong immune response against protein-based and inactivated vaccines, they are almost always administered in conjunction with an adjuvant. Adjuvants are compounds that are added to vaccine formulations to potentiate the immune response of the host. In fact, the word adjuvant is derived from the Latin *adjuvare* which means "to help". While only five adjuvants are approved for use in marketed products, another 10 or so have been administered in human clinical trials [19]. At the most basic level, there are two classes of vaccine adjuvants: those that work based on interactions with Toll-like receptors and those that do not require Toll-like receptor engagement. A couple examples of each class will be briefly discussed. Combining compounds from each class to produce the final vaccine is likely to be the future of the adjuvant field.

Toll-like receptor-independent. Various aluminum salts (e.g., aluminum oxyhydroxide, aluminum hydroxyphosphate, and aluminum hydroxyphosphate sulfate) represent the classic

categories of vaccine adjuvants. Aluminum salts have been used in vaccines since the 1930s when they were added to a diphtheria toxoid antigen [20]. The RiVax antigen of this study is adsorbed to an aluminum hydroxide adjuvant due to a weak immune response against the soluble antigen. For decades, it was assumed that the adjuvant action of these aluminum salts was due to a depot effect in which the antigen was slowly released over time. Thus, complete antigen adsorption was highly preferable. Stanley Hem and colleagues, however, have repeatedly shown that adsorption is not always a requirement for a robust antibody response with certain antigens [21-23]. While the depot effect may contribute to some extent, more recent evidence suggests three, non-mutually exclusive mechanisms: one concerning activation of the Nalp3 inflammasome [24], one positing interactions between the adjuvant and dendritic cell membrane lipids [25], and another involving a signaling cascade caused by extracellularly-[26] and intracellularly-released [27] DNA. Regardless of how aluminum salts exert their stimulating effects, they clearly work as judged by the millions of vaccines that have been dosed with aluminum.

A second adjuvant type which is not dependent on Toll-like receptor agonism is the squalene-based oil-in-water (o/w) emulsion. The European Medicines Agency has approved two O/W emulsion adjuvants as components of vaccines, MF59 (Novartis Vaccines) and AS03 (GlaxoSmithKline). A third o/w emulsion adjuvant, Sanofi's AF03, was shown to be safe and immunostimulatory in humans [28]. Squalene-based oil-in-water emulsions are proposed to potentiate immune responses by triggering the rapid recruitment of leukocytes at sites of injection and have been shown to improve immunogenicity (over aluminum salts) of a number of vaccines and subunit antigens by the i.m. route [29].

Toll-like receptor-dependent. Most recently, much focus has been given to the development of Toll-like receptor (TLR) agonists for use as adjuvants. TLRs are in the family of pattern recognition receptors and recognize pathogen-associated molecular patterns (PAMPs) associated with a range of microbes. Humans express 10 different TLRs and the nomenclature is simply to number them 1 – 10. TLRs 3, 7, 8, and 9 are expressed intracellularly in endosomes while the remaining TLRs are expressed on the surface of the plasma membrane [30]. Almost all TLR agonists cause signaling through the MyD88-dependent pathway, the exception being TLR3 [31]. Engagement of Toll-like receptors biases (to varying extents) the immune response towards a T_h1 response and thus is an attractive means of inducing cell-mediated immunity. Since aluminum salts were the only approved adjuvants for decades, the vast majority of the licensed vaccines that require the use of adjuvants to be effective are not engaging to any large extent (if at all) the cellular T_h1 response.

Monophosphoryl lipid A (MPLA) became the first approved TLR agonist to be included in an FDA approved vaccine when Cervarix was licensed in 2009. Lipid A is a component of the lipopolysaccharides (LPS) found on the outer membrane of gram-negative bacteria; the adjuvant is a detoxified version of LPS. Bacterial lipopolysaccharides are recognized by TLR4 and once detected cause a strong T_h1-biased immune response. In all approved vaccines that contain MPLA, the antigen and MPLA are delivered in conjunction with an aluminum salt adjuvant. In hopes of moving away from the reliance on aluminum salts, several clinical trials have been completed in which the antigen and MPLA are formulated as an o/w emulsion [32-34]. Finally, MPL is also being explored as a liposome-based adjuvant. GSK's liposome-based MPL with QS-21 adjuvant, AS01, has advanced to Phase III trials for a candidate malaria vaccine [35]. It is quite apparent that MPLA has a bright future as a key component of future vaccines.

The other TLR agonist that will be discussed in some detail is unmethylated CpG oligodeoxynucleotides (CpG ODNs). CpG ODN interacts with TLR9 molecules expressed in B cells and plasmacytoid dendritic cells. There are five distinct classes of CpG ODN, the most popular being the Class B type. Class B CpG ODNs strongly stimulate a T_h1 response. They also activate B cells and natural killer (NK) cells [36]. While it appeared this would become the second TLR agonist to be included in an approved vaccine, CpG oligonucleotides recently suffered as setback when Dynavax's hepatitis B vaccine (Heplisav) received a Complete Response Letter from the FDA indicating that there was insufficient data to support the safety of the product, although they overwhelming agreed that it demonstrated immunogenicity. CpG has been tested as a vaccine adjuvant in over a dozen clinical trials and has been successfully delivered in conjunction with an aluminum salt adjuvant [37-39]. In a study involving a biodefense vaccine, the addition of CpG (Type B) resulted in a marked acceleration and enhancement of the toxin-specific neutralizing antibodies when co-administered with anthrax vaccine adsorbed (AVA) [40].

Rational vaccine design and development

The conventional approach to vaccine development leaves a lot (at least scientifically) to be desired due to its reliance on empirical observations. Since the days of Pasteur, the development of a vaccine had essentially three steps: identify and isolate the pathogen responsible for a particular disease, attenuate or inactivate it, and then inject it into a patient. As crude as it may sound, that was essentially the full realization of how vaccines were made for hundreds of years. That being said, the empirical approach has led to every vaccine that was listed in the above section on vaccine classes.

The past decade or so in vaccine research, however, has seen a progressive shift towards a more rational approach towards arriving at a final vaccine candidate. Since this dissertation focuses on the rational design of a vaccine antigen, a short introduction to some of the new approaches used in the design and development of vaccines is appropriate. The following presents a brief introduction to three such vaccinology approaches: reverse, structural, and systems.

Reverse vaccinology. Reverse vaccinology was really the first broadly applicable attempt at a rational method for designing vaccines. Rino Rappuoli and his colleagues introduced the strategy in 2000 using the serogroup B strain of Neisseria meningitides (menB) as proof-of-concept [41]. Reverse vaccinology is a genomics-based technique that relies entirely on the availability of the whole genomic sequence of the disease-causing pathogen [42]. With a genome sequence in hand, an *in silico* search is used to identify suitable vaccine candidates based primarily on whether or not a particular protein can be expressed on the organism's surface. This screen results in a large number of candidates that are then expressed (hopefully), purified, and injected into mice. Quite obviously, the rate limiting step would be actually screening the candidate vaccines for protective immunity in mice. Essentially, the process can be likened to a huge funnel in which the entire genome is considered at the beginning, and after various procedures, one is left with only a handful of the "best" candidate antigens. The reverse vaccinology concept has led to many similar approaches, including those in which high throughput screens are being used to search the transcriptome [43], proteome [44], and immunome [45] of pathogens for candidate antigens. The coronation of the original reverse vaccinology approach was the licensure of Novartis's multicomponent menB vaccine Bexsero by the European Medicines Agency (EMA) in 2013 [46].

Structural vaccinology. The term structural vaccinology was first used by Serruto and Rappuolli in 2006 [47], although the first paper that truly attempted to define structural vaccinology appeared a few years later [48]. Structural vaccinology, as the name suggests, is the application of structural biology to vaccinology. It uses the three dimensional structure of an antigen to determine how to best design a vaccine. In contrast to reverse vaccinology, it is absolutely reliant on the availability of a well-resolved, three dimensional structure of the prospective antigen. Techniques for obtaining such a structure are x-ray crystallography, NMR, and perhaps even cryo-electron microscopy. While structural vaccinology is too young to have any approved products, the first human clinical trials are approaching for one antigen designed using such an approach: Novartis's respiratory syncytial virus fusion (RSV F) subunit protein vaccine [49]. Another group at Novartis designed a broadly protective (in mice), chimeric vaccine against Group B *Streptococcus* [50]. The authors first determined that a particular domain was immunologically dominant across 6 different Group B strains. They then created a single protein that contained the protective domain from each of the six variants with a tetrapeptide spacer between each. The vaccine provided decent protection from all six strains in a mouse model. One has to wonder, however, if the same results would have been achieved with a vaccine comprised of the six individual subunits. A final example of the power of structural vaccinology pertains to the development of another subunit serogroup B meningitis vaccine [51]. This antigen is based on factor H-binding protein which was discovered using reverse vaccinology. The problem with the use of this antigen is that the native protein has many sequence variants. Fortunately, these sequence variants could be grouped into three distinct classes in which any variant in a particular class would provide some amount of protection from the others in that class. To make a broadly protective vaccine, the authors grafted clusters of amino acids from

two of the classes onto the other class to make a single antigen that elicits immunity to all three variants.

The work presented in this dissertation is an exercise in structural vaccinology. Our group along with our collaborators has introduced conformationally-stabilizing mutations into a recombinant ricin A chain subunit vaccine in the hope that the mutated antigens would make a better vaccine. The relationship between antigen stability and the resulting immune response upon immunization, however, is currently unclear. It has been investigated previously in a variety of different systems – a few of which will be discussed below. In a very elegant study, Koide et al. generated a truncated version of outer surface protein A (OspA) antigen for use as a second generation Lyme disease vaccine [52]. The authors found that this truncated version, although it retained native-like structure and three important conformational epitopes, had both reduced vaccine efficacy and conformational stability compared to the full-length OspA. They increased the stability of the truncated version by mutating just three residues. Although the truncated and stabilized version still did not reach the stability of full-length OspA, it was now stable enough to impart the same level of protection as the full length antigen. Another study found a link between the lysosomal proteolytic susceptibility of RNase A and RNase S and the immune response generated by delivering them as antigens [53]. Somewhat counterintuitively, RNase A, being less susceptible to proteolysis, was the more immunogenic protein. While the authors didn't explicitly test for thermodynamic stability in their study, RNase A is indeed the more stable protein [54].

On the contrary, there are other studies that suggest more stable antigens are less immunogenic. Ohkuri et al. used mutant forms of two model antigens, lysozyme and a grass pollen allergen, to show that hyperstable variants of each suppress IgG production [55]. They even went so far as to put a number (>~20 kcal/mol) on the free energy of unfolding that would

suppress antibody production. A group interested in developing anti-cancer immunotoxins also found that stabilizing a foreign protein resulted in decreased immunogenicity [56]. In that study, a disulfide bond was engineered into the toxic arm (domain III of Pseudomonas exotoxin A) of the immunotoxin to increase its stability. The authors found that the disulfide bonded form lowered the amount of antibody raised against the toxic portion. In one study that found essentially no difference, a series of destabilized (8 – 23 kJ/mol less stable) streptococcal pyrogenic exotoxin A mutants were created and tested for antigenicity in mice [57]. Even though all mutants were considerably less stable, the only mutant that generated a significantly weaker protective immune response was the extremely destabilized mutant that contained cysteine to alanine mutations which disrupted a surface-exposed disulfide bond. It has also been observed that adsorbing proteins onto the surface of aluminum salts results in their destabilization, despite the enhanced immunogenicity seen with the use of such adjuvants [58, 59]. In summary, it is difficult to predict *a priori* whether stabilizing or destabilizing mutations will have the intended, enhanced immunogenic consequences.

Systems vaccinology. The final vaccinology approach discussed here will be systems vaccinology. As one might presume from the naming of structural vaccinology, systems vaccinology stems from the integration of systems biology and vaccinology. It is newest of the three vaccinology approaches discussed here having been introduced concomitantly by the Pulendran [60] and Sékaly [61] groups at Emory and McGill, respectively, at the end of 2008. These studies involve a wide array of measurements, including transcriptomics and proteomics, and a wide array of biological systems, from in-vitro stimulated murine innate immune cells to whole blood collected from vaccinated human donors. One of the key goals of systems vaccinology is to be able to identify immune biomarkers (particularly those that appear early in

the response to vaccination) that correlate with an eventual protective immune response [62]. Knowing that the early activation of a particular type of immune cell (for example, macrophages) leads to protective immunity will help researches design better delivery vehicles and adjuvants to provoke such a response. Of course, the confounding problem with this approach is that the immune response in animal models is hardly a mimic for what occurs in humans. Thus, it is likely that one would require clinical trials to begin to use this approach to inform the design of a vaccine against a new pathogen. The continued development of humanized mouse models may turn out to be the key to unleashing the full potential of systems vaccinology [63].

Ricin

Simply put, ricin is one of the world's deadliest toxins. It is produced in the beans of the common castor plant, *Ricinus communis*, of which it constitutes roughly 5% of the dry weight of the bean. It is cultivated primarily for its oil, which is a global commodity used in biofuels, industrial lubricants, and cosmetics. Based primarily on studies in mice, its estimated lethal dose in humans ranges from 1–10 μg/kg body weight when delivered by injection or aerosol [64]. Because of its extreme toxicity and relative ease of acquisition, ricin is classified as a Class B biothreat by the Centers for Disease Control (CDC). At this time, no antidote is commercially available to counter the lethal effects of ricin toxicity.

Ricin has an established history of use in multiple settings. The most infamous use of ricin is that by the Bulgarian secret police in which they injected a ricin pellet from the tip of an umbrella into a dissident's leg. The victim died a few days later. In late 2011, the FBI foiled a plot by several men in Georgia that aimed at using ricin to kill politicians, members of the media, and innocent civilians [65]. More recently, ricin-contaminated mail has been sent to members of

the federal government, including the president [66]. Because developing a ricin vaccine forms the basis for the research initiated in this dissertation, a discussion of the toxin's structure and function; the immunological basis for immunity; as well as an introduction to candidate vaccines is in order.

Structure and function. Ricin is a 64 kDa glycoprotein composed of two polypeptide chains (A and B) joined by a disulfide bond. Each chain is approximately 32 kDa. Ricin belongs to a family of proteins called ribosome inactivating proteins (RIPs) that function by inhibiting protein synthesis at the ribosomal level. Other members of the RIP family include Shiga toxin; type I RIPs (meaning they only contain an "A chain") such as trichosanthin and pokeweed antiviral protein; and type II RIPs such as abrin and cinnamonin. The A chain component of all RIPs shares a nearly identical mechanism of action; the means by which they reach their substrate, however, is toxin-specific.

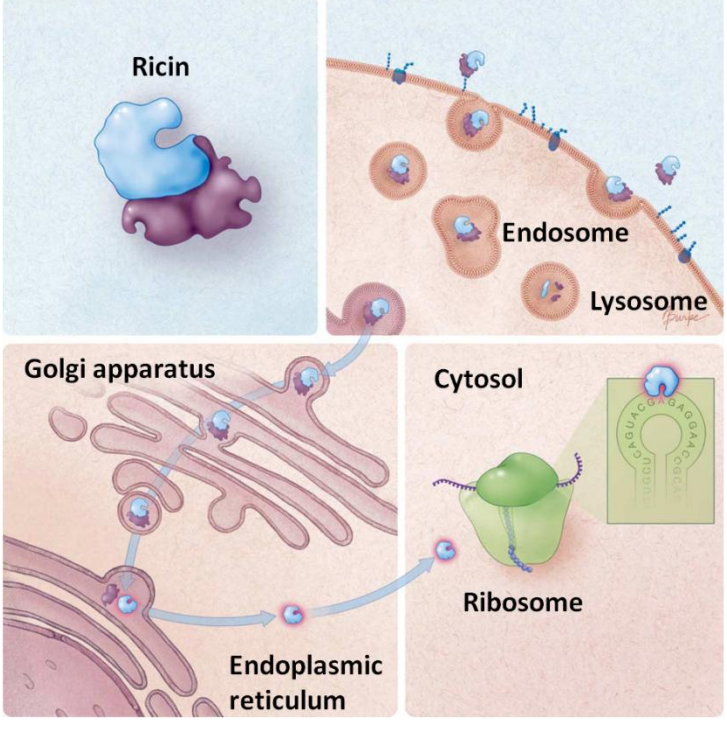

Figure 2. Ricin trafficking in mammalian cells. See accompanying text for a description of the process.

Ricin is more precisely a type II RIP in which each subunit serves a crucial, yet distinct, role in the severe toxicity of the molecule (Figure 2). The B chain acts essentially as a carrier protein that interacts rather promiscuously with terminal galactose residues (e.g., from glycoproteins and glycolipids) or mannose receptors to bind the holotoxin to the cell surface [67]. After gaining

entry into the cell by way of endocytosis, the vast majority of the toxin is either recycled to the cell surface or destroyed in the lysosome. A small fraction of the toxin, however, undergoes retrograde transport through the trans-Golgi network until it reaches the endoplasmic reticulum (ER) [68]. It is in the ER where the disulfide bond joining the two chains is reduced, probably by protein disulfide isomerases [69]. The A chain, now free of its B chain counterpart, apparently undergoes a structural alteration in its C-terminal domain that facilitates its insertion into the ER membrane for subsequent transport into the cytosol [70, 71]. Dislocation of misfolded proteins generally results in ubiquitination and subsequent proteosomal degradation; however, the A chain of ricin contains just two lysine residues which severely limits the extent to which it is degraded [72]. Once in the cytosol, the A chain presumably must refold to its active conformation, perhaps with the aid of host ribosomes [70], before carrying out its toxic function, namely the inhibition of protein synthesis [67, 73]. More recent evidence points to a specific proteosomal subunit cap in preventing unfolded RTA from aggregating after it reaches the cytosol [74]. The precise mechanism of protein synthesis inhibition was shown to be the cleavage of the N-glycosidic bond of adenine residue 4324 within the 28S rRNA of eukaryotic ribosomes [75, 76]. The cleavage of this residue prevents elongation factor binding and thus halts that ribosomes ability to make protein. The A chain can catalyze this reaction at an extraordinary rate—approximately 1400 ribosomes per minute [77, 78]. The depurination event can lead to death in humans as quickly as 36 hours after exposure [79].

Immunity. Given that the B chain of ricin is responsible for the toxin's entry into cells, one might assume that circulating antibodies (as well as memory B and T cells) against the B chain (and more precisely, the galactose-binding sites) would be best at preventing infection. The overly-simplified argument is that the toxin cannot enter the cell due to engagement with

antibodies, with no chance for the A chain to reach the cytosol and depurinate ribosomes. Therefore, it would seem logical that the best antigen to deliver in a vaccine setting would be the B chain. This, however, does not seem to be the case with respect to ricin (and probably other RIPs) [80]. Immunization with holotoxin, A chain alone, or A chain derivatives elicits a response consisting of both neutralizing and non-neutralizing antibodies [80, 81]. How antibodies raised against the A chain provide protection is just starting to be worked out [82, 83]. Remarkably, only six percent of the antibodies raised specifically against the A chain posses detectable ricin neutralizing activity in a Vero cell cytotoxicity assay; of these six percent, approximately 88 % are thought to be conformationally dependent [81]. RiVax, however, is rather unstable [84] – a problem derived from the inherent instability of the free A chain [70]. The fact that the vast majority of anti-A chain antibodies capable of neutralizing the holotoxin recognize some form of higher order antigen structure suggests that a ricin antigen with greater conformational stability might result in a more efficacious vaccine.

Candidate vaccines. A handful of ricin vaccine candidates have been developed over the past couple of decades. The crudest attempt was a formaldehyde-crosslinked toxoid [85-87]. While it was immunogenic in animals, safety concerns with using the active toxin as the starting material, side effects due to the inactivation process, and product variability quickly rendered this a poor option. Another attempt focused on using the unattenuated A chain. This antigen was also immunogenic in animals, but concerns with safety led to this vaccine being abandoned as well.

The previously failed attempts led to the development of attenuated A chain antigens to reduce the inherent toxicity associated with the protein. There are currently two leading recombinant subunit protein vaccines based on the A chain of ricin: RiVax and RVEc (Figure 3).

The RiVax antigen retains the full length of the A chain but contains point mutations V76M and Y80A to attenuate toxicity. The V76M mutation alters a residue shown to induce vascular leak syndrome [88] while the Y80 mutation modifies a residue known to contribute to its enzymatic function [89]. RiVax's immunogenicity and ability to protect animals from lethal ricin challenge has been shown in multiple mouse studies [88, 90-93]. More importantly, it has been administered in Phase 1 clinical trials, both without adjuvant [94] and adsorbed to Alhydrogel [95], and was shown to be safe and somewhat immunogenic.

The RVEc antigen is a significantly truncated version of the A chain. It was designed by comparing the electric field potential of the RTA surface to that of a type I RIP. The authors found significant amounts of hydrophobicity in the C-terminal end of RTA that normally interfaces with the B chain which they proposed led to solubility and stability problems [96]. They thus truncated the final 69 amino acids of the C-terminal sequence to make a more compact A chain with less hydrophobic exposure. Upon truncating those amino acids, they discovered that a disordered loop (residues 34-43) became solvent exposed and contributed significantly to the aggregation propensity of the shortened A chain. After removing the disordered loop, the authors arrived at what is now termed RVEc (or alternatively RTA 1-33/44-198); it has also been shown to be safe and immunogenic in multiple animal studies [96-98]. This candidate has recently entered Phase I clinical trials. More recently, a team at the Army has further increased the stability of RVEc by engineering a disulfide bond between residues 48 and 77 [99].

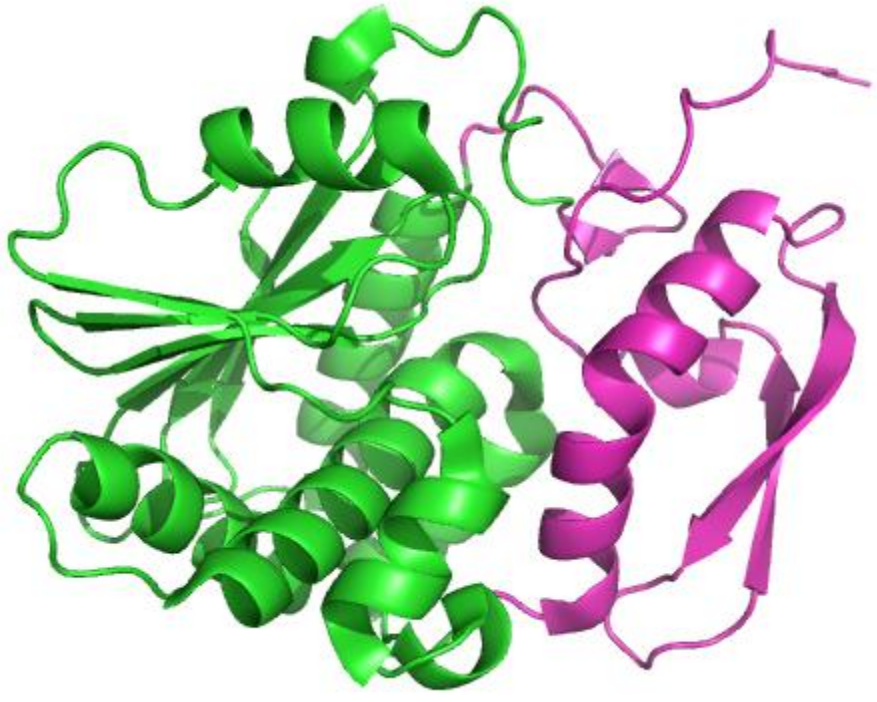

Figure 3. Ribbon diagram of RiVax (PDB accession file 3srp). The regions of the molecule in purple represent the areas that are deleted in RVEc. The region eliminated on RVEc interfaces extensively with the B chain of ricin in the holotoxin.

This dissertation focuses on making mutations to the RiVax antigen. Two problems associated with this antigen will be introduced. As stated previously, RiVax has encountered problems with its marginal stability in solution [84]. Its stability worsens when adsorbed to the surface of Alhydrogel [59], the aluminum salt adjuvant with which it is currently formulated. This instability resulted in multiple lots being used in the first Phase 1 clinical trial [94] and led to subsequent studies to lyophilize the non-adsorbed [93] and adsorbed proteins [100]. As a result of the two lyophilization studies, problems with storage stability should no longer hamper the continued development of the vaccine.

A second, and more important, problem encountered with RiVax is its relatively weak elicitation of toxin neutralizing antibodies (TNA) in the commonly used murine model, especially when compared to RVEc [101]. It is thought that the presence of toxin neutralizing antibodies (and not total antibodies, per se) is critical to the survival of animals that encounter

ricin. Since a ricin vaccine would be approved via the Food and Drug Administration's animal rule, elicitation of TNA in animal models is paramount to the approval (and presumed real-world success) of the vaccine. The TNA assay used throughout this dissertation is a Vero cell cytotoxicity assay that, by the nature of the assay, does not take into account F_c-mediated activity. While F_c effector functions have not yet been shown to play a role in the immune response to ricin, immunity to anthrax toxin does require some amount of F_c effector function involvement to protect from exposure [102]. This dissertation works off the hypothesis that the weak immune response upon vaccination is coupled to the moderate conformational stability of the antigen. Thus, we propose the problem with TNA elicitation can be addressed by designing more stable versions of the antigen. As discussed in the section on structural vaccinology, however, changes to stability tend to have mixed results in terms of the how they impact immunogenicity.

In addition to the aforementioned vaccine candidates, various labs have been investigating small molecule inhibitors [103-105] and monoclonal antibodies [106-108] to thwart ricin exposure. Neither approach, however, offers the obvious advantages of a prophylactic vaccine.

Chapter overview

In Chapters 2 and 3, RiVax antigens containing one mutation each (Chapter 2) and multiple mutations (Chapter 3) are characterized for their conformational stabilities and immunogenicities in a mouse model. Chapter 4 concludes with comments on the implications of the findings presented herein and suggestions for future work. In Appendix A, the development of two stability indicating assays to assist in the further development of a ricin A chain subunit vaccine are described. One involves an ELISA assay developed with the intent of characterizing

Alhydrogel-adsorbed RiVax; the other is a cation exchange chromatography method useful for characterizing charged variants of non-adsorbed RiVax. Appendix B concerns the biophysical characterization of RVEc, the Army's ricin vaccine candidate.

References

1. Andre, F.E., *Vaccinology: past achievements, present roadblocks and future promises.* Vaccine, 2003. 21(7-8): p. 593-5.
2. Plotkin, S.L. and S.A. Plotkin, *A short history of vaccination.*, in *Vaccines.*, S.A. Plotkin and W.A. Orenstein, Editors. 2004, WB Saunders: Philadelphia. p. 1-15.
3. Plotkin, S.A. and S.L. Plotkin, *The development of vaccines: how the past led to the future.* Nat Rev Microbiol, 2011. 9(12): p. 889-93.
4. Salmon, D.E. and T. Smith, *On a new method of producing immunity from contageous diseases.* Am Vet Rev, 1886. 10: p. 63-9.
5. von Behring, E. and S. Kitasato, *Über das zustandekommen der diphtherie-immunität und der tetanus-immunität bie tieren.* Dtsch. Med. Wochenschr, 1890. 16: p. 1113-1114.
6. Ramon, G., *Sur le pouvoir floculant et sur les propriétés immunisantes d'une toxine diphtérique rendue anatoxique (anatoxine).* C R. Acad. Sci. Paris, 1923. 177: p. 1338-1340.
7. Schneerson, R., et al., *Preparation, characterization, and immunogenicity of Haemophilus influenzae type b polysaccharide-protein conjugates.* J Exp Med, 1980. 152(2): p. 361-76.
8. Maugh, T.H., *Maurice R. Hilleman, 85; Scientist Developed Many Vaccines That Saved Millions of Lives.*, in *Los Angeles Times*.
9. Jackson, D.A., R.H. Symons, and P. Berg, *Biochemical method for inserting new genetic information into DNA of Simian Virus 40: circular SV40 DNA molecules containing lambda phage genes and the galactose operon of Escherichia coli.* Proceedings of the National Academy of Sciences of the United States of America, 1972. 69(10): p. 2904-9.
10. Cohen, S.N., et al., *Construction of biologically functional bacterial plasmids in vitro.* Proc Natl Acad Sci U S A, 1973. 70(11): p. 3240-4.
11. Itakura, K., et al., *Expression in Escherichia coli of a chemically synthesized gene for the hormone somatostatin.* Science, 1977. 198(4321): p. 1056-63.
12. CDC, *Principles of Vaccination*, in *Epidemiology and Prevention of Vaccine-Preventable Diseases*, W. Atkinson, S. Wolfe, and J. Hamborsky, Editors. 2012, Public Health Foundation: Washington, D.C.
13. Plotkin, S.A., *Six revolutions in vaccinology.* Pediatr Infect Dis J, 2005. 24(1): p. 1-9.
14. Finn, A., *Bacterial polysaccharide-protein conjugate vaccines.* Br Med Bull, 2004. 70: p. 1-14.
15. Josefsberg, J.O. and B. Buckland, *Vaccine process technology.* Biotechnol Bioeng, 2012. 109(6): p. 1443-60.
16. Kutzler, M.A. and D.B. Weiner, *DNA vaccines: ready for prime time?* Nat Rev Genet, 2008. 9(10): p. 776-88.
17. Liu, M.A. and J.B. Ulmer, *Human clinical trials of plasmid DNA vaccines.* Adv Genet, 2005. 55: p. 25-40.

18. Ulmer, J.B., et al., *RNA-based vaccines.* Vaccine, 2012. 30(30): p. 4414-8.
19. Rappuoli, R., et al., *Vaccines for the twenty-first century society.* Nat Rev Immunol, 2011. 11(12): p. 865-72.
20. Park, W.H., Schroder, M.C., *Diptheria toxin-antitoxin and toxoid: a comparison.* American Journal of Public Health and the Nations Health, 1932. 22(1): p. 7-16.
21. Iyer, S., H. HogenEsch, and S.L. Hem, *Relationship between the degree of antigen adsorption to aluminum hydroxide adjuvant in interstitial fluid and antibody production.* Vaccine, 2003. 21(11-12): p. 1219-23.
22. Romero Mendez, I.Z., et al., *Potentiation of the immune response to non-adsorbed antigens by aluminum-containing adjuvants.* Vaccine, 2007. 25(5): p. 825-33.
23. Noe, S.M., et al., *Mechanism of immunopotentiation by aluminum-containing adjuvants elucidated by the relationship between antigen retention at the inoculation site and the immune response.* Vaccine, 2010. 28(20): p. 3588-94.
24. Eisenbarth, S.C., et al., *Crucial role for the Nalp3 inflammasome in the immunostimulatory properties of aluminium adjuvants.* Nature, 2008. 453(7198): p. 1122-6.
25. Flach, T.L., et al., *Alum interaction with dendritic cell membrane lipids is essential for its adjuvanticity.* Nature medicine, 2011. 17(4): p. 479-87.
26. Marichal, T., et al., *DNA released from dying host cells mediates aluminum adjuvant activity.* Nat Med, 2011. 17(8): p. 996-1002.
27. McKee, A.S., et al., *Host DNA released in response to aluminum adjuvant enhances MHC class II-mediated antigen presentation and prolongs CD4 T-cell interactions with dendritic cells.* Proc Natl Acad Sci U S A, 2013. 110(12): p. E1122-31.
28. Levie, K., et al., *An adjuvanted, low-dose, pandemic influenza A (H5N1) vaccine candidate is safe, immunogenic, and induces cross-reactive immune responses in healthy adults.* J Infect Dis, 2008. 198(5): p. 642-9.
29. O'Hagan, D.T., et al., *The mechanism of action of MF59 - an innately attractive adjuvant formulation.* Vaccine, 2012. 30(29): p. 4341-8.
30. Kumar, H., T. Kawai, and S. Akira, *Toll-like receptors and innate immunity.* Biochem Biophys Res Commun, 2009. 388(4): p. 621-5.
31. Manicassamy, S. and B. Pulendran, *Modulation of adaptive immunity with Toll-like receptors.* Semin Immunol, 2009. 21(4): p. 185-93.
32. Chakravarty, J., et al., *A clinical trial to evaluate the safety and immunogenicity of the LEISH-F1+MPL-SE vaccine for use in the prevention of visceral leishmaniasis.* Vaccine, 2011. 29(19): p. 3531-7.
33. Aide, P., et al., *Four year immunogenicity of the RTS,S/AS02(A) malaria vaccine in Mozambican children during a phase IIb trial.* Vaccine, 2011. 29(35): p. 6059-67.
34. Leroux-Roels, I., et al., *Evaluation of the safety and immunogenicity of two antigen concentrations of the Mtb72F/AS02(A) candidate tuberculosis vaccine in purified protein derivative-negative adults.* Clin Vaccine Immunol, 2010. 17(11): p. 1763-71.
35. Agnandji, S.T., et al., *First results of phase 3 trial of RTS,S/AS01 malaria vaccine in African children.* N Engl J Med, 2011. 365(20): p. 1863-75.
36. Vollmer, J., et al., *Characterization of three CpG oligodeoxynucleotide classes with distinct immunostimulatory activities.* Eur J Immunol, 2004. 34(1): p. 251-62.
37. Brown, T.H., et al., *Comparison of immune responses and protective efficacy of intranasal prime-boost immunization regimens using adenovirus-based and CpG/HH2 adjuvanted-subunit vaccines against genital Chlamydia muridarum infection.* Vaccine, 2012. 30(2): p. 350-60.

38. Cooper, C.L., et al., *Immunostimulatory effects of three classes of CpG oligodeoxynucleotides on PBMC from HCV chronic carriers.* J Immune Based Ther Vaccines, 2008. 6: p. 3.
39. Halperin, S.A., et al., *Comparison of safety and immunogenicity of two doses of investigational hepatitis B virus surface antigen co-administered with an immunostimulatory phosphorothioate oligodeoxyribonucleotide and three doses of a licensed hepatitis B vaccine in healthy adults 18-55 years of age.* Vaccine, 2012. 30(15): p. 2556-63.
40. Rynkiewicz, D., et al., *Marked enhancement of the immune response to BioThrax(R) (Anthrax Vaccine Adsorbed) by the TLR9 agonist CPG 7909 in healthy volunteers.* Vaccine, 2011. 29(37): p. 6313-20.
41. Pizza, M., et al., *Identification of vaccine candidates against serogroup B meningococcus by whole-genome sequencing.* Science, 2000. 287(5459): p. 1816-20.
42. Rappuoli, R., *Reverse vaccinology.* Curr Opin Microbiol, 2000. 3(5): p. 445-50.
43. Grifantini, R., et al., *Previously unrecognized vaccine candidates against group B meningococcus identified by DNA microarrays.* Nat Biotechnol, 2002. 20(9): p. 914-21.
44. Rodriguez-Ortega, M.J., et al., *Characterization and identification of vaccine candidate proteins through analysis of the group A Streptococcus surface proteome.* Nature biotechnology, 2006. 24(2): p. 191-7.
45. Vytvytska, O., et al., *Identification of vaccine candidate antigens of Staphylococcus aureus by serological proteome analysis.* Proteomics, 2002. 2(5): p. 580-90.
46. Vesikari, T., et al., *Immunogenicity and safety of an investigational multicomponent, recombinant, meningococcal serogroup B vaccine (4CMenB) administered concomitantly with routine infant and child vaccinations: results of two randomised trials.* Lancet, 2013.
47. Serruto, D. and R. Rappuoli, *Post-genomic vaccine development.* FEBS Lett, 2006. 580(12): p. 2985-92.
48. Dormitzer, P.R., J.B. Ulmer, and R. Rappuoli, *Structure-based antigen design: a strategy for next generation vaccines.* Trends Biotechnol, 2008. 26(12): p. 659-67.
49. Swanson, K.A., et al., *Structural basis for immunization with postfusion respiratory syncytial virus fusion F glycoprotein (RSV F) to elicit high neutralizing antibody titers.* Proc Natl Acad Sci U S A, 2011. 108(23): p. 9619-24.
50. Nuccitelli, A., et al., *Structure-based approach to rationally design a chimeric protein for an effective vaccine against Group B Streptococcus infections.* Proc Natl Acad Sci U S A, 2011. 108(25): p. 10278-83.
51. Scarselli, M., et al., *Rational design of a meningococcal antigen inducing broad protective immunity.* Sci Transl Med, 2011. 3(91): p. 91ra62.
52. Koide, S., et al., *Structure-based design of a second-generation Lyme disease vaccine based on a C-terminal fragment of Borrelia burgdorferi OspA.* J Mol Biol, 2005. 350(2): p. 290-9.
53. Delamarre, L., et al., *Enhancing immunogenicity by limiting susceptibility to lysosomal proteolysis.* The Journal of experimental medicine, 2006. 203(9): p. 2049-55.
54. Catanzano, F., et al., *Temperature-induced denaturation of ribonuclease S: a thermodynamic study.* Biochemistry, 1996. 35(41): p. 13378-85.
55. Ohkuri, T., et al., *A protein's conformational stability is an immunologically dominant factor: evidence that free-energy barriers for protein unfolding limit the immunogenicity of foreign proteins.* J Immunol, 2010. 185(7): p. 4199-205.

56. Liu, W., et al., *A recombinant immunotoxin engineered for increased stability by adding a disulfide bond has decreased immunogenicity.* Protein Eng Des Sel, 2012. 25(1): p. 1-6.
57. Carra, J.H., et al., *Mutational effects on protein folding stability and antigenicity: the case of streptococcal pyrogenic exotoxin A.* Clin Immunol, 2003. 108(1): p. 60-8.
58. Jones, L.S., et al., *Effects of adsorption to aluminum salt adjuvants on the structure and stability of model protein antigens.* J Biol Chem, 2005. 280(14): p. 13406-14.
59. Peek, L.J., et al., *Effects of stabilizers on the destabilization of proteins upon adsorption to aluminum salt adjuvants.* J Pharm Sci, 2007. 96(3): p. 547-57.
60. Querec, T.D., et al., *Systems biology approach predicts immunogenicity of the yellow fever vaccine in humans.* Nat Immunol, 2009. 10(1): p. 116-25.
61. Gaucher, D., et al., *Yellow fever vaccine induces integrated multilineage and polyfunctional immune responses.* J Exp Med, 2008. 205(13): p. 3119-31.
62. Pulendran, B., S. Li, and H.I. Nakaya, *Systems vaccinology.* Immunity, 2010. 33(4): p. 516-29.
63. Shultz, L.D., et al., *Humanized mice for immune system investigation: progress, promise and challenges.* Nat Rev Immunol, 2012. 12(11): p. 786-98.
64. Audi, J., et al., *Ricin poisoning: a comprehensive review.* JAMA, 2005. 294(18): p. 2342-51.
65. Severson, K. and R. Brown, *Georgia Men Held in Plot to Attack Government*, in *New York Times*.
66. Kindy, K. and J. Achenbach, *Mississippi man suspected in ricin case has been arrested, FBI says*, in *Washington Post*.
67. Olsnes, S., K. Refsnes, and A. Pihl, *Mechanism of action of the toxic lectins abrin and ricin.* Nature, 1974. 249(458): p. 627-31.
68. Rapak, A., P.O. Falnes, and S. Olsnes, *Retrograde transport of mutant ricin to the endoplasmic reticulum with subsequent translocation to cytosol.* Proc Natl Acad Sci U S A, 1997. 94(8): p. 3783-8.
69. Spooner, R.A., et al., *Protein disulphide-isomerase reduces ricin to its A and B chains in the endoplasmic reticulum.* Biochem J, 2004. 383(Pt 2): p. 285-93.
70. Argent, R.H., et al., *Ribosome-mediated folding of partially unfolded ricin A-chain.* J Biol Chem, 2000. 275(13): p. 9263-9.
71. Mayerhofer, P.U., et al., *Ricin A chain insertion into endoplasmic reticulum membranes is triggered by a temperature increase to 37 {degrees}C.* J Biol Chem, 2009. 284(15): p. 10232-42.
72. Deeks, E.D., et al., *The low lysine content of ricin A chain reduces the risk of proteolytic degradation after translocation from the endoplasmic reticulum to the cytosol.* Biochemistry, 2002. 41(10): p. 3405-13.
73. Olsnes, S. and A. Pihl, *Ricin - a potent inhibitor of protein synthesis.* FEBS Lett, 1972. 20(3): p. 327-329.
74. Pietroni, P., et al., *The proteasome cap RPT5/Rpt5p subunit prevents aggregation of unfolded ricin A chain.* Biochem J, 2013.
75. Endo, Y. and K. Tsurugi, *RNA N-glycosidase activity of ricin A-chain. Mechanism of action of the toxic lectin ricin on eukaryotic ribosomes.* J Biol Chem, 1987. 262(17): p. 8128-30.
76. Endo, Y., et al., *The mechanism of action of ricin and related toxic lectins on eukaryotic ribosomes. The site and the characteristics of the modification in 28 S ribosomal RNA caused by the toxins.* J Biol Chem, 1987. 262(12): p. 5908-12.

77. Olsnes, S., et al., *Ribosome inactivation by the toxic lectins abrin and ricin. Kinetics of the enzymic activity of the toxin A-chains.* Eur J Biochem, 1975. 60(1): p. 281-8.
78. Endo, Y. and K. Tsurugi, *The RNA N-glycosidase activity of ricin A-chain. The characteristics of the enzymatic activity of ricin A-chain with ribosomes and with rRNA.* J Biol Chem, 1988. 263(18): p. 8735-9.
79. Wilhelmsen, C.L. and M.L. Pitt, *Lesions of acute inhaled lethal ricin intoxication in rhesus monkeys.* Vet Pathol, 1996. 33(3): p. 296-302.
80. Maddaloni, M., et al., *Immunological characteristics associated with the protective efficacy of antibodies to ricin.* J Immunol, 2004. 172(10): p. 6221-8.
81. O'Hara, J.M., et al., *Folding domains within the ricin toxin A subunit as targets of protective antibodies.* Vaccine, 2010. 28(43): p. 7035-46.
82. Song, K., et al., *Antibody to ricin a chain hinders intracellular routing of toxin and protects cells even after toxin has been internalized.* PloS one, 2013. 8(4): p. e62417.
83. O'Hara, J.M. and N.J. Mantis, *Neutralizing monoclonal antibodies against ricin's enzymatic subunit interfere with protein disulfide isomerase-mediated reduction of ricin holotoxin in vitro.* J Immunol Methods, 2013.
84. Peek, L.J., R.N. Brey, and C.R. Middaugh, *A rapid, three-step process for the preformulation of a recombinant ricin toxin A-chain vaccine.* J Pharm Sci, 2007. 96(1): p. 44-60.
85. Griffiths, G.D., et al., *Protection against inhalation toxicity of ricin and abrin by immunisation.* Human & experimental toxicology, 1995. 14(2): p. 155-64.
86. Hewetson, J.F., et al., *Protection of mice from inhaled ricin by vaccination with ricin or by passive treatment with heterologous antibody.* Vaccine, 1993. 11(7): p. 743-6.
87. Griffiths, G.D., G.J. Phillips, and S.C. Bailey, *Comparison of the quality of protection elicited by toxoid and peptide liposomal vaccine formulations against ricin as assessed by markers of inflammation.* Vaccine, 1999. 17(20-21): p. 2562-8.
88. Smallshaw, J.E., et al., *A novel recombinant vaccine which protects mice against ricin intoxication.* Vaccine, 2002. 20(27-28): p. 3422-7.
89. Ready, M.P., Y. Kim, and J.D. Robertus, *Site-directed mutagenesis of ricin A-chain and implications for the mechanism of action.* Proteins, 1991. 10(3): p. 270-8.
90. Smallshaw, J.E., et al., *Preclinical toxicity and efficacy testing of RiVax, a recombinant protein vaccine against ricin.* Vaccine, 2005. 23(39): p. 4775-84.
91. Smallshaw, J.E., J.A. Richardson, and E.S. Vitetta, *RiVax, a recombinant ricin subunit vaccine, protects mice against ricin delivered by gavage or aerosol.* Vaccine, 2007. 25(42): p. 7459-69.
92. Marconescu, P.S., et al., *Intradermal administration of RiVax protects mice from mucosal and systemic ricin intoxication.* Vaccine, 2010. 28(32): p. 5315-22.
93. Smallshaw, J.E. and E.S. Vitetta, *A lyophilized formulation of RiVax, a recombinant ricin subunit vaccine, retains immunogenicity.* Vaccine, 2010. 28(12): p. 2428-35.
94. Vitetta, E.S., et al., *A pilot clinical trial of a recombinant ricin vaccine in normal humans.* Proc Natl Acad Sci U S A, 2006. 103(7): p. 2268-73.
95. Vitetta, E.S., J.E. Smallshaw, and J. Schindler, *Pilot phase IB clinical trial of an alhydrogel-adsorbed recombinant ricin vaccine.* Clin Vaccine Immunol, 2012. 19(10): p. 1697-9.
96. Olson, M.A., et al., *Finding a new vaccine in the ricin protein fold.* Protein Eng Des Sel, 2004. 17(4): p. 391-7.
97. McHugh, C.A., et al., *Improved stability of a protein vaccine through elimination of a partially unfolded state.* Protein Sci, 2004. 13(10): p. 2736-43.

98. McLain, D.E., et al., *Protective effect of two recombinant ricin subunit vaccines in the New Zealand white rabbit subjected to a lethal aerosolized ricin challenge: survival, immunological response, and histopathological findings.* Toxicol Sci, 2012. 126(1): p. 72-83.
99. Compton, J.R., et al., *Introduction of a disulfide bond leads to stabilization and crystallization of a ricin immunogen.* Proteins, 2011. 79(4): p. 1048-60.
100. Hassett, K.J., et al., *Stabilization of a Recombinant Ricin Toxin A Subunit Vaccine through Lyophilization.* Eur J Pharm Biopharm, 2013.
101. O'Hara, J.M., R.N. Brey, 3rd, and N.J. Mantis, *Comparative efficacy of two leading candidate ricin toxin a subunit vaccines in mice.* Clin Vaccine Immunol, 2013. 20(6): p. 789-94.
102. Abboud, N., et al., *A requirement for FcgammaR in antibody-mediated bacterial toxin neutralization.* J Exp Med, 2010. 207(11): p. 2395-405.
103. Wahome, P.G., J.D. Robertus, and N.J. Mantis, *Small-molecule inhibitors of ricin and Shiga toxins.* Curr Top Microbiol Immunol, 2012. 357: p. 179-207.
104. Wahome, P.G. and N.J. Mantis, *High-throughput, cell-based screens to identify small-molecule inhibitors of ricin toxin and related category b ribosome inactivating proteins (RIPs).* Current protocols in toxicology / editorial board, Mahin D Maines (editor-in-chief) [et al], 2013. Chapter 2: p. Unit 2.23.
105. Stechmann, B., et al., *Inhibition of retrograde transport protects mice from lethal ricin challenge.* Cell, 2010. 141(2): p. 231-42.
106. Hu, W.G., et al., *Conformation-dependent high-affinity potent ricin-neutralizing monoclonal antibodies.* Biomed Res Int, 2013. 2013: p. 471346.
107. Neal, L.M., et al., *A monoclonal immunoglobulin G antibody directed against an immunodominant linear epitope on the ricin A chain confers systemic and mucosal immunity to ricin.* Infect Immun, 2010. 78(1): p. 552-61.
108. O'Hara, J.M., et al., *Plant-based expression of a partially humanized neutralizing monoclonal IgG directed against an immunodominant epitope on the ricin toxin A subunit.* Vaccine, 2012. 30(7): p. 1239-43.

Chapter 2 Effect of single-point mutations on the stability and immunogenicity of recombinant ricin A chain subunit vaccine

Introduction

In this study, we sought to determine whether we could make single residue mutations to RiVax that would improve antigen stability without adversely affecting vaccine efficacy. To test this, we first computationally designed and produced single point mutants of RiVax with differing thermostabilities. The immunogenicity and efficacy of two more thermostable (V18P, C171L) and two less thermostable (T13V, S89T) RTA point mutants was evaluated in a mouse model. After a prime-boost regimen, mice immunized with the more thermostable RTA point mutants (V18P, C171L) produced qualitatively higher levels of serum anti-RTA antibodies, while the less thermostable RTA mutants (T13V, S89T) had lower serum anti-RTA antibody levels than RiVax, suggesting that there is a correlation between immunogenicity and stability. After re-boosting mice that received the more stable antigens, C171L-immunized mice showed a significant increase in RTA-specific antibody titers when compared to RiVax-immunized mice. Much like after the initial boost, the V18P-immunized mice displayed a qualitative increase in anti-RTA IgG; however, the increase did not reach the level of statistical significance. Furthermore, mice immunized with the more thermostable RTA mutants (V18P, C171L) survived a $10LD_{50}$ systemic ricin challenge, indicating that the thermal stability of RiVax can be improved by single point mutations without the loss of vaccine efficacy.

Materials & Methods

Computational design of RiVax mutants. Two different computational approaches were employed to design the set of single-point RiVax mutants. The first method is similar in spirit to one recently published [1]. Briefly, RosettaBackrub [2, 3] was applied to the RiVax crystal structure (PDB ID: 3srp) to generate an ensemble of fifty near-native conformations. Each conformation was analyzed by RosettaHoles [4] to identify underpacked regions in the protein core. RosettaDesign [5, 6] was then used to identify small-to-large or isosteric mutations at these sites that were predicted to stabilize the protein by improving packing. As a final check for predicted stabilization, each mutation was placed in the crystal structure and the backrub motion was applied to a 6 Å radius around the mutated residue. Favorable mutations were those that produced lower total energy than RiVax. Mutations resulting from this approach were V81I, C171L, C171M, V204E, and V204I.

The second design approach was complementary to the structure-based approach, in that it selected mutations on the basis of sequence comparison. This methodology utilized a multi-layered filtering scheme to identify mutations predicted to have enhanced stability. First, the sequence alignment program BLAST [7] and structure alignment program VAST [8] were used to search the NCBI protein database and PDB 3D structure database to identify permitted mutations among other members of the ribosome-inactivating protein family (RIP). This list of mutation candidates was then refined using an amino acid substitution preference matrix [9]. An empirical scoring function developed to discriminate between hyperthermophilic and mesophilic proteins was then applied to further narrow the collection of possible mutations [9]. The predicted thermostability potentials of the remaining mutations were calculated, and only those deemed favorable were considered further [10]. Finally, proteins harboring these predicted stabilizing mutations were created and visually inspected in Molecular Operating Environment (MOE software suite, V. 2009.10, Chemical Computing Group). Energy minimization (force

field: CHARMM27; gradient: 0.01) of these mutants was performed and mutations with the most favorable energies were selected for production and characterization. Mutations resulting from this approach were T13V, V18P, S89T, C171V, Q182R, S228K, and V256L.

Protein production. The gene encoding the RiVax antigen was subcloned into a ligation independent cloning vector, pTBSG [11], to produce the protein in *E. coli* with an N-terminal 6x-histidine tag which can be cleaved by TEV protease. Forward and reverse primers for each mutant were designed using the QuickChange Primer Design Program. Plasmid DNA for each of the mutations was created using Stratagene's QuikChange Site-Directed Mutagenesis Kit (Agilent Technologies, Santa Clara, CA). Plasmid DNA were transformed into *E. coli* DH5α competent cells and positive clones were screened by PCR. Qiagen's QIAprep Spin Miniprep Kit (Qiagen, Valencia, CA) was used to prepare purified plasmid DNA and sequence confirmation was carried out at the Iowa State University Sequencing Facility.
Plasmids containing the cloned genes were transformed via heat shock into the expression host, *E. coli* BL21(DE3) pRARE. Cells were grown in a 1.5 L shaker flask at 37 °C until an optical density value of 0.6-0.8 was obtained. The temperature was then lowered to 15 °C and expression was induced by addition of 0.15 mM Isopropyl β-D-1-thiogalactopyranoside (IPTG). Expression was continued overnight at 15 °C. The cells were harvested by centrifugation, resuspended in a 50 mM Tris (pH 8) buffer containing 400 mM NaCl, then lysed by sonication. The lysed cells were centrifuged, the supernatant collected and filtered through a 0.45 μm syringe, and autoinjected using an ÄKTAXpress system onto a HisTrap HP 5 ml Ni^{2+} affinity column (GE Healthcare, Piscataway, NJ). The column was eluted using a 10-100% gradient of 50 mM Tris (pH 8), 400 mM NaCl, 500 mM imidazole. The eluate corresponding to the protein peak was collected in capillary loops and autoinjected onto a HiLoad 26/60 Superdex 75 pg size

exclusion column (GE Healthcare, Piscataway, NJ). A 20 mM histidine (pH 6) buffer containing 288 mM NaCl was used as the mobile phase for the size exclusion column. Eluate corresponding to the purified protein peak was pooled and concentration was checked before diluting 1:1 by volume with glycerol. RiVax variants were stored at -20 °C in this buffer until analysis.

For RiVax and its mutants used in animal studies, the His-tag was cleaved from the proteins using TEV. TEV was expressed as described previously [12], purified by Ni^{2+}-NTA agarose resin, and stored in 250 mM NaCl, 10 mM Tris-HCl, 50% glycerin, 5 mM DTT, 1 mM EDTA, and 0.05% Triton X-100, pH 8.0 at −20 °C until use. To cleave RiVax variants, TEV was added to the freshly purified proteins (0.5–2 mg/mL, in a solution containing 500 mM NaCl, 50 mM Tris-HCl, pH 8.0, and about 300 mM imidazole) at a ratio of 10:1 (Ricin:TEV, by mass). The reaction was dialyzed against 17 mM sodium phosphate (pH 6.0), 328 mM NaCl, and 15% glycerol at 4 °C overnight. The mutants without his-tag were purified from TEV and uncleaved proteins by passing the reaction mixture through a HisTrap HP 5 ml Ni^{2+} affinity column before a final dialysis into 20 mM histidine (pH 6) buffer containing 288 mM NaCl followed by a 1:1 dilution with glycerol. RiVax variants were stored at -20 °C in this buffer until the mouse studies.

Physical characterization. RiVax variants were dialyzed into 20 mM citrate phosphate buffer at pH values 5, 6, and 7 at 4 °C. The ionic strength of each buffer was adjusted to 0.15 by addition of sodium chloride. Slide-A-Lyzer dialysis cassettes (10K MWCO; Pierce, Rockford, IL) were used during dialysis. After dialysis, RiVax variants were concentrated to 0.5 mg/ml by centrifugation at 4,000 x *g* in an Amicon Ultra centrifugal filter unit and filtered through a 0.22 μm filter.

Differential scanning calorimetry was performed using a MicroCal VPDSC with autosampler (Piscataway, New Jersey). Thermograms of RiVax variants at pH values 5–7 were obtained from 10 to 90 °C using a scan rate of 60 °C/hr. The filled cells were equilibrated for 15 min at 10 °C before beginning each scan. Measurements were made in triplicate. Thermograms of the buffer alone were subtracted from each protein scan prior to analysis. T_m values were calculated and averaged using MicroCal Origin 7.0 software by applying a non-two state model to the individual thermograms.

Far-UV circular dichroism spectra were obtained with a Chirascan-plus circular dichroism spectrometer (Applied Photophysics Ltd., Leatherhead, U.K.) equipped with a 4 position Peltier-controlled cell holder. Spectra were collected in a 1 mm path length cuvette from 200–260 nm in 1 nm increments using a bandwidth of 1 nm and sampling time of 3 s at each wavelength while the temperature was controlled at 10 °C. A buffer blank was subtracted before subsequent manipulation. Three spectra were recorded for each variant, averaged, and smoothed by the Savitsky-Golay method using Pro-Data Chirascan 4.1 (Applied Photophysics Ltd.).

Intrinsic fluorescence measurements were obtained with a Photon Technology International Quantum Master fluorometer (Brunswick, New Jersey) equipped with a 4-position Peltier-controlled cell holder. Triplicate measurements were made using an excitation wavelength of 295 nm (> 95% tryptophan emission) at 10 °C. A 2 x 10 mm quartz cuvette was used and excitation of the proteins was performed along the shorter path length (2 mm). Emission spectra were collected from 305 to 400 nm with a step size of 1 nm. A buffer spectrum was subtracted before normalizing each protein spectrum to the intensity at peak emission.

Immunization. Groups of five BALB/c mice (Taconic Labs, Hudson, NY) approximately 7-9 weeks old were immunized subcutaneously at monthly intervals with 20 μg of each mutant adsorbed to 0.85 mg/ml Alhydrogel® (E.M. Sergeant, Clifton, NJ). Animals were housed under conventional, specific pathogen-free conditions and were treated in compliance with the Wadsworth Center's Institutional Animal Care and Use Committee (IACUC) guidelines. Antigens were dialyzed into 20 mM histidine (pH 6) buffer containing 144 mM NaCl and stored at 4 °C until used for immunization. The antigens were freshly adsorbed to Alhydrogel® 1 hour prior to each vaccination. Blood was collected via the tail vein approximately 10-14 days after each immunization. Finally, vaccinated mice were challenged intraperitoneally with 10 LD_{50}'s of ricin (2ug/mouse) on day 70 (two weeks after the 3rd immunization). Blood glucose levels were monitored as an indicator of ricin intoxication. Survival was also recorded.

ELISA and RTA peptide array. Total serum anti-RTA antibody concentration was determined by ELISA using mouse polyclonal anti-RTA antibody as a standard and native RTA as a capture antigen. The ELISAs were performed as described previously.[13, 14] Statistical analysis of RTA-specific IgG titers was carried out with GraphPad Prism 5 (Graphpad software). Unpaired t-tests with Welch's correction were used where indicated. The significance level threshold was set at $\alpha = 0.05$. Serum toxin neutralizing antibody (TNA) concentrations were normalized (100 ug/ml of anti-RTA serum antibody was serially diluted 1:2 into 10 ng/ml ricin), and assessed in a Vero cell ricin cytotoxicity assay. The assay was performed as described previously [13, 14]. TNA was defined as the concentration of serum anti-RTA antibody required to protect 50% of the Vero cells in triplicate wells.

RTA peptide arrays were performed on vaccine immune sera as previously described.[13, 14] Briefly, Nunc Maxisorb F96 microtiter plates (ThermoFisher Scientific, Pittsburgh, PA)

were coated overnight with individual peptides (1 µg/well or 3-5 µM) in PBS (pH 7.4) before being treated with vaccine immune sera. Horseradish peroxidase (HRP)-labeled goat anti-mouse IgG-specific polyclonal antibodies (SouthernBiotech, Birmingham, AL) were used as the secondary reagent. The ELISA plates were developed using the colorimetric detection substrate 3,3′,5,5′-tetramethylbenzidine (TMB; Kirkegaard & Perry Labs, Gaithersburg, MD) and were analyzed with a SpectroMax 250 spectrophotometer, with Softmax Pro 5.2 software (Molecular Devices, Sunnyvale, CA). The RTA peptide array used in this study consisted of twenty nine 18-mers, each overlapping its neighbors by 9 amino acids, collectively spanning the RTA sequence. The peptides were synthesized, unbound, in 96 individual tubes, in 96-well plate format, and were provided at 3 mg per peptide, on average at >75% purity (NeoBioSci). The peptides were solubilized in DMSO and aliquots were stored at -20 °C.

Results

Stability of RiVax single-point mutants. Between the two computational approaches employed, twelve single-point mutants of RiVax were designed, expressed, and purified. The 50 near-native RiVax structures created by RosettaBackrub are depicted in Figure 1A, whereas the result of processing one of the structures with RosettaHoles is illustrated in Figure 1B. A pictorial example of one of the cavity-filling mutations predicted to increase the stability of RiVax (a cysteine to luceine substitution) is shown in Figure 2. Figure 3 displays representative thermograms of all the RiVax mutants, as obtained by differential scanning calorimetry at pH values 5-7; Table 1 conveniently displays the calculated T_m values of the aforementioned mutants. The four mutants tested in mice were T13V, S89T, V18P, and C171L. Mutants V18P and C171L were 2-4 °C more stable than RiVax depending on solution pH. Conversely, mutants T13V and S89T were 2-4 °C less stable than RiVax depending on solution pH.

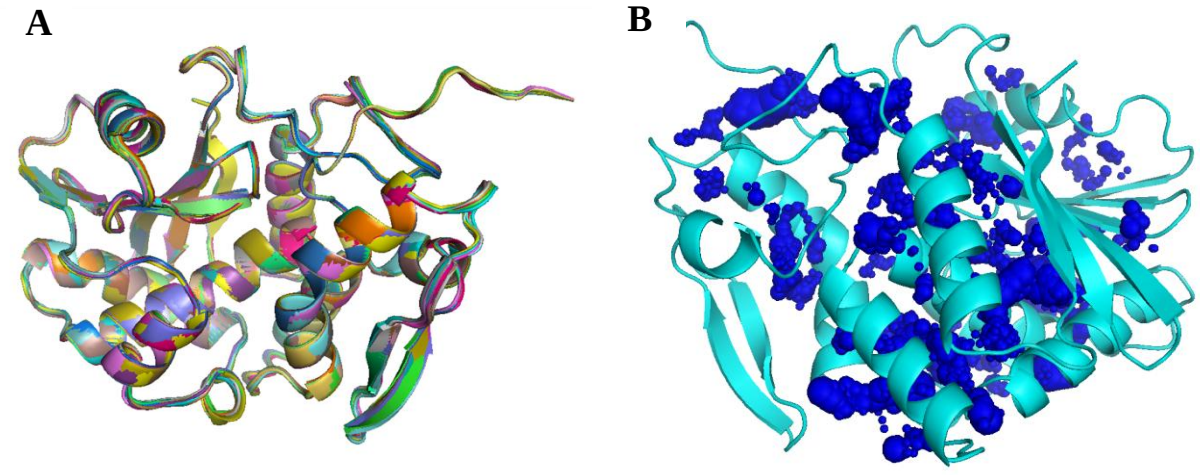

Figure 1. (A) Overlay of the 50 near-native structures created by applying Rosetta Backrub to the RiVax crystal structure. The orientation of the amino acid side chains of each backrubed structure are optimized to find the lowest energy achievable for that particular decoy. This optimization has the potential of opening additional cavities that were not present in the input structure. (B) Example of the application of RosettaHoles to one such structure. The blue spheres represent unoccupied space in the core of the molecule.

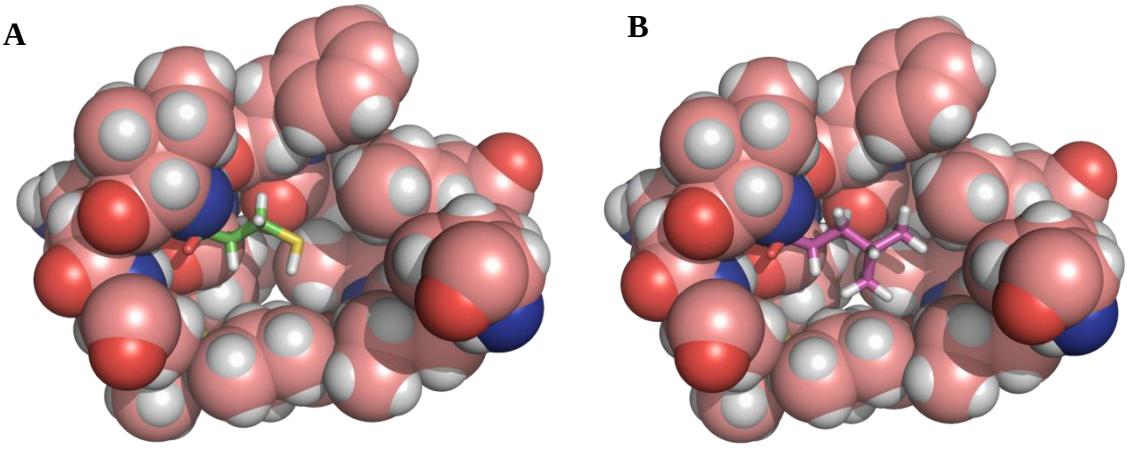

Figure 2. Example of cavity filling mutation. (A) Cysteine 171 in RiVax. (B) Leucine 171 in mutated RiVax.

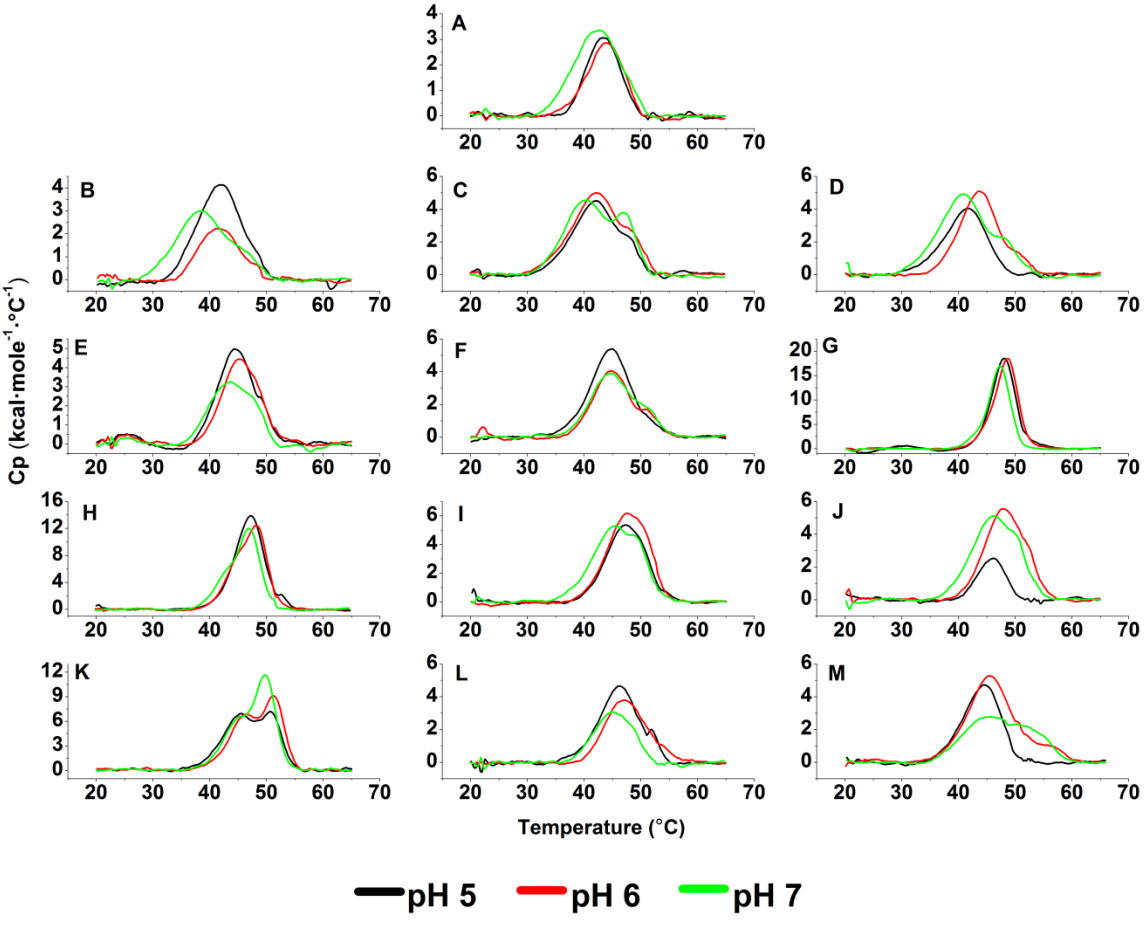

Figure 3. Differential scanning calorimetry thermograms as a function of pH for RiVax and RiVax point mutants. (A) RiVax, (B) T13V, (C) S89T, (D) V256L, (E) V81I, (F) V204I, (G) V18P, (H) C171M, (I) C171L, (J) C171V, (K) Q182R, (L) V204E, and (M) S228K.

Table 1. RiVax point mutations and their respective Tm values

Name	pH 5		pH 6		pH 7	
	$T_{m,1}$	$T_{m,2}$	$T_{m,1}$	$T_{m,2}$	$T_{m,1}$	$T_{m,2}$
RiVax*	43.5 ± 0.1	-[a]	44.3 ± 0.4	-	42.5 ± 0.6	48.4 ± 0.4
T13V*	41.8 ± 0.0	-	41.6 ± 0.2	48.5 ± 0.3	38.6 ± 0.3	45.8 ± 0.2
S89T*	41.5 ± 0.5	48.4 ± 0.4	42.3 ± 0.2	48.9 ± 0.1	40.2 ± 0.1	47.2 ± 0.1
V256L	41.7 ± 0.3	-	43.5 ± 0.2	51.0 ± 0.1	40.8 ± 0.1	48.5 ± 0.1
V81I	44.4 ± 0.1	48.9 ± 0.5	44.4 ± 0.2	48.1 ± 0.6	42.9 ± 0.1	47.6 ± 0.1
V204I	44.3 ± 0.5	-	44.8 ± 0.1	51.6 ± 0.3	44.6 ± 0.3	50.9 ± 0.2
V18P*	47.9 ± 0.0	-	46.5 ± 0.1	49.0 ± 0.0	44.3 ± 0.3	47.5 ± 0.0
C171L*	46.5 ± 0.1	50.1 ± 0.2	46.9 ± 0.1	50.7 ± 0.0	44.9 ± 0.1	49.5 ± 0.1
C171M	47.3 ± 0.2	52.7 ± 0.1	45.3 ± 0.0	48.6 ± 0.0	43.3 ± 0.2	47.3 ± 0.2
C171V	45.4 ± 0.2	-	47.5 ± 0.2	51.9 ± 0.1	45.7 ± 0.1	50.4 ± 0.0
Q182R	45.8 ± 0.3	50.9 ± 0.2	46.3 ± 0.3	51.6 ± 0.2	45.2 ± 0.1	50.0 ± 0.0
V204E	46.2 ± 0.0	51.8 ± 0.6	47.1 ± 0.0	53.6 ± 0.1	44.3 ± 0.0	48.2 ± 0.2
S228K	44.1 ± 0.2	-	45.4 ± 0.0	56.2 ± 0.4	45.9 ± 0.4	50.2 ± 0.2

Thermal transition midpoint (Tm) values of RiVax and RiVax point mutants as determined by differential scanning calorimetry. Thermograms were fit to a non-two state model in MicroCal Origin 7.0 to determine the Tm values. Error bars are standard deviation (n = 3). * Starred mutants were tested for immunogenicity in mice.

Immunogenicity and vaccine efficacy of select RiVax mutants. We sought to investigate the effect(s) of increased thermostability on the overall immunogenicity of RiVax. For these studies, we chose to test two RiVax mutants with increased thermostability (V18P, C171L) and, as controls, two mutants with decreased thermostability (T13V, S89T). These particular mutants were chosen, in part, because their fluorescence and CD spectra (pH 6; 10 °C) were super-

imposable with the spectra of RiVax, indicating that the introduction of these specific point mutations did not impact their overall tertiary or secondary structure (Fig. 4).

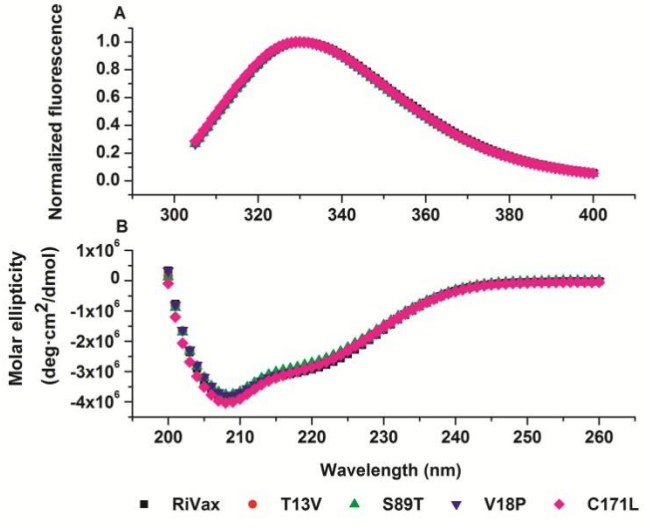

Figure 4. (A) Fluorescence and (B) far-UV circular dichroism spectra of RiVax and RiVax point mutants T13V, V18P, S89T and C171L at pH 6 and 10°C. The mutants' and RiVax antigen spectra are superimposable indicating overall tertiary and secondary structure has not been altered by the mutations.

To assess the immunogenicity of the four different mutants (T13V, S89T, V18P, C171L), the purified recombinant proteins (20 μg) were adsorbed to 0.85 mg/ml aluminum hydroxide (Alhydrogel®) and then administered in a prime-boost regimen to groups of mice by the subcutaneous (SC) route. RiVax (20 μg adsorbed to 0.85 mg/ml Alhydrogel®) was administered to five mice in the same manner to serve as the control to which the mutant antigens were compared. As a vehicle control, a group of five mice were immunized with Alhydrogel® only. Sera were collected from mice 10-14 days after the first booster immunizations and analyzed for total RTA-specific IgG, as well as toxin neutralizing antibody (TNA) titers.

Analysis of serum samples collected after the boost indicated that the V18P- and C171L-immunized mice had slightly higher anti-RTA serum IgG concentrations than did mice immunized with RiVax (Fig. 5A). Both these averages should be viewed with some caution as a single mouse in each group skewed the data due to an uncommonly high anti-RTA antibody concentration. Three of the five mice in the V18P group of animals had demonstrable TNA, as

did four of the five mice with C171L (Table 2). Although in neither case were these differences statistically different from the RiVax immunized mice, the results do at least suggest that more stable RiVax antigens are slightly better immunogens than RiVax itself after a single prime-boost regimen. The less thermostable mutant, T13V, was as effective as RiVax at stimulating anti-RTA antibodies and TNA, while mice immunized with the S89T mutant had RTA-specific titers that were comparable to RiVax immunized mice, but were devoid of TNA activity (Table 2; Fig. 5A).

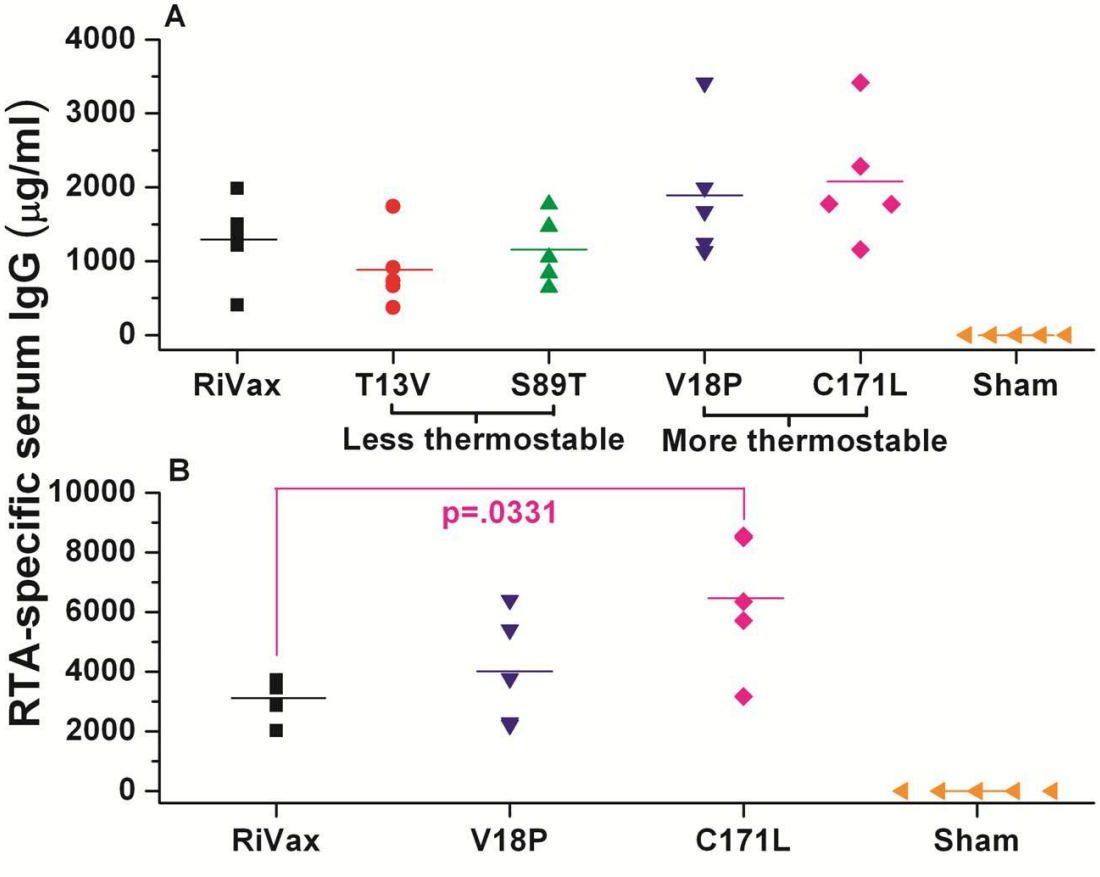

Figure 5. (A) (A) Serum anti-RTA antibody concentrations in mice after first boost with RiVax and four RiVax point mutants T13V, V18P, S89T and C171L. (B) Serum anti-RTA antibody concentrations in mice after a second boost with RiVax and the thermostable mutants, V18P and C171L. Each symbol represents a mouse (n = 5), while a line represents the average anti-RTA antibody concentration for that group. An unpaired t-test with Welch's correction was used to compare antibody titers after second boost in mice immunized with RiVax and C171L.

Table 2. TNA associated with the sera of mice immunized with RiVax and RiVax point mutants.

Mouse	RiVax[a]	T13V	V18P	S89T	C171L
1	-[b]	20	100	-	6
2	20	30	-	-	50
3	50	75	-	-	20
4	-	-	20	-	20
5	40	-	50	50	-

[a]TNA (IC_{50}, μg/ml) were determined using a Vero cell cytotoxicy assay, as described in the Materials and Methods; [b]-, indicates TNA were not detectable.

To confirm that TNA activity in the V18P- and C171L-immunized correlated with immunity, the RiVax-, V18P- and C171L-immunized mice were boosted a second time (i.e., once after the data presented in Fig. 5A) and then challenged 10 days later with 10 LD_{50}s of ricin. Upon re-boost, C171L-immunized mice showed a significant increase in RTA-specific antibody titers when compared to RiVax-immunized mice, whereas V18P mice showed a statistically indistinguishable increase (Fig. 5B). As shown in Figure 6A, mice immunized with RiVax, V18P or C171L survived ricin challenge, whereas the sham immunized animals succumbed to ricin intoxication within 72 h. In addition, blood glucose levels (a surrogate marker of ricin intoxication) of immunized mice remained normal ($\geq$70 mg/dL) in the days following ricin challenge (Fig. 6B), whereas levels in sham-immunized mice declined precipitously within 24 h. These data indicate that the individual point mutations associated with the mutants did not adversely affect the capacity of the antigens to elicit protective immunity.

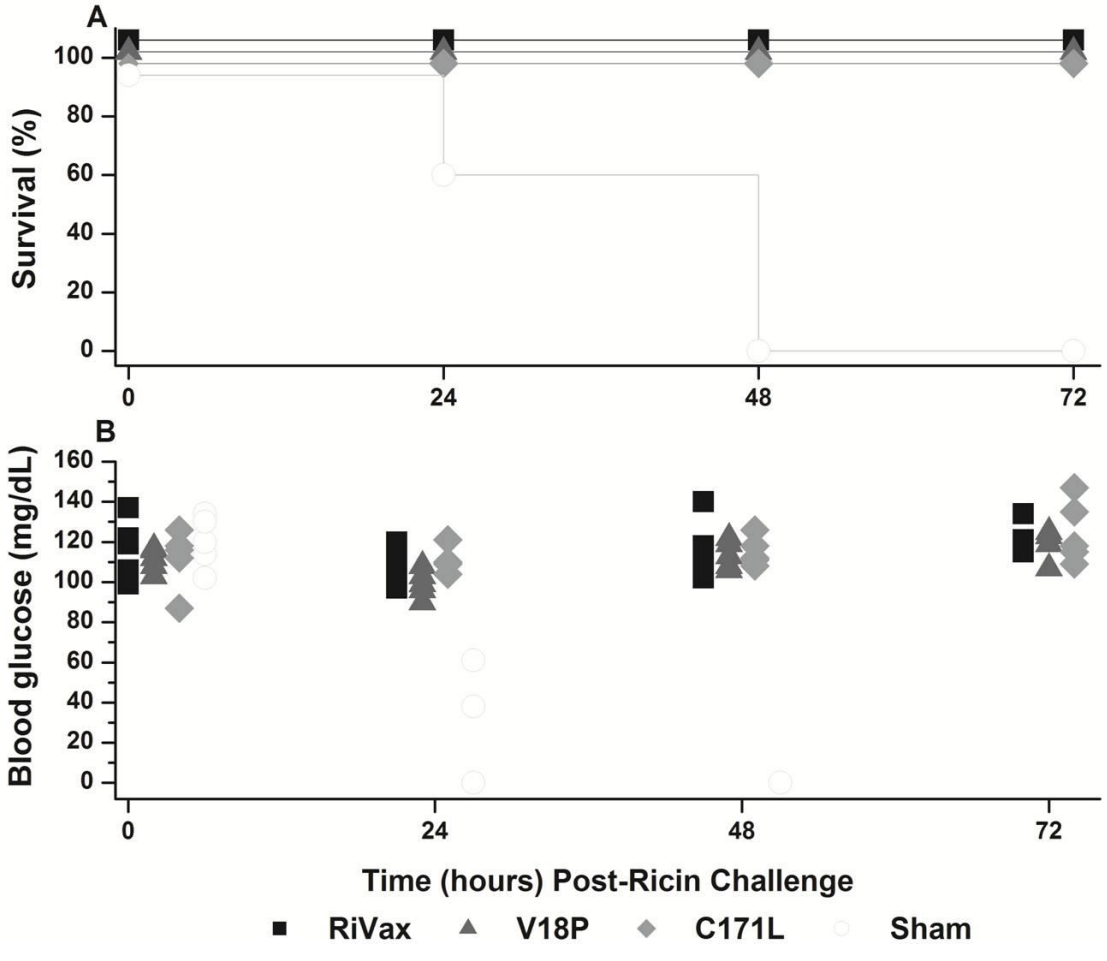

Figure 6. Protective immunity elicited by immunization with RiVax and two RiVax points (V18P and C171L) with enhanced thermostablility. (A) Survival after 10LD50 systemic ricin challenge and (B) Blood glucose as an indicator of ricin intoxication. Blood glucose readings below 40 mg/dL indicate ricin intoxication.

We previously reported that RiVax immune serum reacts with distinct immunodominant linear eptiopes on RTA, as determined by pepscan analysis.[13] To examine whether the V18P and C171L point mutations impact the anti-RTA antibody pepscan profile, serum samples from RiVax-, V18P- and C171L-immunized mice were applied to an array of overlapping 18-mer peptides spanning the length of RTA (Fig. 7A-C). Interestingly, the C171L immune sera gave rise to a collective reactivity profile that was similar to the profile exhibited by sera from RiVax immunized mice, with the exception that C171L immune sera demonstrated several fold more reactivity with peptide A11 (Fig. 7D). Peptide A11 corresponds to residues 91-108, a region of

RTA known to contain two overlapping immunodominant neutralizing B cell epitopes.[15] Antibody bias towards this region could possibly explain why sera from C171L-immunized mice had slightly higher TNA that RiVax immunized mice (Table 2). Pepscan analysis of sera from V18P-immunized mice revealed a reactivity profile that differed considerably from RiVax-immunized mice in that there was increased reactivity with peptide A11 (residues 91-108) as well as with peptides B02-B03 (residues 118-144) and B08-B09 (residues 172-198) (Fig. 7E). Reactivity with peptides containing residues 187-198 is interesting because this represents another immunodominant neutralizing B cell epitope on RTA.[13] Thus, pepscan analysis of sera from both V18P- and C171L-immunized mice reveals interesting differences from RiVax-immunized mice that could account for the increased neutralizing activity.

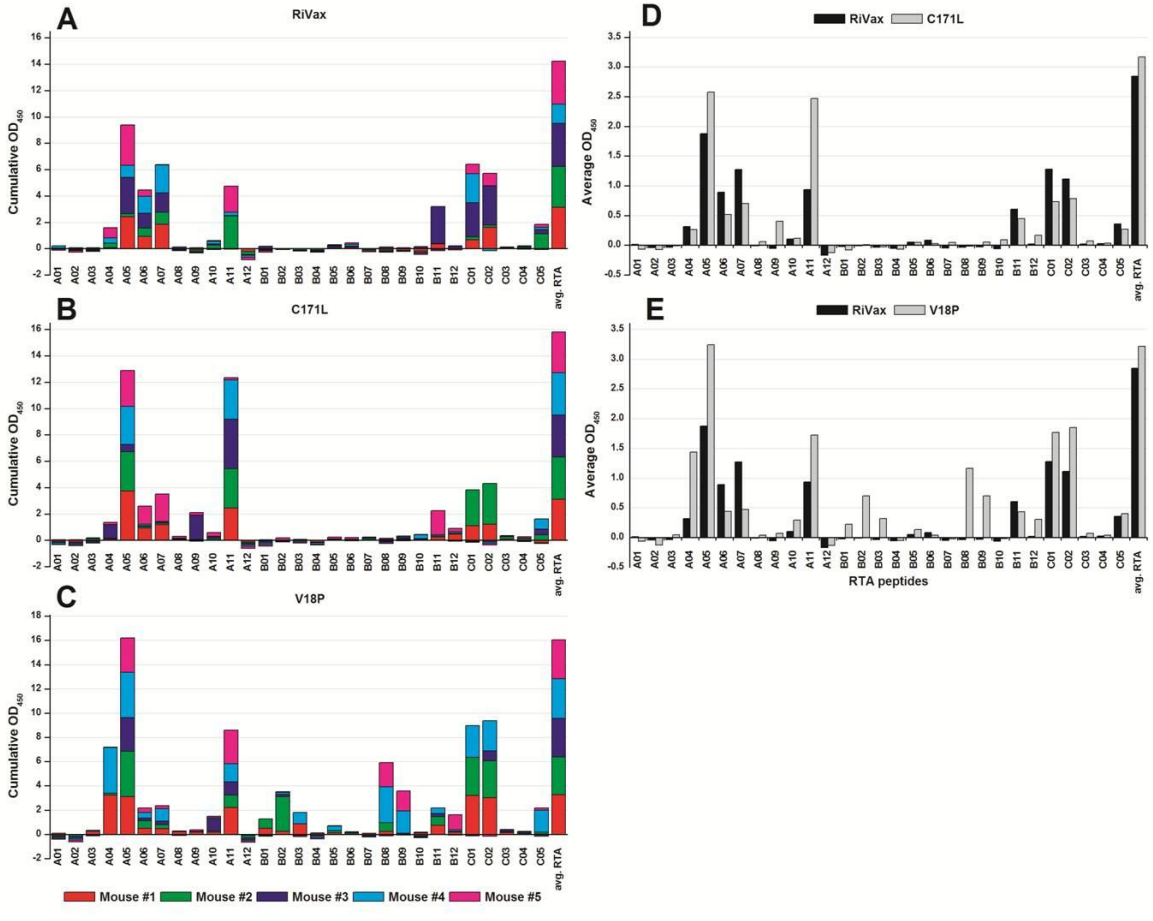

Figure 7. RTA Pepscan analysis of serum antibodies from mice immunized with RiVax and more thermostable RTA mutants V18P and C171L. Sera from mice immunized with RiVax, V18P or C171L RTA mutants were applied to 18-mer overlapping peptides representing the entire length of RTA. A = RiVax, B = C171L RTA, C = V18P RTA. (A–C) Cumulative OD450 on the y-axis represents the level of reactivity of antibodies in the sera with the RTA peptides on the x-axis. Each color represents the reactivity of antibodies in a single mouse serum with each peptide. (D) Comparison of RTA pepscan profi les of RiVax- and C171L-immunized mice. (E) Comparison of RTA pepscan profi les of RiVax- and V18P-immunized mice. The average OD450 on the y-axis represents the average reactivity of antibodies in RTA immune sera (n = 5 mice) with each RTA peptide on the x-axis.

Discussion

An interest in the design and development of highly thermostable and immunogenic biodefense vaccines has emerged in the decade following the intentional dispersal of anthrax spores in the US mail in 2001. A vaccine against ricin toxin is one such vaccine that has recently gained attention, since ricin is frequently cited as one of the most easily accessible of the Category A-C toxins.[16] In this study we investigated the impact of single point mutations that modulate the

thermal stability of an attenuated RTA-based antigen, RiVax, on the parameters associated with protective immunity. We first produced a series of RiVax point mutants and characterized the conformational stability of each by differential scanning calorimetry. We then compared the immunogenicity of four representative RiVax point mutants in a mouse model. The results of this study demonstrate that subtle changes can be made to the RiVax antigen, such as those enhancing thermostability, without loss of vaccine immunogenicity and efficacy. In fact, we found that two point mutations that rendered RiVax slightly more thermostable than RiVax were slightly more effective (though not statistically) at eliciting toxin-neutralizing antibodies in mice in a prime-boost regimen. While this observation needs to be addressed in more detail in future studies, it is intriguing to speculate that enhancing RiVax thermostability (and thus perhaps shelf life) may also render the antigen a more potent vaccine by stimulating higher anti-RTA antibody titers with fewer immunizations.

As indicated in Figure 3 and Table 1, we were successful in producing a collection of RiVax point mutants with a range of different thermal stability properties. The mutants used in the immunogenicity and efficacy studies (V18P, T13V, S89T, and C171L) displayed superimposable secondary and tertiary structures at pH 6 (the formulation pH) as determined by their fluorescence and far-UV circular dichroism spectra (Fig. 4). Because the RiVax vaccine in clinical trials is formulated by adsorbing the protein to an aluminum hydroxide adjuvant, we also adsorbed the mutant antigens to Alhydrogel® prior to administration. The four mutants and RiVax were adsorbed to the adjuvant to the extent of at least 85% (data not shown). All of the antigens tested elicited high levels of RTA-specific antibodies after a single prime-boost regimen (Figure 5A). Interestingly, as noted above, we observed that mutants with greater thermal stability trended towards enhanced total toxin-specific IgG titers after the second immunization; however, because some groups displayed considerable variability in RTA-specific titers, more

animals per experimental group will be needed to definitively address whether point mutations that increase the thermal stability of the RiVax antigen lead to an enhanced immune response after a single prime-boost regimen. Upon re-boost with the more thermostable antigens, a significant increase in RTA-specific IgG was observed in the C171L-immunized mice when compared to the RiVax-treated mice, whereas the mice immunized with the V18P mutant showed no statistical difference (Fig. 5B). Although we cannot formally exclude the possibility that the different mutants adsorbed to the aluminum salt adjuvant with different efficacy, we think it is unlikely considering that the site-specific changes were mostly, if not entirely, buried in the protein interior.

This shortcoming (of too few animals per group) also manifested itself in the TNA response to the different antigens as again a wide range in titers was observed (Table 2). While perhaps secondary in importance to survival against challenge, the elicitation of toxin neutralizing antibodies is vital to the success of the vaccine because these are the antibodies providing protection against the toxin. It should be pointed out that while all RiVax-immunized mice survived challenge with ricin toxin, not all mice displayed detectable TNA. We attribute the discordance between TNA and survival to the limited sensitivity of the Vero cell cytotoxicity assay used to quantify TNA and not the absence of serum TNA per se. We and others have shown, for example, in passive immunization studies that complete protection against ricin challenge can be achieved with very low serum Ab concentrations.[14, 17] While we cannot formally exclude other immune factors playing a role in toxin neutralization, there is no evidence to suggest that immunity to ricin involves more than antibodies. Hence, it is most likely that the pre-existing anti-RTA antibodies raised by immunization confer the needed defense.

Rational design of subunit vaccines by mutagenesis must take in account the fact that single-point mutations may have adverse effects on B (and T) cell epitopes and that generating

mutants with increased thermostability should not come at a cost of decreased vaccine efficacy. Therefore, point mutants are ideally designed with an available B cell epitope map of the antigen of interest. In the case of RiVax, partial B cell epitope maps from mice and humans have been generated.[16] When point mutations are introduced into known epitopes, it is critical to assess the impact of those mutations on vaccine efficacy. In this study, we found that mutations at position C171 consistently gave rise to proteins with increased thermostability as compared to RiVax (Figure 3 and Table 1). Residue C171 is situated within a stretch of amino acids known to constitute a dominant, continuous B cell epitope in humans.[18] For this reason RiVax proteins with mutations at this position are unlikely to be pursued further as a candidate vaccine for humans. Nonetheless, as proof of principle, we chose to examine the immunogenicity of the C171L mutant in mice. At least in mice, this single mutation did not negatively impact the immunogenicity of the antigen as compared to RiVax; in fact, the C171L point mutant was slightly more effective at eliciting RTA-specific antibody titers and TNA than was RiVax.

In conclusion, we have shown that enhancing the stability of the RiVax antigen using rational, computational design methods (mutants V18P and C171L) did not adversely affect the efficacy of the vaccine. A shortcoming of the current study is that we did not immunize with a thermolabile mutant that was also less immunogenic than RiVax. The absence of this experimental group prevents a more conclusive statement as to whether the qualitatively positive effects seen with the more thermostable vaccines was due to increased thermostability. With regard to the marginal stability associated with the RiVax antigen, these mutations with increased conformational stability may allow the vaccine to be stored for longer periods and/or at higher temperatures. While no real-time or accelerated degradation studies were performed on the antigens to address the possibility of longer storage or higher temperature storage, this question will be attended to in future work with the use of multi-point RiVax mutants.

Furthermore, antibody titers after the second immunization indicated that the more thermal stable RiVax mutants tended to elicit a qualitatively better immune response; this observation will be investigated in more detail through future studies utilizing more mice per group.

References

1. Borgo, B. and J.J. Havranek, *Automated selection of stabilizing mutations in designed and natural proteins.* Proc Natl Acad Sci U S A, 2012. **109**(5): p. 1494-9.
2. Friedland, G.D., et al., *A simple model of backbone flexibility improves modeling of side-chain conformational variability.* J Mol Biol, 2008. **380**(4): p. 757-74.
3. Smith, C.A. and T. Kortemme, *Backrub-like backbone simulation recapitulates natural protein conformational variability and improves mutant side-chain prediction.* J Mol Biol, 2008. **380**(4): p. 742-56.
4. Sheffler, W. and D. Baker, *RosettaHoles: rapid assessment of protein core packing for structure prediction, refinement, design, and validation.* Protein Sci, 2009. **18**(1): p. 229-39.
5. Das, R. and D. Baker, *Macromolecular modeling with rosetta.* Annu Rev Biochem, 2008. **77**: p. 363-82.
6. Korkegian, A., et al., *Computational thermostabilization of an enzyme.* Science, 2005. **308**(5723): p. 857-60.
7. Altschul, S.F., et al., *Gapped BLAST and PSI-BLAST: a new generation of protein database search programs.* Nucleic Acids Res, 1997. **25**(17): p. 3389-402.
8. Gibrat, J.F., T. Madej, and S.H. Bryant, *Surprising similarities in structure comparison.* Curr Opin Struct Biol, 1996. **6**(3): p. 377-85.
9. Li, Y., C.R. Middaugh, and J. Fang, *A novel scoring function for discriminating hyperthermophilic and mesophilic proteins with application to predicting relative thermostability of protein mutants.* BMC Bioinformatics, 2010. **11**: p. 62.
10. Li, Y., et al., *PROTS: a fragment based protein thermo-stability potential.* Proteins, 2012. **80**(1): p. 81-92.
11. Qin, H., et al., *Construction of a series of vectors for high throughput cloning and expression screening of membrane proteins from Mycobacterium tuberculosis.* BMC Biotechnol, 2008. **8**: p. 51.
12. Kapust, R.B. and D.S. Waugh, *Controlled intracellular processing of fusion proteins by TEV protease.* Protein Expr Purif, 2000. **19**(2): p. 312-8.
13. O'Hara, J.M., et al., *Folding domains within the ricin toxin A subunit as targets of protective antibodies.* Vaccine, 2010. **28**(43): p. 7035-46.
14. Neal, L.M., et al., *A monoclonal immunoglobulin G antibody directed against an immunodominant linear epitope on the ricin A chain confers systemic and mucosal immunity to ricin.* Infect Immun, 2010. **78**(1): p. 552-61.
15. Vance, D.J. and N.J. Mantis, *Resolution of two overlapping neutralizing B cell epitopes within a solvent exposed, immunodominant alpha-helix in ricin toxin's enzymatic subunit.* Toxicon, 2012. **60**(5): p. 874-7.
16. O'Hara, J.M., A. Yermakova, and N.J. Mantis, *Immunity to ricin: fundamental insights into toxin-antibody interactions.* Curr Top Microbiol Immunol, 2012. **357**: p. 209-41.

17. Lemley, P.V., P. Amanatides, and D.C. Wright, *Identification and characterization of a monoclonal antibody that neutralizes ricin toxicity in vitro and in vivo.* Hybridoma, 1994. **13**(5): p. 417-21.
18. Castelletti, D., et al., *A dominant linear B-cell epitope of ricin A-chain is the target of a neutralizing antibody response in Hodgkin's lymphoma patients treated with an anti-CD25 immunotoxin.* Clin Exp Immunol, 2004. **136**(2): p. 365-72.

Chapter 3 Mutants of a recombinant ricin A chain subunit vaccine antigen elicit a heightened neutralizing antibody response in mice

Introduction

In the present study, we have determined the thermal stabilities and immunogenicities of four mutant variants of the RiVax antigen. The four mutants examined were all considerably more stable than RiVax over a range of pH values, as assessed by differential scanning calorimetry and spectroscopic thermal unfolding curves. Mice were then immunized with one of the five antigens in a prime-boost-boost manner at two dose levels (20 and 5 μg). At the higher 20 μg dose, three of the four mutants were substantially more effective than RiVax at eliciting TNA after both the second and third immunizations. Irrespective of the antigen administered, mice that received this higher dose survived a challenge with a lethal amount of ricin and showed little drop in blood glucose levels (a surrogate marker of ricin toxicity) in the 72 hours post-challenge. At the lower 5 μg dose, only one mutant (V81I/C171L/V204I) showed a statistically significant increase in TNA compared to RiVax. Mice that received the lower dose were not challenged with ricin. Instead, serum was collected from each mouse and analyzed for reactivity with overlapping 18-mer peptides that span the length of RTA. Lending credence to our initial hypothesis, serum reactivity with the peptides was not significantly different between the mutants and RiVax suggesting that the increased neutralizing titers elicited by the triple mutant are due to preservation of the native RTA structure.

Materials & Methods

Protein production. Plasmids (with a tobacco etch virus (TEV)-cleavable, N-terminal hexa-histidine tag) containing the mutations of interest were created from the initial RiVax plasmid using Stratagene's QuikChange Site-Directed Mutagenesis Kit (Agilent Technologies, Santa Clara, CA). The DNA sequences were confirmed by the Iowa State University Sequencing Facility. RiVax mutants were expressed in E. coli BL21(DE3) pRARE upon induction by isopropyl β-D-1-thiogalactopyranoside (IPTG). The bacterial cells were lysed by sonication and the soluble protein was purified using Ni Sepharose affinity chromatography (HisTrap HP; GE Healthcare, Piscataway, NJ) followed by size exclusion chromatography (HiLoad 26/60 Superdex 75 pg; GE Healthcare). The histidine tag was cleaved off using TEV protease and the protein was again passed over the affinity column to remove his-tagged TEV and uncleaved protein. The cleaved and purified RiVax mutants were then passed through a polymyxin B agarose column (Sigma). Finally, the RiVax mutants were dialyzed into 20 mM histidine, 300 mM NaCl, diluted 1:1 with a 20% sucrose solution, and stored at -80 °C until further use. RiVax protein was kindly provided by Soligenix, Inc. SDS-PAGE indicated all proteins migrated predominantly as a single monomeric species (>95 %) at the appropriate molecular weight (data not shown).

Assessment of conformational stability. Proteins were dialyzed overnight at 4 °C into 20 mM citrate phosphate buffers (Sigma-Aldrich) (pH 5 – 8) at a constant ionic strength of 0.15; ionic strength was adjusted by the addition of sodium chloride (ThermoFisher Scientific). The proteins were assayed at a concentration of 0.1 mg/ml for the spectroscopic experiments and 0.5 mg/ml for the differential scanning calorimetry experiments. For the spectroscopic techniques, spectra were recorded every 2.5 °C from 10 – 75 °C using an equilibration time of 3 minutes at each

temperature. Transition melting temperatures at a given pH were calculated for each individual replicate before calculating the average and standard deviations.

Circular dichroism. Secondary structure stability was assessed by recording circular dichroism spectra from 195 – 260 nm in 1 nm increments on an Applied Photophysics Chirascan CD spectrometer (Leatherhead, Surrey, UK) equipped with a four-position, Peltier-controlled cell holder. Measurements were made in a 1 mm pathlength cuvette. The CD signal at 208 nm was plotted as a function of temperature.

Tryptophan fluorescence. Tertiary structure stability was assessed by monitoring tryptophan fluorescence emission from 310 – 400 nm in 1 nm increments in a Photon Technology International spectrofluorometer (Birmingham, NJ) equipped with a four-position, Peltier-controlled cell holder. An excitation wavelength of 295 nm was used to selectively excite the lone tryptophan residue. In addition, the aggregation behavior of the proteins was monitored by simultaneously collecting light scattering at the incident wavelength. Light scattering detection was accomplished in a second detector positioned 180° to the detector used to collect tryptophan fluorescence. Tryptophan peak position was determined using a center of spectral mass method and plotted as a function of temperature. This method artificially red-shifted the true peak position by ~ 15 nm. For each sample, the light scattering signal at 295 nm was normalized between 0 and 1 and plotted as a function of temperature.

Differential scanning calorimetry. Differential scanning calorimetry was performed with a MicroCal VP-Capillary DSC (GE Healthcare). The temperature was ramped from 15 – 75 °C using a ramp rate of 60 °C/hr. The sample cell was equilibrated for 15 min at the start

temperature before beginning data acquisition. Transition melting temperatures at a given pH were calculated for each individual replicate using a non-two-state equilibrium model in Origin 7.0 (OriginLab; Northampton, MA) before calculating the average and standard deviations. DSC was only performed on mutants at pH values 5 – 7 because pH 8 consistently resulted in lower thermal stability as assessed by the spectroscopic techniques.

Immunization. The proteins were first dialyzed from their frozen storage buffer into a buffer consisting of 10 mM histidine (pH 6) and 144 mM sodium chloride. Groups of eight BALB/c mice (female, 8 wk) from Taconic Labs (Hudson, NY) were immunized subcutaneously three times spaced three weeks apart with one of the four mutated RiVax proteins, RiVax, or vehicle control. The proteins (200 or 50 μg) were adsorbed to Alhydrogel® adjuvant (0.85 mg aluminum; E.M. Sergeant, Clifton, NJ) in a final volume of 1 ml for 1 hr prior to each immunization. Between immunizations, the non-adsorbed proteins were stored at 4 °C. The first experiment dosed each mouse with 20 μg/immunization, while a second study dosed each mouse with 5 μg/immunization. Animals were housed under conventional, specific pathogen-free conditions and were treated in compliance with the Wadsworth Center's Institutional Animal Care and Use Committee (IACUC) guidelines. Blood was collected by tail bleed from the mice ~7 days after the second and third injections to determine the concentration of toxin neutralizing antibodies in the sera. Four mice from each group were challenged with ricin intraperitoneally (2 μg/mouse) ten days after the third immunization. Blood glucose levels were used to monitor morbidity using ACCU-CHEK® Aviva System Blood Glucose Meter (Roche Diagnostics) and were recorded directly before ricin administration and every 24 hours following challenge. Mice were euthanized when blood glucose levels fell below 20 mg/dL.

ELISA and RTA peptide array. Nunc Maxisorb F96 microtiter plates (ThermoFisher Scientific) were coated with 1 μg/ml ricin overnight (for ELISA) or individual peptides in PBS (10 □g/ml) (for peptide array) and then treated with mouse sera obtained after the second or third immunization. Horseradish peroxidase (HRP)-labeled goat anti-human IgG (Invitrogen) was used as the secondary reagent and the plates were developed using 3,3',5,5' tetramethylbenzidine (Kirkegaard & Perry Labs, Gaithersburg, MD). The plates were analyzed with a SpectroMax 250 spectrophotometer with Softmax Pro 5.4.5 software (Molecular Devices, Sunnyvale, CA). The RTA peptide array consisted of 29 18-mer peptides, each overlapping its neighbors by 9 amino acids, which spans the RTA sequence (Neo-peptide, Cambridge, MA).
Statistical analysis was performed using an unpaired t-test comparing each mutant to RiVax.

Ricin cytotoxicity assay. To determine toxin-neutralizing antibody levels, Vero cells (5×10^4 cells/ml) were seeded into white 96-well plates (Corning Life Sciences, Corning, NY) (100 μl/well) and incubated at 37 °C overnight. Dilutions of mouse sera combined with ricin (10 μg/ml) were added to the cells and incubated for 2 hr. After washing, fresh DMEM was added and the cells were incubated for an additional 48 hr. Cell viability was assessed using CellTiter-GLO reagent (Promega, Madison, WI). Treatments were performed in triplicate. Cells treated with media only were used as a control with 100% viability. Statistical analysis of TNA was performed using an unpaired t-test comparing each mutant to RiVax.

Results

Antigen structure. The RiVax mutants were constructed by combining point mutations that were found to be stabilizing in a previous study [1]. That study used two independent and orthogonal computational approaches (one structure-based, the other sequence-based) to predict stabilizing

point mutations. The potential for further stability increases by combining stability-enhancing point mutations is well established [2-5]. Nine total mutants were produced and purified from E. coli; however, only four mutants were selected (on the basis of highest thermal stability) for immunogenicity studies in mice. These four variants are: V81I/V204I, V81I/C171L/V204I, V18P/C171V, and C171V/S228K. The mutations V81I, V204I, and C171L were designed (using the Rosetta software suite) to fill packing defects in the wild type structure by increasing the volume of sidechains adjacent to cavities. V18P, C171V, and S228K were selected on the basis of a scoring function that was shown to accurately predict the relative stability of proteins and their mutants [6]. Combining mutations from the first group gave mutants RA (V81I/V204I) and RB (V81I/C171L/V204I), while combining from the second group gave SA (V18P/C171V) and SB (C171V/S228K). With regard to the location of each mutation, V81 is immediately adjacent to active site residue Y80 in RTA. Its side chain does not form part of the active site cleft, but instead faces inward toward the protein core to contribute to extensive apolar contacts that maintain the interface between folding domains I and II. V204 is situated in α-helix G and helps maintain apolar contacts with helix F. C171 is within α-helix E, which also contributes to the interface between domains I and II. More importantly, this helix constitutes a known B cell epitope in humans [7] and mice [8, 9]. V18 is the N-terminal residue on α-helix A, which is spatially adjacent to a region that elicits both neutralizing [10] and non-neutralizing antibodies [9]. S228 is in RTA's C terminus and situated near the RTB interface in the holotoxin. Helix and domain nomenclature were adopted from that proposed by Katzin [11].

As stated in the introduction, it is well-established that immunization with RiVax elicits a protective response in mice. For that reason, we first sought to ensure that the mutants retained native-like RiVax structure. To accomplish this, we used circular dichroism and tryptophan fluorescence spectroscopy to assess the secondary and tertiary structures of RiVax and each of

the mutants. We found that the RiVax structure remains largely intact in the four mutants (Figure 1A/B). RB, SA, and SB displayed nearly identical CD spectra when compared to RiVax (Fig. 1A). This suggests the overall secondary structure content of the three mutants is virtually the same as that of RiVax. RA displayed a slight increase in molar ellipticity values in the 210 – 240 nm region compared to RiVax (Fig. 1A). Because this region contains various contributions from overlapping alpha helix and beta sheet bands, it is difficult to attribute this increase to a distinct structural change. With regard to tertiary structure, at each pH value there were subtle shifts in the fluorescence emission maximums (1 – 2 nm) of some of the mutants that suggest the environment surrounding the single tryptophan residue differs very slightly (more or less polar depending on the direction of the shift) than the tryptophan environment of RiVax (Fig. 1B). In summary, the tryptophan environment — and by inference the active site — is exceptionally similar between the mutants and RiVax.

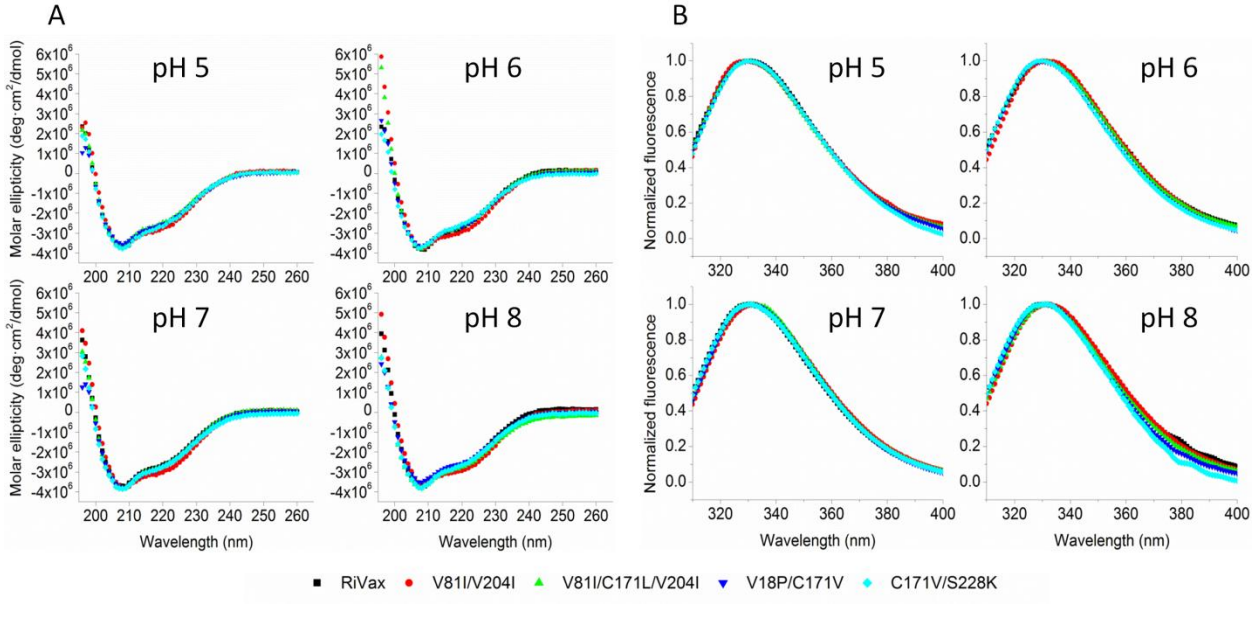

Figure 1. Circular dichroism (A) and fluorescence emission spectra (B) of RiVax and RiVax mutants as a function of pH at 10 °C.

Antigen stability. Having confirmed the mutants retained native-like RiVax structure, we next sought to determine the effect of the mutations on protein stability. We used a combination of CD, tryptophan fluorescence, Rayleigh light scattering, and DSC to examine the effect of increasing temperatures on the stability of each protein. Circular dichroism at 208 nm was followed to assess changes in helical content. Many of the neutralizing antibodies characterized to date interact with helical regions of RTA [9] so the stability of such regions may be important to the success of a ricin vaccine. We found that the mutations did not have a large impact on the thermal stability of regions of the proteins which are helical (Figure 2A and Table 1). SA and SB gain an average of 3 – 4 ºC of stability across the four pH values, RB gains ~ 2 ºC, and RA does not show any marked improvement in stability when compared to RiVax. Because the sole tryptophan residue is located in the active site, we next used tryptophan fluorescence spectroscopy to monitor the thermal stability of this region. At least one neutralizing antibody has been isolated that interacts directly with discontinuous residues in the active site cleft [8], although the nature of ricin's toxicity would suggest that there are likely to be others. Thus, keeping this region intact may also play an important role in eliciting protective immunity. Much like the CD results, we found the thermal stability of the active site environment was only moderately affected by the mutations (Figure 2B and Table 2). All proteins were prone to aggregation and precipitation as the temperature was increased as indicated by increases in light scattering (Figure 2C and Table 3) and by visual inspection upon completion of the experiment.

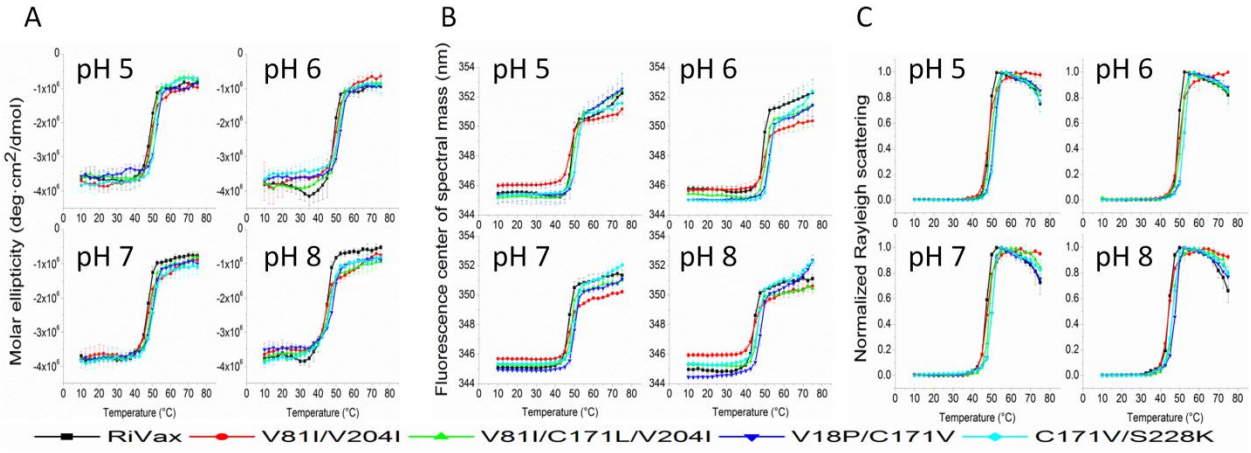

Figure 2. Circular dichroism at 208 nm (A), tryptophan fluorescence center of spectral mass peak position (B), and Rayleigh scattering at 295 nm (C) as a function of pH and temperature for RiVax and RiVax mutants. Error bars represent standard deviation (n = 3).

Table 1. Thermal transition temperatures (Tm) of RiVax and RiVax mutants as a function of pH as measured by circular dichroism at 208 nm.

Mutant	T_m			
	pH 5	pH 6	pH 7	pH 8
RiVax	48.3 ± 0.3	48.1 ± 1.1	46.8 ± 0.6	44.5 ± 0.3
V18P/C171V	51.9 ± 0.5	52.3 ± 0.7	49.9 ± 0.2	47.8 ± 0.2
C171L/V204I/V81I	50.0 ± 0.6	50.9 ± 0.3	48.9 ± 0.5	45.5 ± 0.2
V81I/V204I	49.0 ± 0.4	50.1 ± 0.2	47.2 ± 0.7	44.2 ± 0.1
C171V/S228K	51.4 ± 0.6	52.1 ± 0.9	49.9 ± 0.3	46.5 ± 0.7

Table 2. Thermal transition temperatures (T_m) of RiVax and RiVax mutants as a function of pH as measured by tryptophan fluorescence emission peak position.

Mutant	T_m			
	pH 5	pH 6	pH 7	pH 8
RiVax	48.5 ± 0.3	49.1 ± 0.4	46.9 ± 0.4	44.2 ± 0.2
V18P/C171V	51.5 ± 0.5	52.2 ± 0.8	49.9 ± 0.4	47.7 ± 0.4
C171L/V204I/V81I	49.6 ± 0.4	50.4 ± 0.4	48.3 ± 0.3	46.0 ± 0.1

V81I/V204I	47.7 ± 0.2	49.8 ± 0.3	47.9 ± 0.3	44.6 ± 0.3
C171V/S228K	51.3 ± 0.5	52.9 ± 0.4	50.1 ± 0.5	46.5 ± 0.9

Table 3. Thermal transition temperatures (T_m) of RiVax and RiVax mutants as a function of pH as measured by normalized Rayleigh light scattering at 295 nm.

Mutant	T_m			
	pH 5	pH 6	pH 7	pH 8
RiVax	48.3 ± 0.3	49.0 ± 0.3	46.9 ± 0.5	44.3 ± 0.1
V18P/C171V	51.1 ± 0.3	52.0 ± 0.5	49.8 ± 0.3	47.5 ± 0.3
C171L/V204I/V81I	49.7 ± 0.3	50.4 ± 0.5	48.6 ± 0.2	46.4 ± 0.1
V81I/V204I	48.3 ± 0.2	49.9 ± 0.2	47.7 ± 0.2	44.2 ± 0.2
C171V/S228K	51.4 ± 0.6	52.0 ± 0.4	49.9 ± 0.5	46.3 ± 0.7

Upon examination of the RiVax crystal structure [12], we noted that circular dichroism and tryptophan fluorescence may not provide a complete readout of protein structural changes (due to a dearth of helicity in the C-terminal region and the presence of only one tryptophan in the protein). We therefore used differential scanning calorimetry to report on structural changes throughout the protein. The stability measurements from differential scanning calorimetry suggest that full-length RTA-based proteins undergo two distinct changes in response to increasing temperature (Figure 3), the first of which was not detected by the spectroscopic techniques described in Figure 1. In RiVax, the midpoint of this first structural change occurs at fairly low temperature (~34 °C at pH 7). This suggests the region of RiVax responsible for this first event may be disordered under physiological conditions. The mutations exert most of their stabilizing effect on this first transition (Table 4), particularly when compared to changes observed for the second transition. For RA, SB, and RB, the first transition is raised such that it

collapses the two transitions into a broad peak with a leading shoulder. Deconvolution of the thermograms allowed an estimation of the contribution of each transition. Depending upon mutant and pH, the gain in stability of this first transition ranges from 7 – 15 °C (Table 4). The largest difference was seen in RB at pH 7, but SB was most consistent at raising the Tm of the first transition across all pH values. SA retains the general shape of the RiVax thermogram, but both transitions are shifted to higher temperature. Changes in the temperature at which the second DSC transition occurs are modestly correlated with the transition temperatures measured by the spectroscopic techniques ($r > 0.8$), and show stability increases ranging from 2 – 8 ºC, depending upon the protein variant and the pH (Table 4). All proteins showed a trend towards increasing stability (of both DSC transitions) at lower pH values.

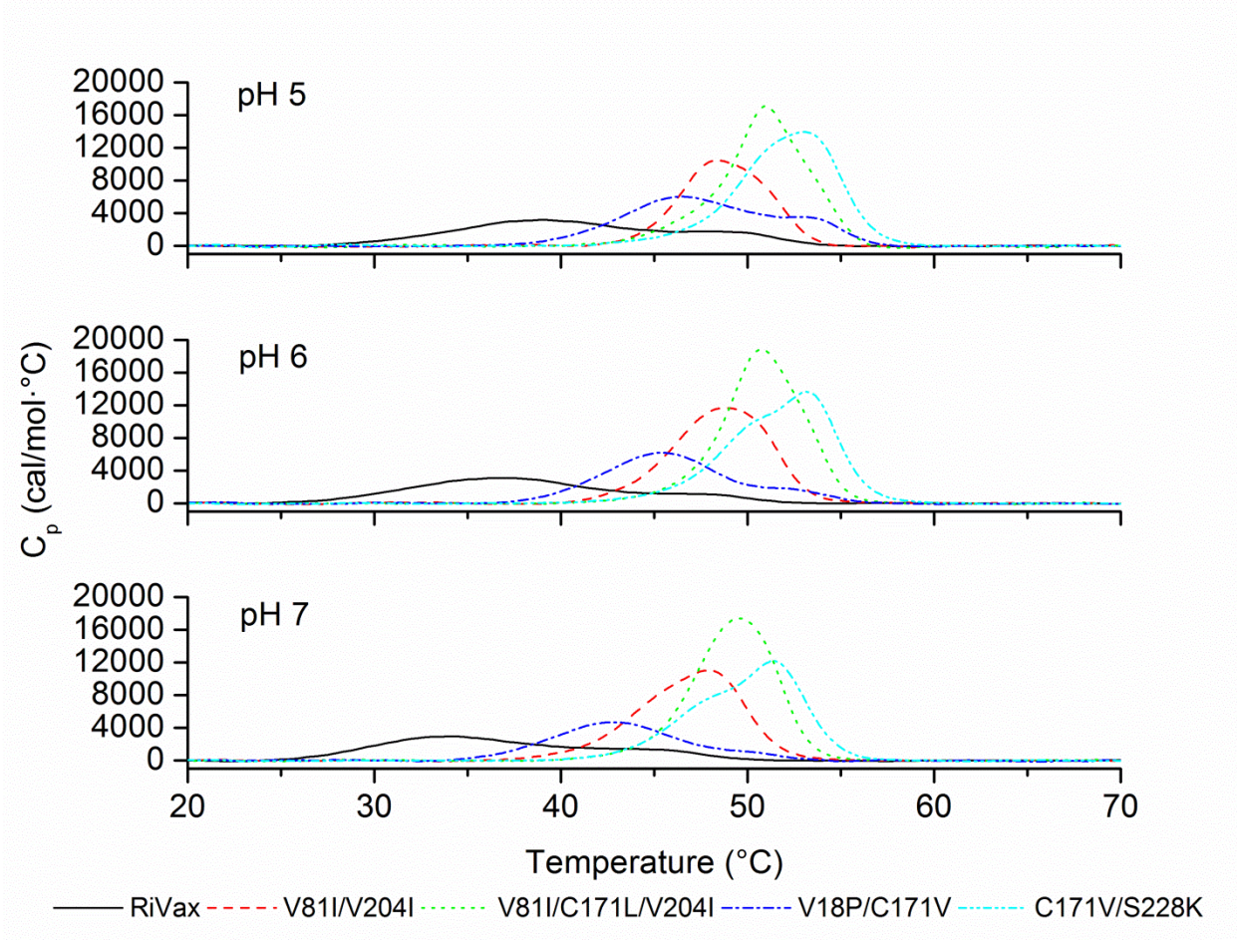

Figure 3. Representative differential scanning calorimetry thermograms of RiVax and RiVax mutants as a function of pH.

Table 4. Transition temperatures of RiVax and RiVax mutants as a function of pH as measured by differential scanning calorimetry (n=3).

Mutant	$T_{m,1}$			$T_{m,2}$		
	pH 5	pH 6	pH 7	pH 5	pH 6	pH 7
RiVax	39.1 ± 0.2	36.8 ± 0.3	34.0 ± 0.2	48.9 ± 0.1	47.4 ± 0	43.8 ± 0
V18P/C171V	46.7 ± 0.1	45.4 ± 0.1	42.8 ± 0.1	53.3 ± 0.2	52.7 ± 0	50.0 ± 0.1
C171L/V204I/V81I	46.6 ± 0.4	46.8 ± 0.2	49.4 ± 0	51.2 ± 0.2	51.0 ± 0	-
V81I/V204I	48.2 ± 0.1	47.9 ± 0.1	45.8 ± 0.1	50.9 ± 0	50.4 ± 0.1	48.5 ± 0
C171V/S228K	51.4 ± 0	50.7 ± 0	48.2 ± 0	53.8 ± 0	53.6 ± 0	51.7 ± 0

Vaccine immunogenicity and efficacy. We proceeded to test RiVax and the four RiVax mutants for immunogenicity in a mouse model at a dose of 20 μg protein and 85 μg aluminum adjuvant per immunization. Analysis of serum samples after the first boost indicated that mice immunized with the mutant antigens elicited a statistically significant increase in anti-ricin antibody titers when compared to those immunized with RiVax (Figure 4A, top panel). After the third immunization, however, only RA and SB elicited a statistically significant increase in anti-ricin antibody titers compared to RiVax (Figure 4A, bottom panel). Comparing anti-ricin antibody titers from the second to third immunizations, RiVax, RA, and SB displayed an increase in total antibody titers ($p < 0.05$, values not explicitly shown) whereas RB and SA did not shown any statistically significant differences (Figure 4A). SA, SB and RB all elicited statistically significant increases in toxin neutralizing antibodies compared to RiVax after both the second and third immunizations (Figure 4B). TNA raised by immunization with RA was statistically indistinguishable from that of RiVax (Figure 4B) after both booster immunizations. Mice receiving vehicle control did not display detectable TNA in their sera (data not shown). All antigens, with the exception of RA, displayed a statistically significant ($p < 0.05$, values not explicitly shown) boost in TNA from the second to third immunizations (Figure 4B).

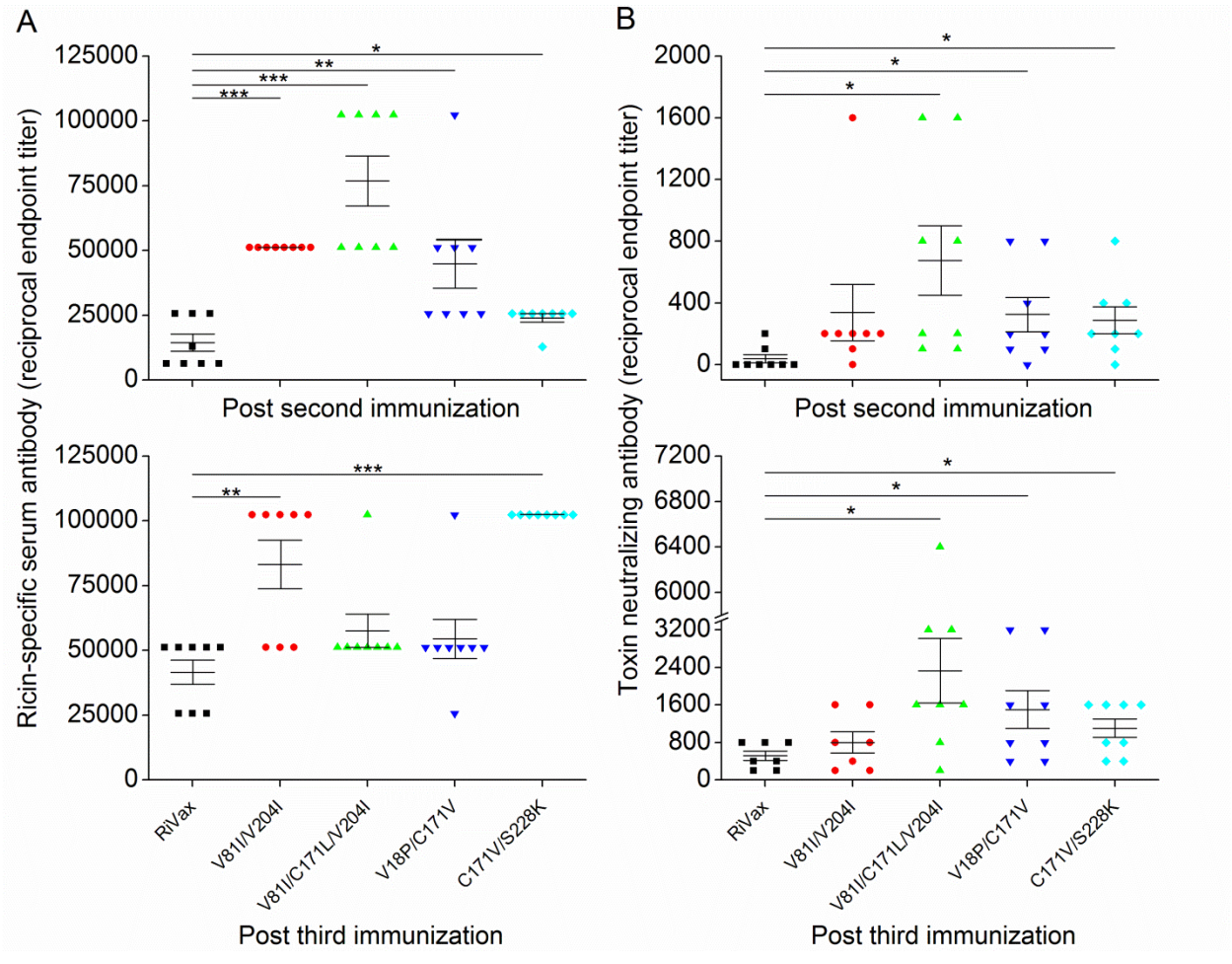

Figure 4. Ricin-specific serum antibody (A) and toxin-neutralizing antibody (B) of mice immunized with 20 µg of RiVax or a RiVax mutant. Error bars represent standard error (n = 8). An unpaired t-test was used to compare the differences in serum antibody levels and TNA.* $p < 0.05$, ** $p < .01$, and *** $p < 0.001$.

Due to our previous experience with RiVax mutants and expectation that all mice would survive challenge, only four mice in each group were subjected to a lethal dose of ricin toxin. As anticipated, all mice immunized with RiVax or a RiVax mutant survived the challenge while the mice immunized with vehicle control succumbed within 72 hours (Figure 5A). Additionally, the mutants showed little drop (<20 %) in blood glucose levels when compared to RiVax in the 72 hours after challenge (Figure 5B). Blood glucose levels are a surrogate marker of ricin intoxication.

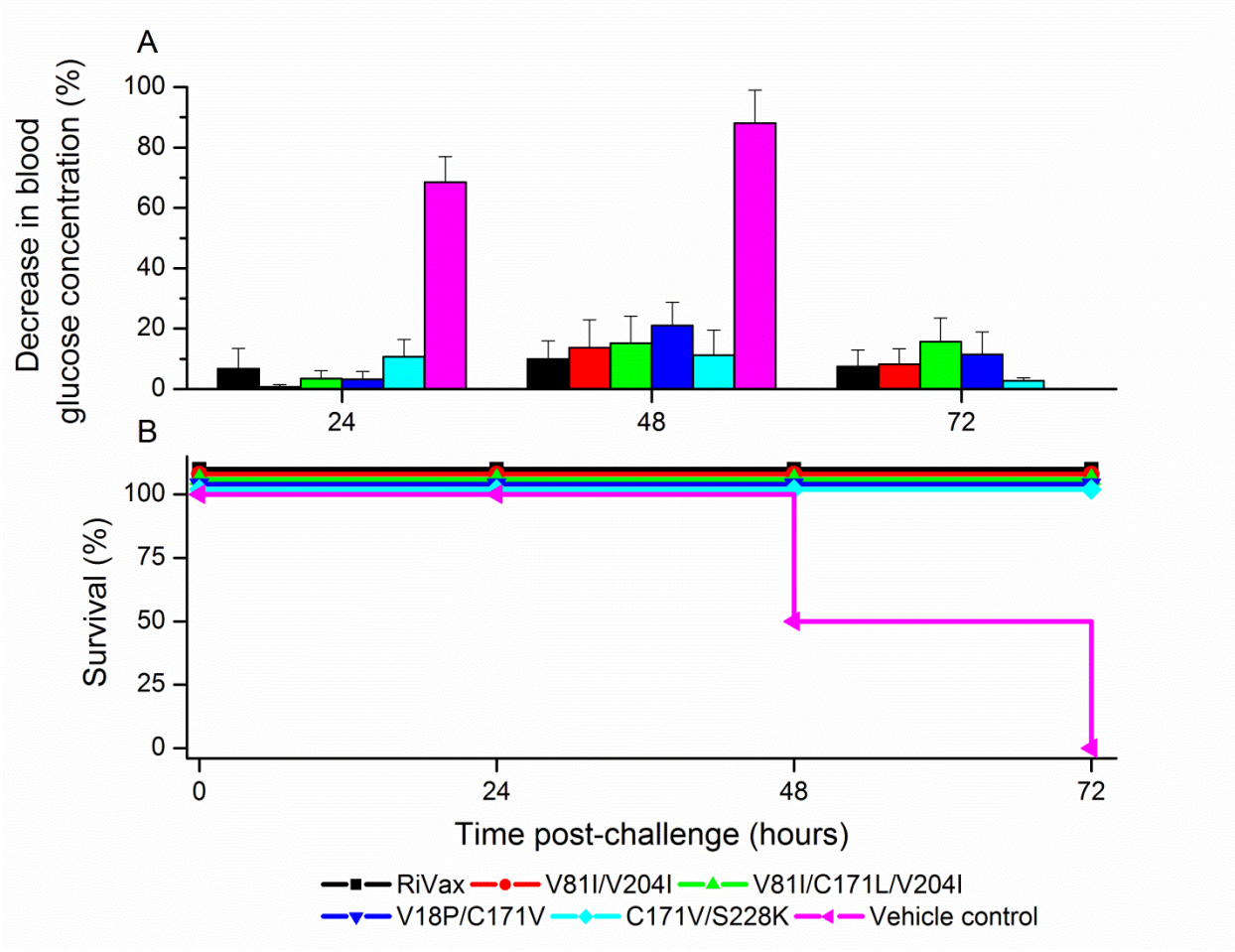

Figure 5. Decrease in blood glucose (A) and survival (B) of mice immunized with RiVax or a RiVax mutant as a function of time post-ricin challenge. Error bars represent standard error (n = 4).

Encouraged by the results with a high dose of antigen, we next sought to investigate the effects of a lower dose of antigen (5 μg) on the murine immune response. Analysis of serum samples after the first boost indicated that mice immunized with RB and SA elicited a statistically significant increase in anti-ricin antibody titers when compared to those immunized with RiVax (Figure 6A, top panel). After the third immunization, mutant elicitation of anti-ricin antibodies was indistinguishable from that of RiVax (Figure 6A, bottom panel). Comparing anti-ricin antibody titers from the second to third immunizations, only SA displayed an increase in total antibody titers over that of RiVax ($p < 0.05$). RB was the only mutant to elicit statistically significant increases in toxin neutralizing antibodies compared to RiVax after both the second

and third immunizations (Figure 6B). Again, mice receiving vehicle control did not display any detectable TNA in their sera (data not shown). RA and RB displayed a statistically significant ($p < 0.05$) boost in TNA from the second to third immunizations.

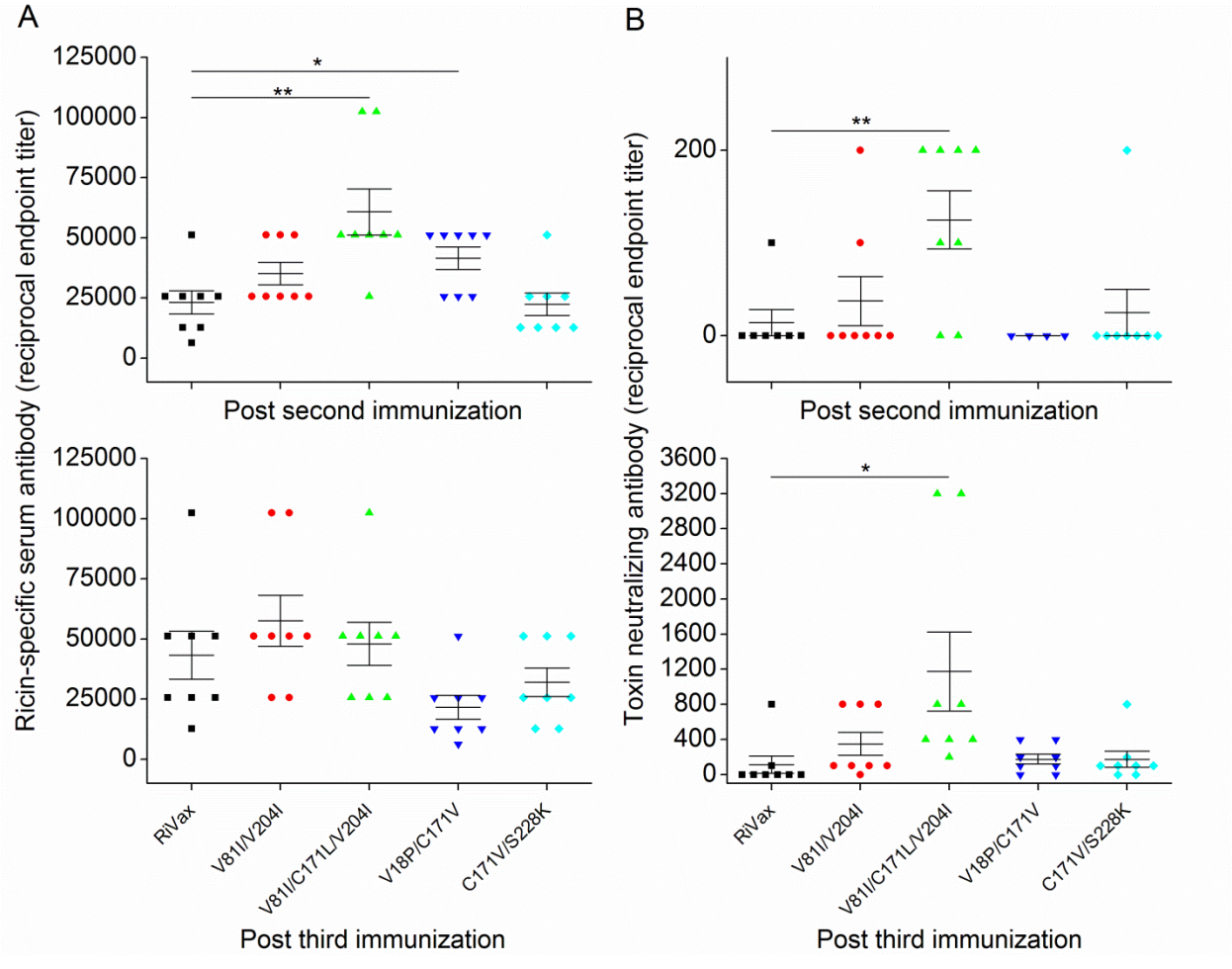

Figure 6. Ricin-specific serum antibody (A) and toxin neutralizing antibody (B) of mice immunized with 5 µg of RiVax or a RiVax mutant. Error bars represent standard error (n = 8). An unpaired t-test was used to compare the differences in serum antibody levels and TNA.* $p < 0.05$, and ** $p < .01$.

Instead of challenging the mice in the low dose study with a lethal amount of ricin toxin, we analyzed their serum for reactivity with overlapping 18-mer peptides that span the length of RTA. Because the reactivity profiles were so similar among the antigens, only the difference in the cumulative reactivity of sera drawn from mice immunized with RB and RiVax is shown (Figure 7A). Sera collected from mice immunized with RB showed heightened reactivity against

four peptides, namely A5, A7, A11, and B9. In contrast, sera collected from mice immunized with RiVax showed increased reactivity against a variety of peptides, most prominently B11 and C1. Peptides A5 and A11 consistently reacted with the serum of multiple mice. Thus, the average reactivity against theses peptides is plotted for all of the mutant antigens. The average serum reactivity against peptide A5 was only statistically different when comparing the sera isolated from RiVax-immunized mice to mice immunized with RA; the mutant performed better (Figure 7B, top panel). The average serum reactivity against peptide A11 was statistically indistinguishable between mice sera isolated from three of the four mutants and RiVax (Figure 7B, bottom pannel). RiVax, however, did outperform SA in terms of A11 reactivity.

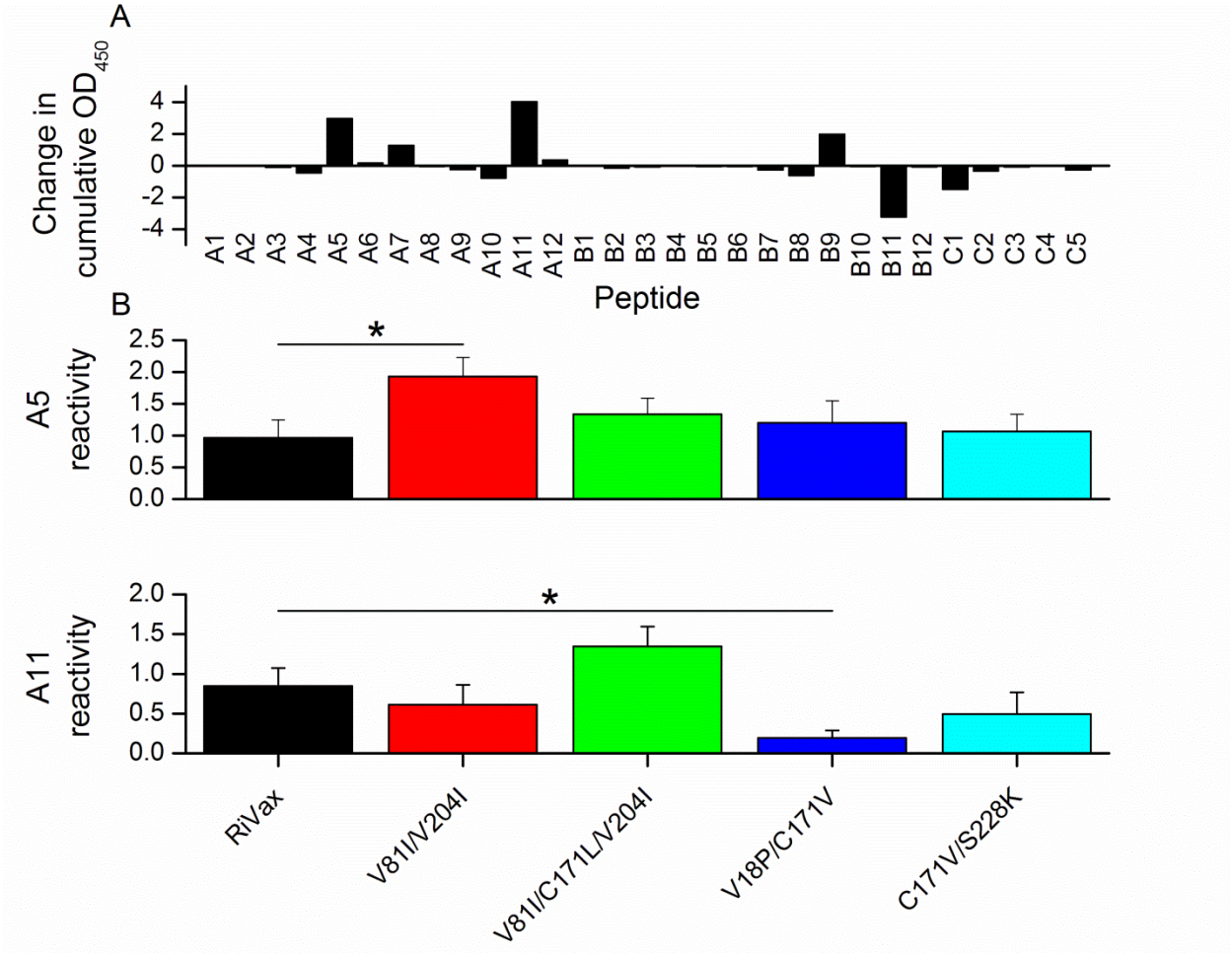

Figure 7. RTA pepscan analysis of sera from RiVax- and RiVax mutant-immunized mice. (A) Difference in the cumulative reactivities of sera taken from mice immunized with RiVax or mutant V81I/C171L/V204I. Positive values indicate that sera from triple mutant-immunized mice were more reactive against that peptide; negative deflections from the x-axis indicate sera from RiVax-immunized mice were more reactive.

(B) A5 and A11 peptide reactivity from mice immunized with RiVax or a RiVax mutant. Peptide A5 contains both a non-neutralizing epitope and the majority of a neutralizing epitope. Peptide A11 is a neutralizing epitope. Error bars represent standard error (n = 8). An unpaired t-test was used to compare the differences in peptide reactivity.* $p < 0.05$. OD450, optical density at 450 nm.

Discussion

With the recent events regarding government officials receiving ricin-tainted letters, there has been a renewed interest in the development of antidotes to treat or prevent ricin poisoning. The approval of a prophylactic ricin vaccine would be the ultimate safeguard in that it would presumably provide protection against the toxin for a number of years after an individual was vaccinated. RiVax is one of two leading ricin vaccine candidates; however, it suffers from a less than optimal elicitation of toxin neutralizing antibodies which we hypothesized was linked to its moderate conformational stability. In a previous study, we demonstrated that RiVax can retain its immunogenicity and protective capacity while accommodating single-point mutations designed to increase its thermal stability [1]. In this study, we have characterized the stabilities and immunogenicities of four new RiVax variants produced by combining previous mutations. The four mutants all increased the transition temperature of the earliest structural change of RiVax, as assessed by differential scanning calorimetry. Additionally, SA, SB, and RB all enhanced the toxin neutralizing antibody response in mice to a statistically significant level when delivered at a high dose. When immunized at a lower dose, only RB showed significant increases in TNA. The results show a positive relationship between antigen thermal stability and the elicitation of TNA for this antigen. An important caveat to this observation is that additional unanticipated differences between these variants may have also contributed to the improved immunological performance of some of the mutants. Furthermore, all studies were performed with a single lot of each protein; however, more comprehensive studies will be conducted in the future with additional lots.

As Figure 1 demonstrates, the mutants investigated in this paper retain the native structure of RiVax. We carried out a battery of biophysical techniques to determine what effect, if any, the set of mutations had on thermal stability. Results from spectroscopic measurements indicated that thermal stability was generally increased across the pH values examined compared to that of RiVax. The various spectroscopic techniques employed suggest the majority of mutants have been stabilized by 2-4 °C relative to RiVax, depending on the protein variant and the pH (Figure 2 and Tables 1 – 3).

In contrast to the spectroscopic techniques, differential scanning calorimetry detected an early transition in both RiVax and the four variants (Figure 3). The various mutations had a remarkable effect on this first transition, with stability increases ranging from 7 – 15 ºC relative to RiVax. The second transition in DSC correlated well with the changes in stability detected by the spectroscopic techniques. The seeming disagreement in which the spectroscopic techniques are not identifying a transition detected by DSC may be explained by the distinct folding domains of ricin A chain (and derivatives thereof) [11]. McHugh and colleagues speculated that ricin A chain (and presumably any full-length A chain variant) undergoes structural change at its C-terminal end prior to the unfolding of the remainder of the protein [13]. Our data appear to support their hypothesis. Interestingly, the final 48 residues (220 – 267) of RiVax contain only one small helix (a four residue 3_{10} helix) and the sole tryptophan residue resides at position 211. Taken together, these two facts may explain why the spectroscopic techniques did not detect this low temperature event: changes were not occurring in the parts of the protein monitored by circular dichroism at 208 nm and tryptophan fluorescence. By detecting changes in heat capacity, meanwhile, DSC would prove capable of reporting on conformational changes across the entire protein, including the C-terminal region. The precise nature of how the mutations introduced into RiVax might have affected the structural change of this C-terminal region is presently unclear.

We next sought to determine whether these antigen variants were more effective than RiVax at eliciting a robust murine immune response. All antigens elicited ample amounts of ricin-specific antibodies after the first 20 μg boost, with the antigen variants clearly outperforming RiVax (Figure 4A). Upon re-boost, however, only mice receiving the RA or SB variants retained their superiority over RiVax in eliciting ricin-specific antibodies. At the lower dose (5 μg), RA and RB elicited a stronger total anti-ricin antibody response; whereas after reboost, the variants were indistinguishable from RiVax itself.

While elicitation of total ricin-specific antibodies is important, the elicitation of toxin neutralizing antibodies is even more critical to the protection of animals exposed to a wide variety of pathogens. These toxin neutralizing antibodies are presumably the ones that give rise to protection upon exposure to the lethal toxin. They may also be the most useful indicators when developing vaccines against biothreat agents, since efficacy studies cannot be performed in humans. Thus, the approval of a ricin vaccine would be heavily reliant on neutralizing antibody titers raised in relevant animal models. We assessed the amount of TNA elicited by the different antigens using a commonly employed Vero cell cytotoxicity assay [1, 9, 14]. After the second and third immunizations of a 20 μg dose, RA, SA, and SB elicited an increase in TNA when compared to the response elicited by RiVax (Figure 4B). RB elicited the strongest TNA response after both the second and third immunizations; furthermore, the mutants demonstrated a more rapid TNA response compared to RiVax with substantial elicitation of neutralizing antibodies after just the second immunization. In fact, the TNA elicited by RB after the second immunization was (on average) higher than that elicited by RiVax after the third immunization; this difference, however, did not reach a statistically significant level. At a 5 μg dose, only mice immunized with RB displayed a heightened TNA response after either of the boosts (Figure 6B). The ricin vaccine antigens tested here are not the first to display an increased TNA response

when compared to RiVax. In a head-to-head comparison, RVEc also consistently displayed a more robust TNA response than RiVax [14].

Nonetheless, the impressive gains observed in terms of a neutralizing antibody response would be inconsequential if they did not translate into protection from lethal ricin challenge. Not surprisingly, the mice in the high dose group that received antigen did not display any serious signs of ricin intoxication after challenge with a 10LD50 dose of ricin toxin, while mice that received vehicle control exhibited a precipitous drop in blood glucose levels (Figure 5A). Accordingly, all mice that received antigen survived the toxic challenge, whereas mice that received vehicle control died within 72 hours (Figure 5B). Mice from the low dose group were not challenged. Instead, serum was isolated from the blood of each mouse and subjected to pepscan analysis. Sera from mice immunized with RB showed increased reactivity against peptides A5, A7, A11, and B9 (Figure 7A). Interestingly, peptides A5, A11, and B9 all contain residues in putative neutralizing antibody epitopes, although A5 contains a known non-neutralizing epitope as well [9, 10]. To date, no monoclonal antibodies have been isolated that bind to an epitope in the region that peptide A7 spans. Peptides A5 and A11 showed reactivity against serum isolated from multiple mice in all of the antigen groups; however, the increase in triple mutant sera reactivity against A7 and B9 was solely attributed to a single mouse's serum (data not shown). When the average sera reactivity against peptide A5 was compared among the mutants, a statistically significant difference was only observed when comparing RiVax to RA (Figure 7B, top panel); this difference implies that RA is better at eliciting antibodies to this particular region. It is unknown whether this enhanced reactivity can be primarily attributed to neutralizing or non-neutralizing antibodies. Similarly, when the average sera reactivity against peptide A11 was compared amongst the mutants, a statistically significant difference was only observed when comparing RiVax to SA (Figure 7B, bottom panel). Peptide C1, which reacted

better with sera isolated from RiVax-immunized mice than triple mutant-immunized mice, contains some of the amino acids in a known non-neutralizing epitope [9] so less reactivity against this region is beneficial in the development of a ricin vaccine. Peptide B11 also reacted better with sera isolated from RiVax-immunized mice. To date, no monoclonal antibodies have been isolated that bind to an epitope in the region spanned by peptide B11.

The relationship between antigen stability and immunogenicity, if one exists, remains an enigma. Some reports provide evidence that increased antigen stability has a positive effect on immunogenicity [15, 16]. Others have found quite the opposite effect [17, 18]. We propose that RiVax's weak elicitation of toxin neutralizing antibodies can be attributed at least partially to structural variation in the C-terminal region, to which we attribute the first peak in the DSC thermograms. While many of the ricin-neutralizing antibodies directed against the A chain have been identified using peptide arrays of RTA (and probably aren't strictly dependent on native secondary or tertiary structure), the majority of the neutralizing RTA-specific antibodies elicited during immunization (~90 %) are directed towards conformational epitopes [9]. By stabilizing this domain in the four mutant RiVax antigens, we propose that the immune response is steered away from non-native RiVax conformations that would not be present in the native toxin. Instead, by keeping the C-terminal domain more native-like, the immune response might direct itself to the core region of the A chain which gives rise to the majority of neutralizing antibodies [14]. Alternatively, antibodies might be engaging previously unrecognized conformational epitopes in the C-terminal domain, and thus elicit a greater quantity of conformationally-sensitive toxin neutralizing antibodies. Pepscan analysis seems to support this suggestion, as reactivity against known neutralizing regions is not significantly different between RiVax and the mutants (Figure 7). As it relates to RA at the 20 μg dose, the positive effects associated with the gain in stability may have been counteracted by the change in secondary structure detected

by circular dichroism (Figure 1A). In addition, the fact that SA and SB are not better than RiVax at eliciting TNA at a low dose may be attributed to the low dose accentuating unaccounted-for features. It is interesting to note that besides being more stable than RiVax, the three mutants that elicited the best neutralizing response all contain a mutation to cysteine 171. Peptides containing this cysteine residue are known to be bound with high affinity by ricin neutralizing antibodies isolated from humans [7] and mice [8, 9]. It is unclear at this time if the more hydrophobic mutations (V and L) confer additional benefits to the increased neutralizing antibody response through a mechanism unrelated to antigen stability — for example, by better engaging the various receptors (T and/or B cell) or MHC molecules of the mouse immune system — or if this was merely coincidence.

In conclusion, we have designed mutants of the RiVax antigen that elicit a robust toxin-neutralizing antibody response in mice. Our hypothesis at the outset of this study was that RiVax antigens with enhanced stability would give rise to a more potent neutralizing response, because they would maintain a more native-like structure. This hypothesis is supported by that data presented above, though there may be other additional factors that played a role in making these variants better antigens. Because of its superiority over RiVax and the other mutants at a low immunization dose, RB warrants further evaluation and development as a ricin vaccine antigen. This RiVax variant appears to have solved the most significant problem encountered with the development of RiVax, namely the rate and quantity at which toxin-neutralizing antibodies are elicited.

References

1. Thomas, J.C., et al., *Effect of single-point mutations on the stability and immunogenicity of a recombinant ricin A chain subunit vaccine antigen.* Hum Vaccin Immunother, 2013. **9**(4): p. 740-48.

2. Wells, J.A., *Additivity of mutational effects in proteins.* Biochemistry, 1990. **29**(37): p. 8509-17.
3. Zhang, X.J., et al., *Enhancement of protein stability by the combination of point mutations in T4 lysozyme is additive.* Protein engineering, 1995. **8**(10): p. 1017-22.
4. Declerck, N., et al., *Hyperthermostabilization of Bacillus licheniformis alpha-amylase and modulation of its stability over a 50 degrees C temperature range.* Protein Eng, 2003. **16**(4): p. 287-93.
5. Korkegian, A., et al., *Computational thermostabilization of an enzyme.* Science, 2005. **308**(5723): p. 857-60.
6. Li, Y., C.R. Middaugh, and J. Fang, *A novel scoring function for discriminating hyperthermophilic and mesophilic proteins with application to predicting relative thermostability of protein mutants.* BMC Bioinformatics, 2010. **11**: p. 62.
7. Castelletti, D., et al., *A dominant linear B-cell epitope of ricin A-chain is the target of a neutralizing antibody response in Hodgkin's lymphoma patients treated with an anti-CD25 immunotoxin.* Clin Exp Immunol, 2004. **136**(2): p. 365-72.
8. Maddaloni, M., et al., *Immunological characteristics associated with the protective efficacy of antibodies to ricin.* J Immunol, 2004. **172**(10): p. 6221-8.
9. O'Hara, J.M., et al., *Folding domains within the ricin toxin A subunit as targets of protective antibodies.* Vaccine, 2010. **28**(43): p. 7035-46.
10. O'Hara, J.M. and N.J. Mantis, *Neutralizing monoclonal antibodies against ricin's enzymatic subunit interfere with protein disulfide isomerase-mediated reduction of ricin holotoxin in vitro.* J Immunol Methods, 2013.
11. Katzin, B.J., E.J. Collins, and J.D. Robertus, *Structure of ricin A-chain at 2.5 A.* Proteins, 1991. **10**(3): p. 251-9.
12. Legler, P.M., et al., *Structure of RiVax: a recombinant ricin vaccine.* Acta Crystallogr D Biol Crystallogr, 2011. **67**(Pt 9): p. 826-30.
13. McHugh, C.A., et al., *Improved stability of a protein vaccine through elimination of a partially unfolded state.* Protein Sci, 2004. **13**(10): p. 2736-43.
14. O'Hara, J.M., R.N. Brey, 3rd, and N.J. Mantis, *Comparative efficacy of two leading candidate ricin toxin a subunit vaccines in mice.* Clin Vaccine Immunol, 2013. **20**(6): p. 789-94.
15. Koide, S., et al., *Structure-based design of a second-generation Lyme disease vaccine based on a C-terminal fragment of Borrelia burgdorferi OspA.* J Mol Biol, 2005. **350**(2): p. 290-9.
16. Delamarre, L., et al., *Enhancing immunogenicity by limiting susceptibility to lysosomal proteolysis.* The Journal of experimental medicine, 2006. **203**(9): p. 2049-55.
17. Ohkuri, T., et al., *A protein's conformational stability is an immunologically dominant factor: evidence that free-energy barriers for protein unfolding limit the immunogenicity of foreign proteins.* J Immunol, 2010. **185**(7): p. 4199-205.
18. Liu, W., et al., *A recombinant immunotoxin engineered for increased stability by adding a disulfide bond has decreased immunogenicity.* Protein Eng Des Sel, 2012. **25**(1): p. 1-6.

Chapter 4 Conclusions and future directions

Conclusions

Due to the recent events involving ricin-contaminated letters, the Department of Defense's interest in a prophylactic vaccine heightened resulting in a request for information "for a pre-exposure prophylaxis ricin vaccine that provides balanced onset and duration of protection for administration to healthy individuals." Because of its extreme toxicity and relative ease of acquisition, it is a prominent threat to be used as a bioterrorism agent [1]. Thus, the development and approval of a vaccine against ricin exposure is of great importance [2]. Neither of the current ricin vaccine antigen candidates, RiVax and RVEc, elicits a potent neutralizing antibody response in animal models [3-6]. Quite surprisingly, RiVax, the more advanced of the two, is the worse of the two in eliciting a strong neutralizing antibody response [7]. RiVax, however, has already completed two Phase I trials in healthy adults which determined the vaccine was safe and moderately immunogenic [8, 9]; results have yet to be disclosed for the initial Phase I trial administering RVEc to healthy adults.

This dissertation sought to design an improved antigen candidate based on RiVax. To facilitate this, two complimentary computational design approaches were employed to create antigens that were predicted to have increased stability. Single-point mutants were created, expressed in *E. coli*, and purified by chromatographic methods. In all, eleven single-point RiVax mutants were characterized across a range of pH values by differential scanning calorimetry, near- and far-UV circular dichroism, optical density at 350 nm, and tryptophan fluorescence spectroscopy. This characterization was performed on mutants the retained the TEV-cleavable hexahistidine tag. As assessed by differential scanning calorimetry, the conformational

stabilities of the designed mutants ranged from 4°C less stable to 4.5°C more stable than RiVax, depending on solution pH. Two more thermostable (V18P, C171L) and two less thermostable (T13V, S89T) mutants that displayed native-like secondary and tertiary structures (as determined by circular dichroism and fluorescence spectral analysis, respectively) were tested for their capacity to elicit RTA-specific antibodies and toxin-neutralizing activity. Following a prime-boost regimen, we found qualitative differences with respect to specific antibody titers and toxin neutralizing antibody levels induced by the different mutants. Upon a second boost with the more thermostable mutant C171L, a statistically significant increase in RTA-specific antibody titers was observed when compared with RiVax-immunized mice. Notably, the results indicate that single residue changes can be made to the RiVax antigen that increases its thermal stability without adversely impacting the efficacy of the vaccine.

In Chapter 3, nine additional RiVax mutants were created based on results from the biophysical characterization of RiVax single point mutants. Single point mutations that provided an enhancement in RiVax thermal stability were combined in various ways to create dual-point (and a triple-point) mutants. After expression and purification in *E. coli*, these second-generation mutants (devoid of any tag and cleavage site residues) were subjected to thermal stress across a range of pH values. Techniques used to assess thermal stability included circular dichroism (CD), fluorescence spectroscopy, Rayleigh light scattering and differential scanning calorimetry (DSC). The spectroscopic techniques indicated apparent two-state unfolding with changes in stability ranging from no change to ~ 4 °C. DSC indicated multi-state unfolding which included an early transition not detected by the spectroscopic techniques. This dichotomy between the results from DSC and spectroscopy may be explained by the unique spatial distribution of alpha helices (CD was followed at 208 nm, which monitors changes in helical content) and the location of the lone tryptophan residue (residue 211) in the three dimensional structure of RiVax. We

speculate that the early DSC transition is detecting a conformational change in the C-terminal domain due to its lack of helices and tryptophan residue. We are not the first to suggest an early unfolding event in the C-terminal domain of ricin A chain derivatives [10]. The work presented above has resulted in the identification of a new candidate ricin antigen, namely RiVax mutant V81I/C171L/V204I.

Future directions

Because it is unethical to test the efficacy of a ricin vaccine in humans, the new antigen candidate (V81I/C171L/V204I) indentified in this dissertation will next progress into studies in rhesus macaques. Non-human primates, while certainly not perfect, are the most relevant animal model for assessing the protective capacity of ricin vaccines. Should non-human primate studies recapitulate the immunogenicity and protective ability observed in mouse studies, the vaccine would then progress into Phase 1 trials in heathy adult volunteers. Given that the future of RiVax-based vaccines resides in the lyophilized formulation developed by Hassett and co-workers [4], these studies might be best carried out using a lyophilized formulation of the triple mutant adsorbed to Alhydrogel as opposed to the conventional liquid formulation.

The chapters of this dissertation have provided evidence that the conformational stability of RiVax-based antigens plays a role in the resulting immune response. If one wanted to further improve the stability of the RiVax antigen, one straightforward idea would be to simply make a RiVax antigen comprised of five mutations: the triple mutant plus V18P and S228K. Mutants containing V18P and S228K seemed to have a slightly more stabilizing effect on the non C-terminal region than those containing V81I, C171L, and V204I mutations. Thus, the combination of all five mutations may increase the stability of RiVax even further. Since it is

unclear how each of the individual mutations precisely contribute to the protein's increased stability, it may also be the case the many of the mutations are stabilizing the same unfolding pathway. Adding more mutations to RiVax in this scenario would probably not lead to a further increase in stability. To assess the unfolding pathway of RiVax, one might consider using hydrogen-deuterium exchange coupled with mass spectrometry (H/D-MS) [11, 12]. Local solvent exposure would be quantified by measuring the kinetics of amide H/D exchange in short peptide segments (from protease digestion) of RiVax (and mutants) by determining segment-averaged rate constants for exchange. Increased solvent exposure is defined by large rate constants for exchange. Conversely, regions that remain shielded from solvent are defined by small rate constants. The regions of the protein that initiate the unfolding process will expose residues initially shielded from the solvent at a faster rate than regions that unfold later. After identifying these early unfolding region(s), one could design mutations that attempt to stabilize such region(s) and therefore the unfolding of the protein. The Volkin and Weis labs at KU are already set up for such studies [13, 14]. The Middaugh lab also has a few techniques to assess the "global" dynamics of a protein, including high resolution ultrasonic spectroscopy and temperature dependent second derivate absorbance spectroscopy [15-17], which would provide complimentary information to the H/D-MS results.

Even with the enhanced toxin neutralizing antibody response in mice observed with some of the RiVax mutants, it is almost certain that the response will not be enough to confer protection even when scaled up for human use. Monomeric, recombinant protein-based vaccines have historically faced a difficult time gaining approval from the FDA due to poor performance in clinical trials. In fact, the problem is so severe that upwards of 1000 of such vaccines have reached the clinic, yet exactly zero have made it out [18]. Monomeric toxoid vaccines (i.e., anthrax, diphtheria, and tetanus) are the occasionally exceptions. The primary reason for failure

is most often poor immunogenicity. Thus, the success of ricin and any protein-based vaccine will be intimately tied to the adjuvants with which it is co-delivered. As discussed in the introduction to this dissertation, the new wave of adjuvants based on Toll-like receptor antagonism is revolutionalizing vaccine development. The first TLR-based adjuvant to be included in a marketed product gained approval in the United States in 2009 (GSK'S Cervarix) so this area of vaccinology is very young. It is still to be seen how large an impact these types of adjuvants will have on vaccine research. To date there has been only one unpublished study in which RiVax has been formulated with one of these new TLR agonists. A synthetic TLR4 agonist, PHAD™, has been co-delivered with aluminum salt-adsorbed RiVax and administered to mice. Although there was a slight boost in the elicitation of antibodies (both total and neutralizing), the level to which these were boosted were not as impressive as was hoped going into the study (unpublished results). One could make the argument that additional TLR agonists should be tested; however, most of these agonists work by skewing the immune response towards a Th1-bias in the classical Th1/Th2 model [19]. It is unclear whether steering an immune response towards a cell-mediated Th1 response would be beneficial for a ricin vaccine. If another agonist is to be tried, the most appropriate one would probably be a CpG oligonucleotide. In a related protein-based vaccine, the addition of CpG to BioThrax®, the vaccine that protects against anthrax disease (anthrax is an A_2B toxin similar to ricin), resulted in striking acceleration and enhancement of toxin-specific neutralizing antibodies [20]. What is known, however, is that a vaccine against ricin should result in the production of significant amounts of plasma cells that secrete toxin neutralizing antibodies. Such an effect is typically associated with Th2 responses. In fact, aluminum salt adjuvants strongly promote a Th2 response with little no now involvement of Th1 helper cells. Yet, as mentioned previously, the current aluminum salt-adjuvanted RiVax vaccine elicits an inadequate neutralizing antibody

response in humans and other animals. Squalene based oil-in-water emulsions, such as MF59, are an attractive alternative to aluminum salt adjuvants since they show a slight bias towards a humoral response as well [21, 22]. It has been proposed that such adjuvants potentiate immune responses by triggering the rapid recruitment of leukocytes at sites of injection. They have been shown to improve immunogenicity over that induced by aluminum salts of a number of vaccines [23-25].

Further development of a ricin vaccine may rely on delivering the antigen using a multivalent presentation platform. Currently, there are two FDA-approved recombinant vaccines based on multivalent presentation: the hepatitis B vaccine (HBV) and the human papillomavirus vaccine (HPV). Both are formulated as virus-like particles, in which multiple copies of a surface antigen are displayed in a repetitive fashion for detection by the immune system. It is likely that the success of these two vaccines is a result of the VLPs more naturally mimicking the wild pathogen which natively expresses multiple copies of antigen on its surface. Ricin, being a heterodimeric protein, does not have such natural multivalency. Nonetheless, it would be well worth the effort to present a ricin antigen multivalently. There is evidence that multivalent display of anthrax protective antigen results in improved antibody titers and survival from lethal challenge compared to the monomer [26]. There is also a report in which a self crosslinked protein was more immunogenic than the monomeric form [27]. A similar study completed by a different group with a different antigen, however, found that a multimeric form was not any better than the monomer in terms of antibody elicitation [28]. A possibly effective way to display an antigen multivalently would be by conjugating it to a polymeric backbone. This could potentially stimulate T-cell independent pathways of the immune response. These types of responses can, in fact, generate memory B cells [29, 30]. One would have to investigate the

effect of antigen density [31, 32] and vehicle size [33, 34] on the resulting immune response to fine tune any such vaccine.

Another interesting idea perhaps worth pursuing would be to deliver an antigen comprised of an attenuated A chain joined (via the natural disulfide bond or through chemical crosslinking) to an attenuated B chain. Recent evidence suggests that a diverse set of toxin neutralizing antibodies interfere with the reduction of the holotoxin into individual chains once it reaches the endoplasmic reticulum [35]. It is not a big leap to hypothesize that a vaccine antigen that maintains the contact between the two chains would be a better immunogen than either individual chain. Work from nearly 40 years ago suggested that conformational epitopes exist on the intact toxin that are not present on the isolated chains [36]. Furthermore, the general belief is that the more similar a vaccine is to the disease-causing entity (in the case of ricin, a disease-causing protein), the better the immune response to the vaccine. In a related idea in which a formaldehyde-inactivated ricin vaccine was delivered to mice, the inactivated toxin was immunogenic. Since the vaccine was comprised of the wild type toxin, however, concerns about residual toxicity due to incomplete inactivation eliminated the candidate [37, 38]. It is imperative that both chains be attenuated because attaching an attenuated A chain to a native B chain (RTB) might be hazardous due to residual toxicity since the antigen would now be able to enter cells and reach the cytosol. There is already significant literature investigating attenuation of the galactose binding ability of the B chain by mutagenesis. One report suggests that simply removing the glycosylation sites in the B chain renders it devoid of lectin activity [39]. Another suggests that substituting a binding site asparagine with alanine abrogates more than 99 % of its lectin binding ability [40]. Some mutant B chains did not associate readily with the native A chain so this must be taken into account if the two chains are to be joined by a native disulfide bond [41]. Due to the presence of the intramolecular disulfide bonds in native RTB and the

intermolecular disulfide bond connecting the A chain and B chain, one would probably have to express the protein in an E. coli strain with an enhanced ability to form proper disulfide bonds in the cytoplasmic space, such as the Origami™ or SHuffle® strains. Alternatively, the two chains can be expressed separately (and even in separate expression systems) and recombined after purification.

In conclusion, there is a long road ahead before the eventual approval of a vaccine against ricin. Many more experiments will have to be undertaken on the triple mutant disclosed in Chapter 3 if that is to become a lead RiVax-based candidate. If, as expected, the immunogenicity of the triple mutant will still be too weak to present a viable option in humans, one could turn to either of the two suggestions presented above. In regard to multivalent presentation of the antigen, a collaboration has already been initiated with the Forrest and Berkland labs to conjugate the ricin antigen to a hyaluranic acid backbone for vaccine purposes.

References

1. Bradberry, S.M., et al., *Ricin poisoning.* Toxicol Rev, 2003. **22**(1): p. 65-70.
2. Reisler, R.B. and L.A. Smith, *The need for continued development of ricin countermeasures.* Adv Prev Med, 2012. **2012**: p. 149737.
3. Thomas, J.C., et al., *Effect of single-point mutations on the stability and immunogenicity of a recombinant ricin A chain subunit vaccine antigen.* Hum Vaccin Immunother, 2013. **9**(4): p. 740-48.
4. Hassett, K.J., et al., *Stabilization of a Recombinant Ricin Toxin A Subunit Vaccine through Lyophilization.* Eur J Pharm Biopharm, 2013.
5. Meagher, M.M., et al., *Process development and cGMP manufacturing of a recombinant ricin vaccine: an effective and stable recombinant ricin A-chain vaccine-RVEc.* Biotechnol Prog, 2011. **27**(4): p. 1036-47.
6. McLain, D.E., et al., *Protective effect of two recombinant ricin subunit vaccines in the New Zealand white rabbit subjected to a lethal aerosolized ricin challenge: survival, immunological response, and histopathological findings.* Toxicol Sci, 2012. **126**(1): p. 72-83.
7. O'Hara, J.M., R.N. Brey, 3rd, and N.J. Mantis, *Comparative efficacy of two leading candidate ricin toxin a subunit vaccines in mice.* Clin Vaccine Immunol, 2013. **20**(6): p. 789-94.

8. Vitetta, E.S., et al., *A pilot clinical trial of a recombinant ricin vaccine in normal humans.* Proc Natl Acad Sci U S A, 2006. **103**(7): p. 2268-73.
9. Vitetta, E.S., J.E. Smallshaw, and J. Schindler, *Pilot phase IB clinical trial of an alhydrogel-adsorbed recombinant ricin vaccine.* Clin Vaccine Immunol, 2012. **19**(10): p. 1697-9.
10. McHugh, C.A., et al., *Improved stability of a protein vaccine through elimination of a partially unfolded state.* Protein Sci, 2004. **13**(10): p. 2736-43.
11. Maier, C.S. and M.L. Deinzer, *Protein conformations, interactions, and H/D exchange.* Methods Enzymol, 2005. **402**: p. 312-60.
12. Zhang, Z. and D.L. Smith, *Thermal-induced unfolding domains in aldolase identified by amide hydrogen exchange and mass spectrometry.* Protein Sci, 1996. **5**(7): p. 1282-9.
13. Majumdar, R., et al., *Effects of Salts from the Hofmeister Series on the Conformational Stability, Aggregation Propensity, and Local Flexibility of an IgG1 Monoclonal Antibody.* Biochemistry, 2013.
14. Manikwar, P., et al., *Correlating excipient effects on conformational and storage stability of an IgG1 monoclonal antibody with local dynamics as measured by hydrogen/deuterium-exchange mass spectrometry.* J Pharm Sci, 2013. **102**(7): p. 2136-51.
15. Esfandiary, R., et al., *Temperature dependent 2nd derivative absorbance spectroscopy of aromatic amino acids as a probe of protein dynamics.* Protein Sci, 2009. **18**(12): p. 2603-14.
16. Kamerzell, T.J. and C.R. Middaugh, *The complex inter-relationships between protein flexibility and stability.* J Pharm Sci, 2008. **97**(9): p. 3494-517.
17. Ramsey, J.D., et al., *Using empirical phase diagrams to understand the role of intramolecular dynamics in immunoglobulin G stability.* J Pharm Sci, 2009. **98**(7): p. 2432-47.
18. Friede, M., *Challenges to using adjuvants*, 2012.
19. Manicassamy, S. and B. Pulendran, *Modulation of adaptive immunity with Toll-like receptors.* Semin Immunol, 2009. **21**(4): p. 185-93.
20. Rynkiewicz, D., et al., *Marked enhancement of the immune response to BioThrax(R) (Anthrax Vaccine Adsorbed) by the TLR9 agonist CPG 7909 in healthy volunteers.* Vaccine, 2011. **29**(37): p. 6313-20.
21. Baudner, B.C., et al., *MF59 emulsion is an effective delivery system for a synthetic TLR4 agonist (E6020).* Pharmaceutical research, 2009. **26**(6): p. 1477-85.
22. Calabro, S., et al., *The adjuvant effect of MF59 is due to the oil-in-water emulsion formulation, none of the individual components induce a comparable adjuvant effect.* Vaccine, 2013. **31**(33): p. 3363-9.
23. O'Hagan, D.T., et al., *The mechanism of action of MF59 - an innately attractive adjuvant formulation.* Vaccine, 2012. **30**(29): p. 4341-8.
24. Khurana, S., et al., *Vaccines with MF59 adjuvant expand the antibody repertoire to target protective sites of pandemic avian H5N1 influenza virus.* Science translational medicine, 2010. **2**(15): p. 15ra5.
25. Ott, G., G.L. Barchfeld, and G. Van Nest, *Enhancement of humoral response against human influenza vaccine with the simple submicron oil/water emulsion adjuvant MF59.* Vaccine, 1995. **13**(16): p. 1557-62.
26. Manayani, D.J., et al., *A viral nanoparticle with dual function as an anthrax antitoxin and vaccine.* PLoS pathogens, 2007. **3**(10): p. 1422-31.

27. Kubler-Kielb, J., et al., *Long-lasting and transmission-blocking activity of antibodies to Plasmodium falciparum elicited in mice by protein conjugates of Pfs25.* Proc Natl Acad Sci U S A, 2007. **104**(1): p. 293-8.
28. Qian, F., et al., *Immunogenicity of self-associated aggregates and chemically cross-linked conjugates of the 42 kDa Plasmodium falciparum merozoite surface protein-1.* PLoS One, 2012. **7**(6): p. e36996.
29. Obukhanych, T.V. and M.C. Nussenzweig, *T-independent type II immune responses generate memory B cells.* J Exp Med, 2006. **203**(2): p. 305-10.
30. Defrance, T., M. Taillardet, and L. Genestier, *T cell-independent B cell memory.* Curr Opin Immunol, 2011. **23**(3): p. 330-6.
31. Dintzis, H.M., R.Z. Dintzis, and B. Vogelstein, *Molecular determinants of immunogenicity: the immunon model of immune response.* Proc Natl Acad Sci U S A, 1976. **73**(10): p. 3671-5.
32. Dintzis, R.Z., et al., *The immunogenicity of soluble haptenated polymers is determined by molecular mass and hapten valence.* J Immunol, 1989. **143**(4): p. 1239-44.
33. Bachmann, M.F. and G.T. Jennings, *Vaccine delivery: a matter of size, geometry, kinetics and molecular patterns.* Nat Rev Immunol, 2010. **10**(11): p. 787-96.
34. Reddy, S.T., et al., *In vivo targeting of dendritic cells in lymph nodes with poly(propylene sulfide) nanoparticles.* J Control Release, 2006. **112**(1): p. 26-34.
35. O'Hara, J.M. and N.J. Mantis, *Neutralizing monoclonal antibodies against ricin's enzymatic subunit interfere with protein disulfide isomerase-mediated reduction of ricin holotoxin in vitro.* J Immunol Methods, 2013.
36. Olsnes, S. and E. Saltvedt, *Conformation-dependent antigenic determinants in the toxic lectin ricin.* J Immunol, 1975. **114**(6): p. 1743-8.
37. Griffiths, G.D., et al., *Protection against inhalation toxicity of ricin and abrin by immunisation.* Human & experimental toxicology, 1995. **14**(2): p. 155-64.
38. Griffiths, G.D., et al., *Liposomally-encapsulated ricin toxoid vaccine delivered intratracheally elicits a good immune response and protects against a lethal pulmonary dose of ricin toxin.* Vaccine, 1997. **15**(17-18): p. 1933-9.
39. Zhan, J., et al., *Restoration of lectin activity to a non-glycosylated ricin B chain mutant by the introduction of a novel N-glycosylation site.* FEBS Lett, 1997. **407**(3): p. 271-4.
40. Vitetta, E.S. and N. Yen, *Expression and functional properties of genetically engineered ricin B chain lacking galactose-binding activity.* Biochim Biophys Acta, 1990. **1049**(2): p. 151-7.
41. Frankel, A., et al., *Double-site ricin B chain mutants retain galactose binding.* Protein Eng, 1996. **9**(4): p. 371-9.

Appendix A Stability-indicating assays for the development of RiVax-based antigens

Introduction

The development of stability-indicating assays is critical for successfully developing vaccines. In this study, two assays were developed to assist with the continued development of RiVax, although the methods should be applicable to RiVax mutants as well. One assay is ELISA-based and uses the R70 monoclonal antibody to characterize the aluminum salt-adsorbed protein. An accelerated stability study revealed that the aluminum salt adjuvant destabilized the antigen to a great extent. Since development, the assay has been used by our industrial collaborator to evaluate lyophilized, aluminum salt-adsorbed RiVax during process development and scale-up. The second stability-indicating assay is a cation exchange chromatography method useful for characterizing charge heterogeneity of the non-adsorbed antigen. The method was tested for its stability-indicating ability by forced degradation studies, including elevated pH and temperature and oxidation by hydrogen peroxide. Under forced deamidation conditions (elevated pH and temperature), an increase in acidic species was detected as a function of incubation time at 37 °C. A particular pre-main species peak and numerous early eluting peaks gave rise to the majority of the additional acidic species. Forced oxidation conditions also gave rise to an increase in acidic species. This increase was confined largely to the most prominent acidic peak and was prevented by alkylation of a free cysteine residue. Given the results of the forced oxidation studies, the major acidic peak likely contains a significant amount of RiVax variants with C259 oxidized to sulfinic or sulfonic acid.

Materials & Methods

Preparation of materials for ELISA assay. RiVax was dialyzed at 4 °C into a buffer consisting of 10 mM histidine (pH 6) and 144 mM NaCl. An adequate amount of RiVax was then adsorbed onto Alhydrogel in amounts such that the final formulation consisted of 0.85 mg/ml aluminum and 0.2 mg/ml RiVax. This solution was stirred at 60 rpm for 1 hour at 4 °C to facilitate adsorption and subsequently aliquoted into microcentrifuge tubes (1 mL each). Additionally, non-adsorbed RiVax (0.2 mg/ml) and appropriate blanks were aliquoted in the same manner. Half of each of the adsorbed and non-adsorbed formulations and blanks were stored at 4 °C and the other half were stored at 40 °C

R70 ELISA accelerated stability study. At each time point of the study, the adsorbed RiVax formulations were washed twice with fresh histidine buffer by centrifugation at 14,000 *g* for 5 minutes. After the final re-suspension, the samples were diluted 20-fold in histidine buffer. The soluble RiVax formulations were centrifuged once at 14,000 *g* for 5 minutes to pellet any aggregates that formed during storage. The supernatant was diluted 20-fold in histidine buffer. The resulting solutions were plated (100 µL) onto a Nunc-Immuno MediSorp (Nalge Nunc International, Wiesbaden, Germany) 96-well plate overnight at 4 °C; the plates were then washed four times with tris-buffered saline (TBS), blocked with Superblock T20 in TBS® (ThermoScientific) and incubated at room temperature (RT) for one hour. The plates were then washed another four times with TBS. R70 monoclonal antibody was diluted 1:10,000 in the blocking buffer, plated (100 µL) and allowed to incubate on the plate for one hour at RT. The plates were washed as above and then 100 µL of HRP-conjugated goat anti-Mouse monoclonal antibody (Sigma) diluted 1:5,000 in blocking buffer was added and allowed to incubate at RT for one hour. The plates were washed again as above after which 100 µL of 3,3',5'-

TetraMethylBenzidine (TMB) substrate (100mL) (Sigma) was added. After 30 minutes at RT, 2M HCl (100mL) was added to quench the reaction and plates were read using a SpectraMax M3 plate reader (Molecular Devices, Sunnyvale, CA) at 450nm.

Cation exchange chromatography. A pH-gradient cation exchange chromatography method was developed on a Dionex ProPac WCX-10 column (4 x 250 mm) (ThermoScientific) on a Shimadzu HPLC system with UV detection at 280 nm. Mobile phase A consisted of 10 mM ACES, 10 mM HEPES, and 50 mM NaCl adjusted to a pH value of 6.1 while mobile phase B consisted of the same species, but adjusted to a pH value of 8.2. The temperature of the column was maintained at 30 ºC and that of the autosampler at 5 ºC. The flow rate was set to 1 ml/min. The following gradient was used:

Time (min)	% B
0	0
5	0
35	100
40	100
40.1	0
50	0

Forced deamidation study. RiVax was dialyzed at 4 ºC into a buffer consisting of 100 mM sodium phosphate (pH 8.0), 100 mM sodium chloride, and 10 mM EDTA. The protein was concentrated to 2 mg/ml using centrifugal filters and then diluted 1:1 with glycerol and placed in

a 37 ºC incubator. Aliquots were removed at 0, 1, and 4 days, buffer exchanged with a solution of 10 mM histidine (pH 6), 150 mM sodium chloride and 10 % sucrose using centrifugal filters, centrifuged to remove insoluble material, and stored at -80 ºC until analysis. All samples were buffered exchanged again into mobile phase A on the day of analysis. The cation exchange method described above was used to determine the percentage of charged variants at each time point. Size exclusion chromatography (SEC) was performed on the day 0 and 4 samples to determine if any soluble fragmentation or dimerization occurred during incubation. SEC was executed on a TSKgel BioAssist G3SWxl column (TOSOH, King of Prussia, PA). The mobile phase consisted of 100 mM sodium phosphate (pH 7) and 300 mM NaCl. The temperature of the column was maintained at 30 ºC and that of the autosampler at 5 ºC. The flow rate was set to 0.5 ml/min.

Forced oxidation study. RiVax was dialyzed at 4 ºC into a buffer consisting of 10 mM histidine pH 6), 144 mM sodium chloride and concentrated to 0.5 mg/ml. Hydrogen peroxide was added at 0.005 % wt/vol and incubated at room temperature in the dark for 24 hours. Aliquots were removed at 0, 4, 12, and 24 hours and the reaction quenched with 100 mM methionine. The quenched solutions were stored at 4 °C until all the samples were simultaneously buffer exchanged into mobile phase A. The cation exchange method described above was used to determine the percentage of charged variants at each time point. An SDS-PAGE gel was used to determine if any fragmentation or aggregation occurred during incubation. For experiments in which RiVax was alkylated with iodoacetamide (Pierce, Rockford, IL), the alkylation was preformed following manufacturer's instructions.

Results & Discussion

R70 ELISA. R70 recognizes the continuous epitope N97 – F108. The crystal structure of RiVax shows this stretch of amino acids forms a solvent-exposed helix [1]. It is probably the dominant continuous epitope targeted by neutralizing antibodies, at least in mice, since monoclonal antibodies to this region have been isolated on at least four separate occasions [2-5]. In passive protection studies in mice, these antibodies against N97-F108 provided protection against lethal toxin challenge [2, 4, 5]. Thus, an ELISA method developed on the basis of R70 recognition of its epitope on RiVax would be a valuable tool in assessing the vaccine product.

Figure 1 displays the results of the accelerated stability testing of RiVax using the R70 ELISA. Not surprisingly, soluble RiVax stored at 4 °C performed best in terms of retaining the ability to be bound by mAb R70. It retained ~ 70 % of its binding ability after nearly three months of storage. Soluble RiVax stored at 40 °C lost approximately half of its ability to be bound by R70 over this same time period. It is probable that the majority of these losses were due to insoluble aggregation of the protein since that is a major route of degradation for RiVax. Alhydrogel-adsorbed RiVax stored at 4 °C lost roughly 70 % of its ability to bind the antibody during its 84 days of storage. This is not surprising since Alhydrogel has been previously shown to lower the thermal transition of RiVax, which suggests adsorption to Alhydrogel destabilizes the protein [6]. The adsorbed RiVax stored at 40 °C was not detected by the antibody after just two days. This is again not surprising given the aforementioned observation. Further evidence supporting complete destabilization of Alhydogel-adsorbed RiVax stored at 40 °C is a mouse study in which such a formulation stored at 40 °C for 60 days did not protect mice from lethal ricin challenge [7], presumably due to a loss of the protein's native structure. Due to the destabilization of RiVax on aluminum salt adjuvants in solution, experiments were undertaken to lyophilize Alhydrogel-bound RiVax [8]. This formulation completely protected mice from lethal

ricin challenge after storage at 40 °C for 4 weeks. Such results imply that the storage stability problems initially encountered during the development of RiVax have been at least substantially mitigated, if not completely.

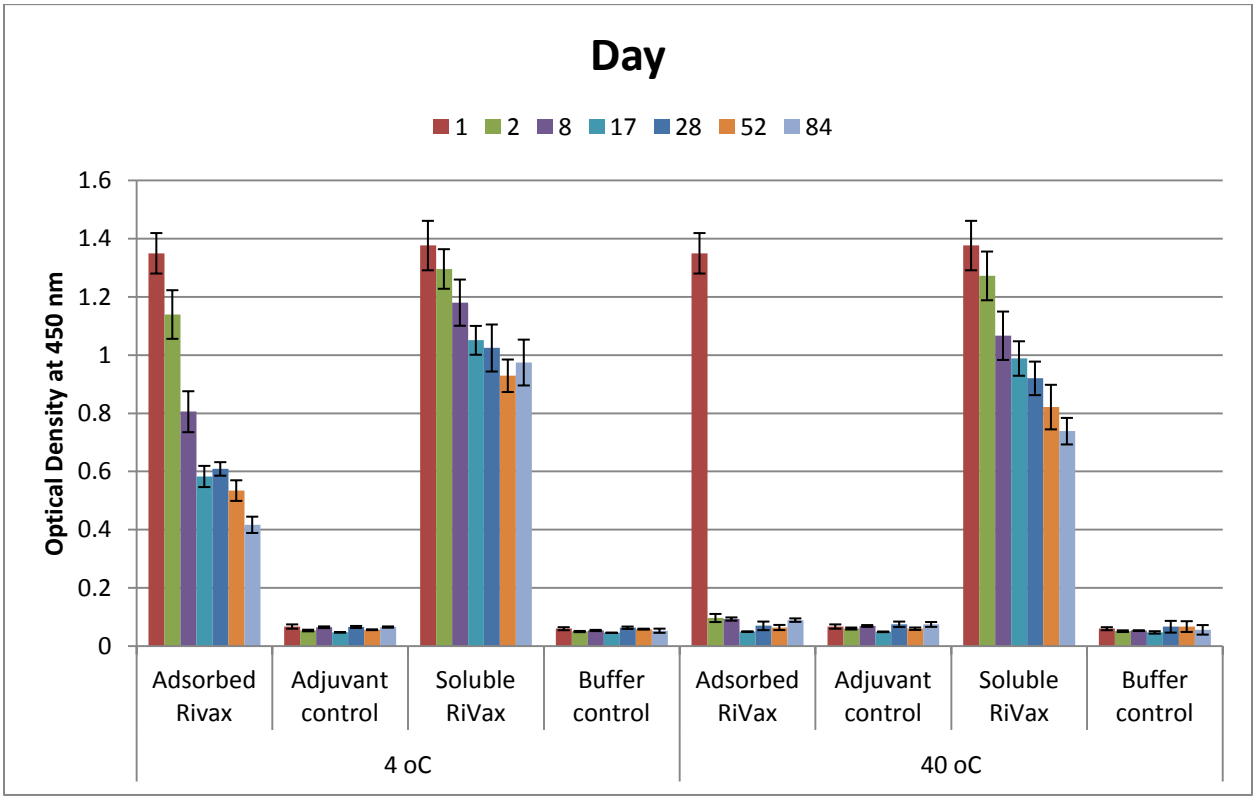

Figure 1. Accelerated stability of adsorbed and non-adsorbed RiVax formulations as a function of time and incubation temperature. R70 monoclonal antibody was used to detect the epitope N97 – F108.

Detection of charged RiVax variants. The ability to detect chemical modifications of proteins is critical to ensure a safe and efficacious product will be delivered to humans. Two prominent methods for the detection of charged chemical modifications are ion exchange chromatography and imaged capillary isoelectric focusing (icIEF). Initial attempts at developing an icIEF method for the quantification of charged RiVax variants proved unsuccessful. The application of current during the focusing steps combined with the lack of salt in the injected sample gave rise to

aggregation and/or precipitation of RiVax within the capillary. Evidence to support this was primarily based on repeated fouling of new capillaries after just a handful of injections. The fouling resulted in irreproducible peaks in the electorpherogram of both RiVax samples and hemoglobin standards. Thus, a cation exchange chromatography method was developed to quantify charged RiVax variants. Cation exchange chromatography is most commonly employed using a linear gradient in salt concentration at a specific pH value. Alternatively, one may use a linear gradient in pH at a specific salt concentration [9, 10].

One common experiment performed during the development of biotechnology products involves the forced deamidation of the protein. Forced deamidation conditions generally combine elevated pH values and temperature, which greatly accelerate the rate of deamidation so that the reaction occurs on a manageable time scale for research purposes. Deamidation events in a protein often result in the introduction of negative charge(s) as aspargine residues (and sometimes gluatmines) are converted to aspartic acid and/or isoaspartic acid. Due to the precipitation problems associated with RiVax under forced deamidation conditions, 50 % glycerol was included in the buffer to prevent such events. During excipient screening, glycerol was found to stabilize both the conformation and aggregation propensity of RiVax [11]. Even with the inclusion of 50% glycerol, some precipitation was observed during the incubation period; analysis was only performed on the soluble fraction remaining after centrifugation. The charge characteristics of the species that precipitated are unknown. Of the species that remained soluble at each time point, it is clear that they became increasingly more acidic at increasing incubation times (Figures 2 and Table 1). The main peak species decreased concomitantly with the increasing acidic peaks. The precise modifications these acidic species contain, however, are uncertain but are actively being pursued by LC-MS methods. Analysis of the day zero and four samples by size exclusion chromatography revealed a slight increase in high molecular weight

species and the appearance of a low molecular weight species (Figure 3 and Table 2). Of particular interest are the low molecular weight species. Depending on where the protein backbone was fragmented, the clipped RiVax could possess a greater negative charge density and thus run acidic to the main peak on a cation exchange column.

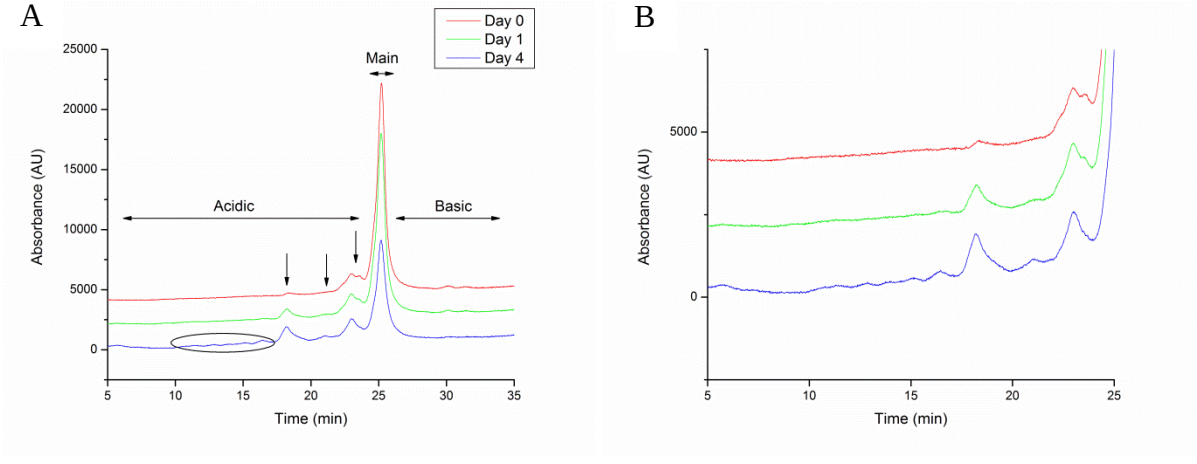

Figure 2. Chromatographic analysis of the forced deamidation of RiVax. Cation exchange chromatography was used to separate the various species produced during incubation at elevated pH and temperature. (A) Full chromatogram. (B) Chromatogram zoomed in to highlight acidic species.

Table 1. Quantification of acidic, unmodified, and basic species resulting from the forced deamidation of RiVax.

Day	% Acidic	% Main	% Basic
0	14.2 ± 0.5	81.7 ± 0.4	4.1 ± 0.2
1	19.2 ± 0.9	78.3 ± 1.3	2.5 ± 0.6
4	34.0 ± 0.6	64.9 ± 0.3	1.1 ± 0.4

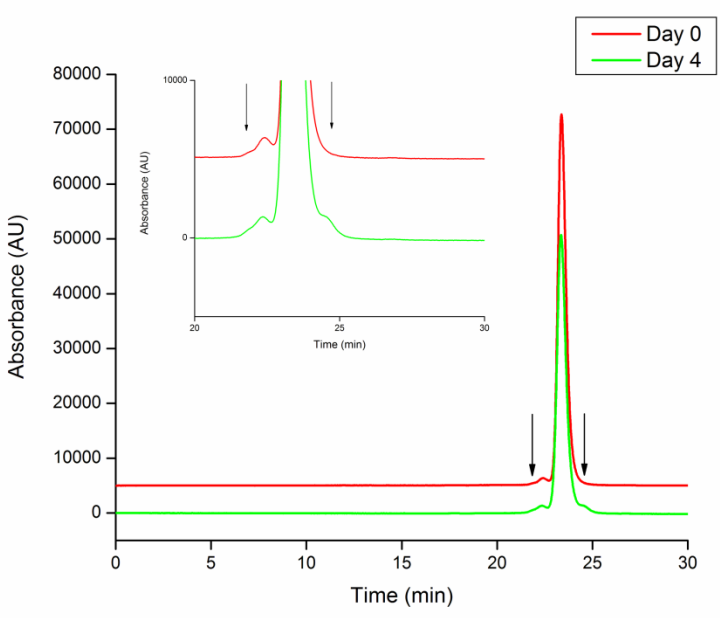

Figure 3. Chromatographic analysis of the forced deamidation of RiVax. Size exclusion chromatography was used to separate the various species produced during incubation at elevated pH and temperature.

Table 2. Quantification of the species produced during the forced deamidation of RiVax. HMWS = high molecular weight species; LMWS = low molecular weight species

Day	% HMWS	% Monomer	% LMWS
0	2.0 ± 0	98.0 ± 0	-
4	2.8 ± 0.2	95.2 ± 0.2	2.0 ± 0.1

The inclusion of 50 % glycerol could potentially have impacted the results [12, 13]. Unfortunately, glycerol had to be included in the solvent due to the precipitation problems mentioned above. Glycerol, an excluded solute, tends to compact the native state ensemble into its most compact form [14, 15]. This could lead to normally solvent exposed asparagine (and glutamine) residues becoming less exposed and accessible to water, a necessary component for the generation of charged deamidation variants. Additionally, compaction could make regions of the protein containing asparagines less flexible, which would slow the rate of deamidation. Furthermore, adding glycerol lowers the dielectric constant which would slow the rate of

deamidation by disfavoring formation of the charged intermediates in the cyclization pathway [16]. The increased viscosity of the glycerol-containing buffer would also disfavor deamidation, although the effect mediated by the change in solvent dielectric would probably have a greater contribution to decreasing deamidation rates [17].

A second common experiment performed during the development of biotechnology products involves the forced oxidation of the product. Oxidation does not generally introduce charge into a protein. Most commonly, methionine residues are oxidized to the sulfoxide and/or sulfone derivatives, which carry no additional charge. Nonetheless, the cation exchange method was applied to oxidized RiVax samples. Incubation with 0.005% hydrogen peroxide produced a striking increase in acidic species over the course of 24 hours that was almost entirely confined to one particular peak (Figures 4A and Table 3). An SDS-PAGE gel did not reveal any new bands or shifts in bands suggesting that there was not any clipping of the protein backbone nor aggregation of the protein (disulfide mediated or otherwise) (Figure 5). The most likely event is oxidation of the free, surface-exposed cysteine to its sulfinic or sulfonic derivative [18, 19]. To test the cysteine oxidation hypothesis, RiVax was alkylated with iodoacetamide and subjected to the same oxidation conditions. Alkylation of the solvent-exposed cysteine completely abrogated the increase in acidic species upon incubation with hydrogen peroxide (Figure 4B). While the alkylation experiment suggests the main acidic peak may contain RiVax variants with an oxidized cysteine, the precise nature of the modification(s) is currently being pursued by LC-MS methods.

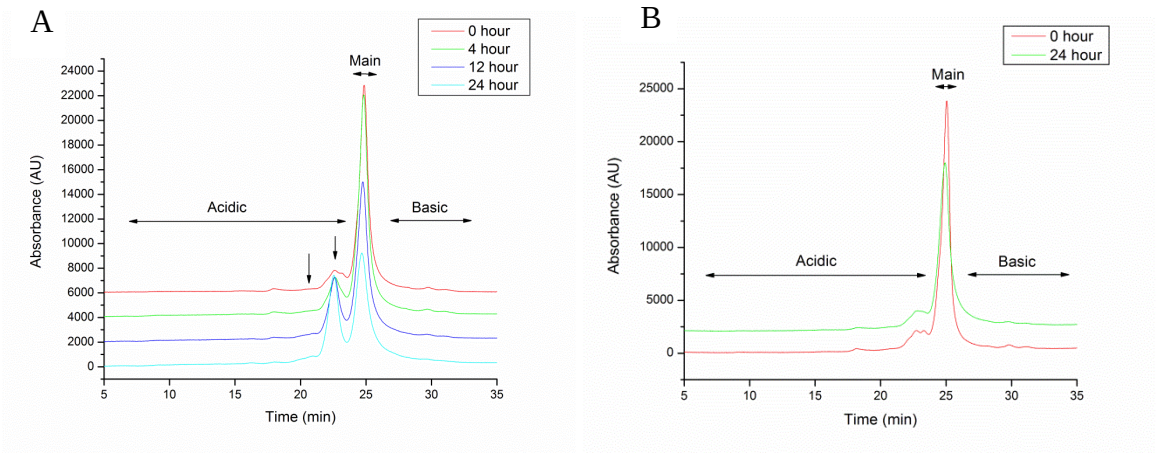

Figure 4. Chromatographic analysis of the forced oxidation of (A) RiVax and (B) RiVax alkylated with iodoacetamide. Cation exchange chromatography was used to separate the various species produced during incubation with 0.005 % hydrogen peroxide.

Table 3. Quantification of the species produced during the forced oxidation of RiVax.

Hour	% Acidic	% Main	% Basic
0	14.9 ± 0.1	82.9 ± 0.1	2.9 ± 0.1
4	18.1 ± 0.1	79.1 ± 0.2	2.8 ± 0.1
12	27.4 ± 0.1	69.9 ± 0.3	2.7 ± 0.3
24	38.9 ± 0.4	58.9 ± 0.4	2.2 ± 0.3

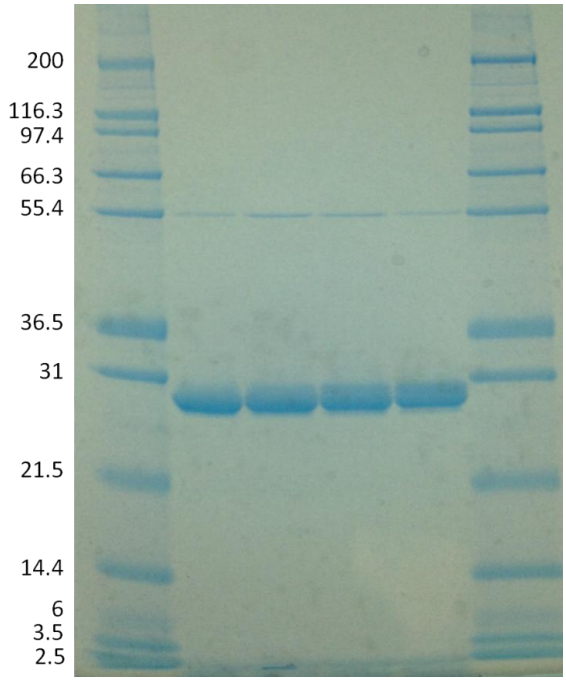

Figure 5. SDS-PAGE gel of the four time points of the forced oxidation experiment. Lanes 1 and 6 are markers. Lanes 2 – 5 are time points 0, 4, 12, and 24 hours, respectively.

In conclusion, two new methods are now available to assess the integrity of adsorbed and non-adsorbed RiVax. The R70 ELISA method is being actively employed by our industrial collaborator, primarily to assess the impact of different lyophilization parameters on the final vaccine product. The cation exchange chromatography method will prove valuable in ensuring that the protein adsorbed to Alhydrogel is consistent from lot to lot. It is presently unclear whether the non-main peak species negatively impact the immune response to the protein, which is a significant concern. Nonetheless, consistency of the final product is also an essential part of the successful development of vaccines and the cation exchange method furthers the achievement of this goal.

References

1. Legler, P.M., et al., *Structure of RiVax: a recombinant ricin vaccine.* Acta Crystallogr D Biol Crystallogr, 2011. 67(Pt 9): p. 826-30.
2. Neal, L.M., et al., *A monoclonal immunoglobulin G antibody directed against an immunodominant linear epitope on the ricin A chain confers systemic and mucosal immunity to ricin.* Infect Immun, 2010. 78(1): p. 552-61.
3. Mantis, N.J., et al., *Immunoglobulin A antibodies against ricin A and B subunits protect epithelial cells from ricin intoxication.* Infection and immunity, 2006. 74(6): p. 3455-62.
4. O'Hara, J.M., et al., *Folding domains within the ricin toxin A subunit as targets of protective antibodies.* Vaccine, 2010. 28(43): p. 7035-46.
5. Lemley, P.V., P. Amanatides, and D.C. Wright, *Identification and characterization of a monoclonal antibody that neutralizes ricin toxicity in vitro and in vivo.* Hybridoma, 1994. 13(5): p. 417-21.
6. Peek, L.J., et al., *Effects of stabilizers on the destabilization of proteins upon adsorption to aluminum salt adjuvants.* J Pharm Sci, 2007. 96(3): p. 547-57.
7. Barrett, B.S., *Formulation and Development of Recombinant Protein Vaccines,* in *Department of Pharmaceutical Chemistry*2009, University of Kansas.
8. Hassett, K.J., et al., *Stabilization of a Recombinant Ricin Toxin A Subunit Vaccine through Lyophilization.* Eur J Pharm Biopharm, 2013.
9. Farnan, D. and G.T. Moreno, *Multiproduct high-resolution monoclonal antibody charge variant separations by pH gradient ion-exchange chromatography.* Anal Chem, 2009. 81(21): p. 8846-57.
10. Rea, J.C., et al., *Validation of a pH gradient-based ion-exchange chromatography method for high-resolution monoclonal antibody charge variant separations.* J Pharm Biomed Anal, 2011. 54(2): p. 317-23.
11. Peek, L.J., R.N. Brey, and C.R. Middaugh, *A rapid, three-step process for the preformulation of a recombinant ricin toxin A-chain vaccine.* J Pharm Sci, 2007. 96(1): p. 44-60.
12. Stratton, L.P., et al., *Controlling deamidation rates in a model peptide: effects of temperature, peptide concentration, and additives.* Journal of pharmaceutical sciences, 2001. 90(12): p. 2141-8.
13. Wakankar, A.A. and R.T. Borchardt, *Formulation considerations for proteins susceptible to asparagine deamidation and aspartate isomerization.* Journal of pharmaceutical sciences, 2006. 95(11): p. 2321-36.
14. Priev, A., et al., *Glycerol decreases the volume and compressibility of protein interior.* Biochemistry, 1996. 35(7): p. 2061-6.
15. Vagenende, V., M.G.S. Yap, and B.L. Trout, *Mechanisms of protein stabilization and prevention of protein aggregation by glycerol.* Biochemistry, 2009. 48(46): p. 11084-96.
16. Brennan, T.V. and S. Clarke, *Spontaneous degradation of polypeptides at aspartyl and asparaginyl residues: effects of the solvent dielectric.* Protein science : a publication of the Protein Society, 1993. 2(3): p. 331-8.
17. Li, R., et al., *Effects of solution polarity and viscosity on peptide deamidation.* The journal of peptide research : official journal of the American Peptide Society, 2000. 56(5): p. 326-34.
18. Griffiths, S.W., J. King, and C.L. Cooney, *The reactivity and oxidation pathway of cysteine 232 in recombinant human alpha 1-antitrypsin.* J Biol Chem, 2002. 277(28): p. 25486-92.
19. Kettenhofen, N.J. and M.J. Wood, *Formation, reactivity, and detection of protein sulfenic acids.* Chem Res Toxicol, 2010. 23(11): p. 1633-46.

Appendix B Biophysical characterization of RVEc

Introduction

Throughout the Chapters of this dissertation, there have been multiple references to RVEc, the other leading ricin vaccine antigen candidate. As a reminder, RVEc, also referred to as RTA 1-33/44-198, is being developed by the US Army Medical Research Institute for Infectious Diseases (USAMRIID) as their candidate ricin antigen. A Phase 1, dose escalating clinical trial of the vaccine in healthy adults was completed in March 2013, although results have not yet been made public. A second trial was initiated which sought to re-enroll only those volunteers in the initial 50 μg cohort to deliver a fourth round of immunizations. Whether this is a positive or negative development for the candidate is unclear. Regardless, USAMRIID was gracious enough to send us their candidate antigen for our own characterization purposes. In this study, the ricin vaccine candidate being developed by the US Army Medical Research Institute for Infectious Diseases, RVEc, was characterized as a function of temperature and pH by circular dichroism, intrinsic fluorescence, Rayleigh light scattering, and ANS fluorescence. The experimental conditions used to assess the stability of RVEc were the same as those used by Peek and co-workers during their initial characterization of RiVax [1].

Materials & Methods

Protein preparation. 25 mM citrate-phosphate (CP) buffers containing 1 M NaCl (Sigma-Aldrich) were prepared (pH values 3 – 8) using citric acid monohydrate (Fisher Scientific) and sodium phosphate dibasic anhydrous (Fisher). RTA 1-33/44-198 was kindly provided by the U.S. Army Medical Research Institute for Infectious Diseases (USAMRIID). The protein was dialyzed into CP buffers at 4 °C using Slide-A-Lyzer® Dialysis Cassettes, 10,000 kDa MWCO

(Pierce, Rockford, IL). The dialyzed protein was diluted to 0.26 mg/mL before analysis. Protein concentration was determined by Ultraviolet (UV) spectroscopy using an extinction coefficient of 0.721 mL/mg·cm. The stability of the protein at pH values 3 and 4 was not determined due to the formation of insoluble aggregates. In the same conditions, RiVax was soluble at pH 4 but insoluble at pH 3.

Circular dichroism. Circular dichroism (CD) spectra were obtained at 10 °C using a Jasco J-815 spectropolarimeter furnished with a 6-position Peltier temperature controller (Easton, MD). The CD signal was monitored from 195 – 260 nm using a scanning speed of 20 nm/min and 1 nm resolution. Thermal melts were performed by following the CD signal at 207 nm every 0.5 °C from 10 – 90 °C. The temperature was ramped at a rate of 15 °C/hour and the samples were equilibrated for 1 minute at each temperature. An appropriate buffer spectrum was subtracted before analysis.

Intrinsic fluorescence. Fluorescence spectra were acquired on a Photon Technology International spectrofluorometer (Lawrenceville, NJ) equipped with a 4-position Peltier temperature controller. Since the single tryptophan of RiVax is deleted in RVEc, an excitation wavelength of 280 nm was used and emission spectra were collected from 290 – 380 nm to monitor tyrosine fluorescence. The scattering of light at the excitation wavelength was followed as a measure of aggregation. Spectra were collected every 2.5 °C from 10 – 87.5 °C with an equilibration time of 5 minutes at each temperature Appropriate buffer spectra were subtracted before analysis. The fluorescence intensity at the peak emission position and the light scattering at 280 nm were plotted as a function of temperature.

Extrinsic fluorescence. 8-Anilino-1-napthalene sulfonate (ANS) (Sigma-Aldrich) was used to monitor the accessibility of apolar sites upon thermal stress. Each sample contained a 10-fold molar excess of ANS to protein. An excitation wavelength of 375 nm was used and emission spectra were collected from 400 – 600 nm. Spectra were obtained every 2.5 °C from 10 – 87.5 °C with an equilibration time of 5 minutes at each temperature. An appropriate buffer spectrum was subtracted before analysis. The fluorescence intensity at the peak emission position was plotted as a function of temperature.

Empirical Phase Diagram. An empirical phase diagram (EPD) was constructed using CD molar ellipticity, fluorescence intensity, and ANS intensity data. The original EPD technique was used to remain consistent with the previous analysis of RiVax [2]. Empirical phase diagrams are a convenient way to represent multi-dimensional data in a two-dimensional, colored plane. An important point about these diagrams is that they do not represent a true thermodynamic phase diagram in that no equilibrium is implied between different states. Also, the various colors are purely arbitrary in this early version of the EPD. The transitions in color, however, represent a change in the data used to construct the diagram and therefore a change in the physical state of the protein.

Results & Discussion

Secondary structure. Figure 1 shows the CD spectrum of RVEc at 10 °C for the four pH values studied. The spectra are characteristic of a mixture of α-helix and β-sheet structure. These spectra are consistent with the crystal structure of a version of the protein that contains an

engineered disulfide bond to improve the crystalizability of the protein [3]. These spectra are also consistent with previously published papers describing this protein's stability [4, 5]. The effect of temperature and pH on the stability of RVEc is shown in Figure 2. Similarly to Peek and co-workers results with RiVax, pH 6 (T_m ~ 52.5) affords the greatest stability against secondary structure thermal unfolding followed closely by pH 7 (T_m ~ 51.5) [1]. In contrast to the previous work are the stabilities of RVEc at pH 5 and 8. Peek's work revealed that RiVax had identical secondary structure stability at pH values 5 and 7, with pH 8 affording the least stability towards thermal stress. The Army variant is least stable at pH 5 (T_m ~ 45.5), with pH 8 (T_m ~ 48.5) having a stability intermediate to that of pH 5 and 7. Given the insolubility of RVEc at pH values 3 and 4, it is clear that acidic pH has destabilizing effect on RVEc. The precise molecular mechanism of this destabilization is unclear.

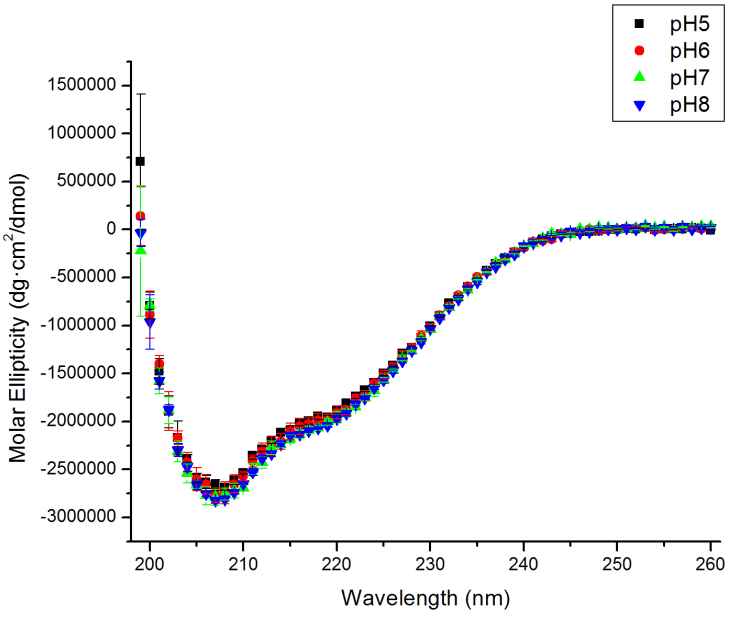

Figure 1. Circular dichrosim spectra of RVEc at 10 °C and the indicated pH values.

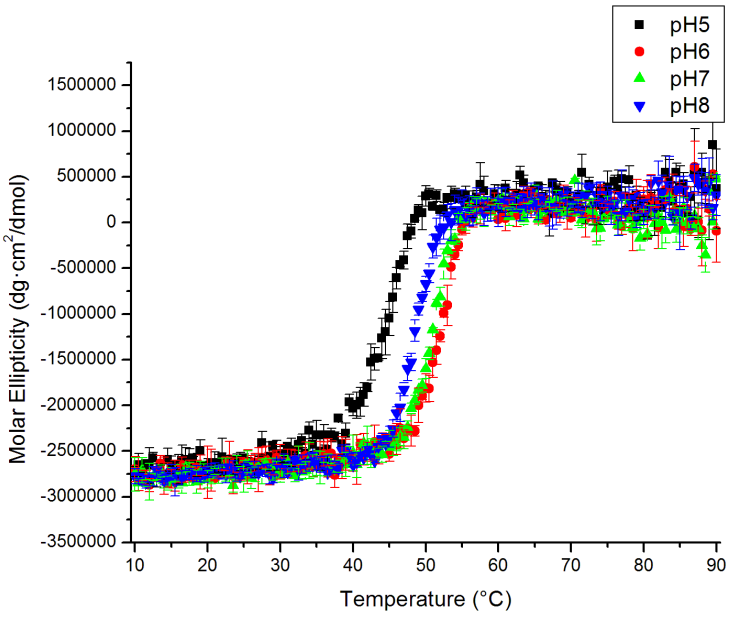

Figure 2. Thermal melting curves of RVEc as a function of temperature obtained by following mollar ellipticity at 207 nm.

Tertiary structure. The lone tryptophan residue in full length RTA occurs at site 212. Thus, RVEc does not contain any tryptophan residues due to its C-terminal truncation. As a result, an excitation wavelength of 280 nm was used to monitor changes in tertiary structure. Because tyrosine residues are notoriously insensitive to the polarity of their environment, changes in fluorescence intensity were used instead of changes in peak position. No differences were observed in the 10 °C fluorescence emission spectra of RVEc at pH values 5 – 8 (Figure 3). The effect of increasing temperature on the tertiary structure of RVEc is shown in Figure 4. The relative stabilities of RVEc as a function of pH remain the same as those observed in the CD melts (i.e., pH 6 > pH 7 > pH 8 > pH 5). Figure 5 presents the static light scattering of the protein at the incident wavelength as a function of temperature and pH. The figure clearly shows that the protein is particularly prone to aggregation at pH 5 when compared to the other pH conditions. In comparing Figures 4 and 5, it appears that the dramatic increase in intrinsic

fluorescence intensity is probably detecting increased scattering at 303 nm rather than a change in tertiary structure.

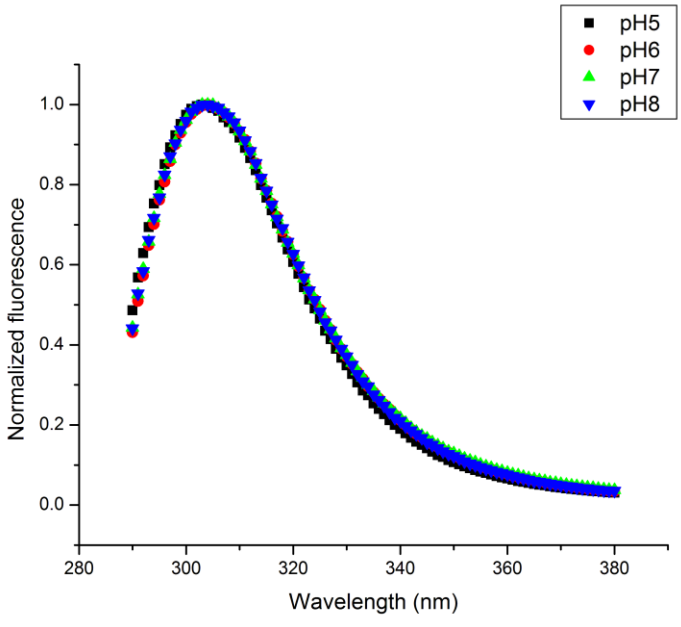

Figure 3. Fluorescence emission spectra of RVEc at 10 °C and the indicated pH values.

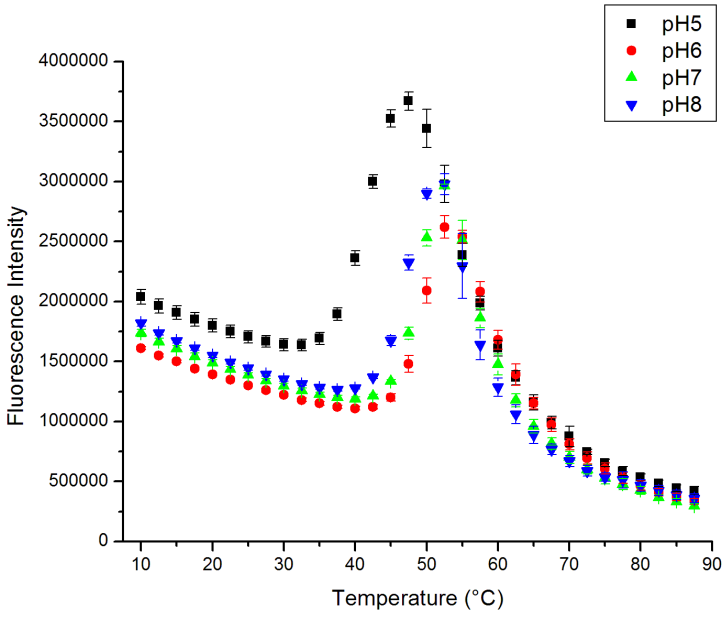

Figure 4. Thermal melting curves of RVEc as a function of temperature obtained by following the change in fluorescence intensity.

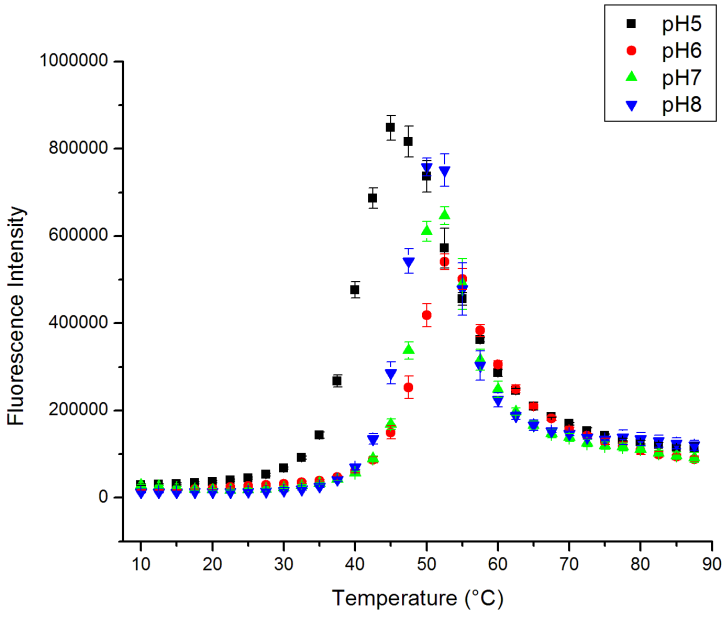

Figure 5. Thermal melting curves of RVEc as a function of temperature obtained by following the change in light scattering at 280 nm.

ANS fluoresces when it binds to apolar regions of a molecule. In a protein, these regions are typically buried in its native state and become more exposed upon unfolding. Thus, one should observe an increase in ANS intensity as the molecule unfolds. The possibility of an electrostatic component to this binding, however, cannot be ruled out. The relative stabilities as a function of pH are again unchanged compared to that observed in the CD and fluorescence melting curves (Figure 6). The value of the fluorescence intensity in the transition region may indicate that at pH 5 the protein unfolds differently than at other pH values, apparently by exposing a larger apolar surface area.

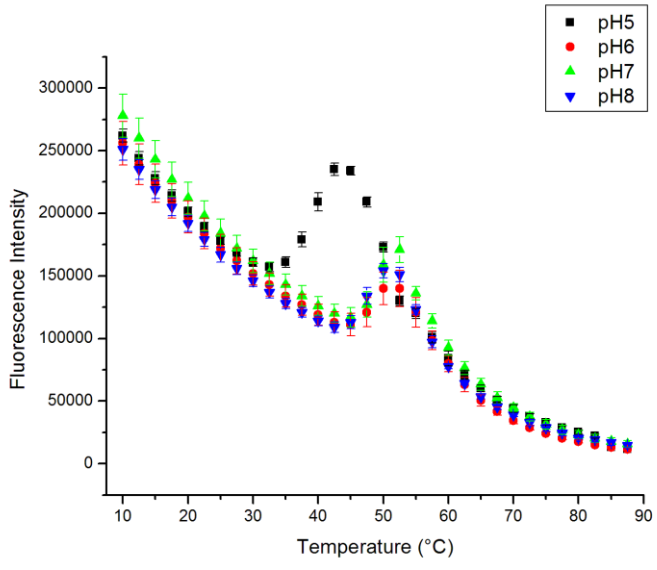

Figure 6. Thermal melting curves of RVEc as a function of temperature obtained by following ANS fluorescence intensity.

Empirical Phase Diagram. An empirical phase diagram (EPD) for RVEc was constructed based on the CD thermal melts, fluorescence intensity thermal melts, and ANS intensity thermal melts (Figure 7). It is quite similar to the one developed by Peek for RiVax [1]. In fact, it is difficult to conclude that this antigen is more stable than RiVax as once thought by comparing the EPDs except at pH 5, as noted in the paragraphs above, although much of the work stability data produced by the Army is in phosphate-buffered saline. The EPD reiterates the stability trends observed from the individual techniques: pH 6 > pH 7 > pH 8 > pH 5. The trends observed previously by Peek with RiVax were pH 6 > pH 7 ≈ pH 5 > pH 8.

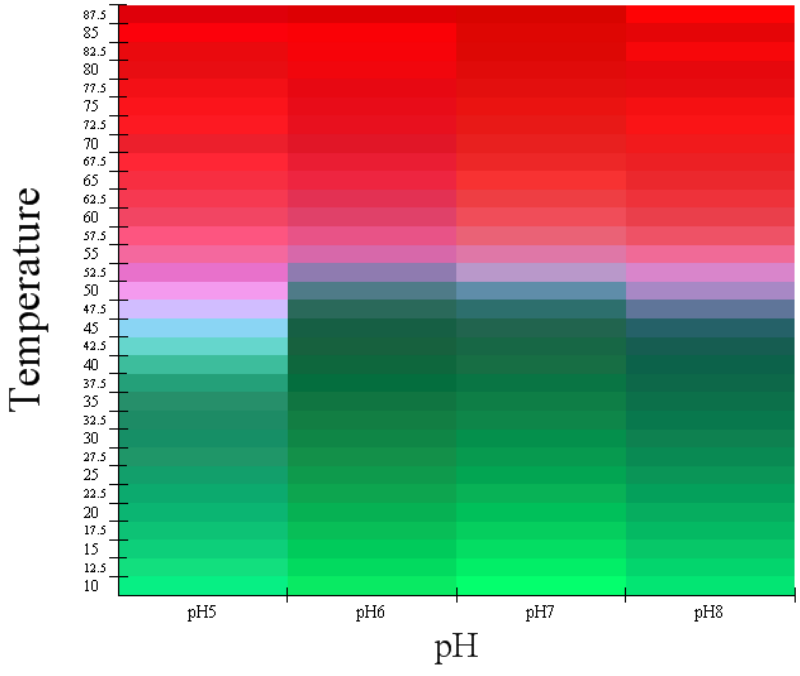

Figure 7. Empirical phase diagram (EPD) for RVEc created using molar ellipticity at 207 nm, fluorescence intensity, and ANS fluorescence.

References

1. Peek, L.J., R.N. Brey, and C.R. Middaugh, *A rapid, three-step process for the preformulation of a recombinant ricin toxin A-chain vaccine.* J Pharm Sci, 2007. 96(1): p. 44-60.
2. Kueltzo, L.A., et al., *Derivative absorbance spectroscopy and protein phase diagrams as tools for comprehensive protein characterization: a bGCSF case study.* J Pharm Sci, 2003. 92(9): p. 1805-20.
3. Compton, J.R., et al., *Introduction of a disulfide bond leads to stabilization and crystallization of a ricin immunogen.* Proteins, 2011. 79(4): p. 1048-60.
4. McHugh, C.A., et al., *Improved stability of a protein vaccine through elimination of a partially unfolded state.* Protein Sci, 2004. 13(10): p. 2736-43.
5. Olson, M.A., et al., *Finding a new vaccine in the ricin protein fold.* Protein Eng Des Sel, 2004. 17(4): p. 391-7.